



Title	Heterogeneous Catalysis for the Synthesis of Chemicals using Dehydrogenation/Hydrogenation Properties of Metal Nanoparticles and Hydrophobicity of Acidic Zeolites
Author(s)	Poly, Sharmin Sultana
Citation	北海道大学. 博士(工学) 甲第13813号
Issue Date	2019-09-25
DOI	10.14943/doctoral.k13813
Doc URL	http://hdl.handle.net/2115/90495
Type	theses (doctoral)
File Information	Sharmin_Sultana_Poly.pdf



[Instructions for use](#)

**Heterogeneous Catalysis for the Synthesis of
Chemicals using Dehydrogenation/Hydrogenation
Properties of Metal Nanoparticles and
Hydrophobicity of Acidic Zeolites**

Sharmin Sultana Poly

2019

Graduate School of Chemical Sciences and Engineering

Hokkaido University

Table of contents

Chapter 1- General Introduction

1.1 Introduction	2
1.1.1 Acceptorless dehydrogenative coupling (ADC) reaction of alcohols	2
1.1.2 ADC reaction of alcohols by heterogeneous catalyst	4
1.1.3 Synthesis of heterocycles by ADC of alcohols using heterogeneous catalyst	6
1.2 Hydrophobic substrates (alkynes, epoxides and glycerol) in polar solvent	7
1.2.1 Hydration reaction of alkynes and epoxides by heterogeneous catalyst	9
1.2.2 Acetalization of glycerol by heterogeneous catalyst	11
1.3 A new catalytic method: combination of metal nanoparticle and Brønsted acid catalysts	12
1.3.1 Chemical utilization of CO ₂	13
1.3.2 Hydrogenation of CO ₂ to value added chemicals	13
1.3.3 Catalytic methylation of <i>m</i> -xylene with CO ₂ /H ₂	14
1.4 Summary	15
1.5 Outline of thesis	15
References	19

Chapter 2 Acceptorless dehydrogenative synthesis of pyrimidine from alcohols and amidines catalyzed by supported platinum nanoparticles

2.1 Introduction	23
2.2 Experimental	25
2.3 Results and discussions	39
2.4 Conclusion	45
References	45

Chapter 3 Acceptorless dehydrogenation reaction of alcohols to pyridine by heterogeneous Pt catalyst

3.1 Introduction	62
3.2 Experimental	63
3.3 Results and discussions	65

3.4 Conclusion	66
References	67

Chapter 4 High silica H β zeolites for catalytic hydration of hydrophobic epoxides and alkynes in water

4.1 Introduction	75
4.2 Experimental	77
4.3 Results and discussions	83
4.4 Conclusion	90
References	91

Chapter 5 Acetalization of glycerol with ketones and aldehydes catalyzed by high silica H β Zeolite

5.1 Introduction	107
5.2 Experimental	108
5.3 Results and discussions	109
5.4 Conclusion	112
References	113

Chapter 6 Methylation of *m*-xylene by hydrogenation of CO₂ using TiO₂-supported Re and HBEA zeolite catalysts

6.1 Introduction	123
6.2 Experimental	124
6.3 Results and discussions	124
6.4 Conclusion	125
References	126

Chapter 7- General conclusion 134

Acknowledgements

Chapter 1

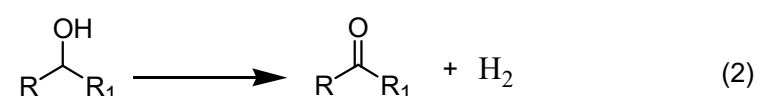
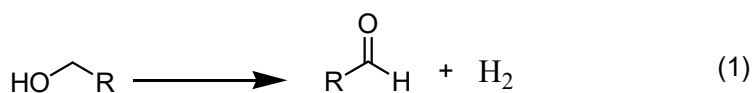
General Introduction

1.1 Introduction

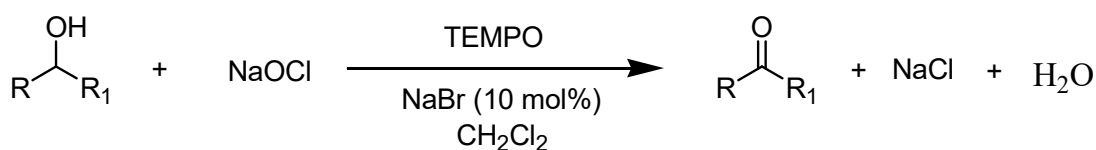
The ‘green chemistry’ perspective, new and economically efficient processes that do not rely on the use or formation of toxic and hazardous materials are critically important. In this point of view, green chemistry and ‘sustainable technology’ approaches have recently attracted substantial attention from academic and industrial chemists.¹ The ultimate goal in catalytic and organic chemistry is to reach the ideal synthesis of catalytic activity, selectivity, atom-efficiency and step-efficiency. The introduction gives an overview of the current research in the area of *acceptorless dehydrogenative* coupling of alcohols using supported metal catalysts, which expands the formation of C-C and C-N bonds. Another important target in modern synthetic catalysis is the transformation of hydrophobic substrates to important chemicals in polar environment. Recently homogeneous transition metal catalysts are used for this synthetic process. However, these homogeneous methods have problems such as difficulties in catalyst/product separation, catalyst reuse and the necessity of additives in the reaction mixture. From the environmental and economical viewpoints, the development of reusable heterogeneous catalysts is important. For this case, Bronsted acidic zeolite catalysts have been demonstrated for the hydration of hydrophobic substrates and acetalization of glycerol in a polar environment. According to the concept of previous methods, combination of supported metal nanoparticle and zeolite chemistry can be a new efficient catalytic approach for the utilization of CO₂ to activate C-H bond of aromatic ring via the hydrogenation reaction.

1.1.1 Acceptorless Dehydrogenative coupling (ADC) reaction of alcohols

The dehydrogenation of alcohols is widely applicable in organic synthesis because of the importance in medicines, agricultural chemicals and fragrances. Alcohols are unreactive and require strong inorganic oxidants to convert to synthetically useful carbonyl compounds. One of the important subjects of the transformation of nitrogen-containing heterocycles, which have broad applicability in pharmaceuticals, agrochemicals, flavoring agents and other functional chemicals.

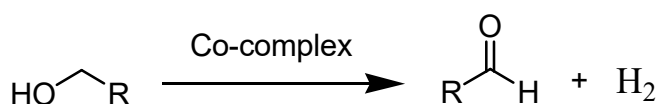


There are several methods studied for the acceptorless dehydrogenation reaction in recent years. In organic synthesis, the dehydrogenation is carried out using different types of oxidants such as: Chromium (IV) reagents, pressurized oxygen or peroxides, in addition of various kinds of additives, co-catalysts and catalytic systems introduced with metal complexes and TEMPO (2,2,6,6-tetramethylpiperidiny-1-oxyl).²⁻⁴ But pressurized oxygen and peroxides act as explosion hazards. In homogeneous system dehydrogenation of alcohols by TEMPO-catalyzed with sodium hypochlorite has been developed and commonly used in both small and large-scale applications.



Scheme 1. Acceptorless dehydrogenation of alcohols using acceptor

To overcome these problems, dehydrogenation methods without use of conventional oxidants were established. That means, Alcohols are readily dehydrogenated to carbonyl compounds without using oxidants or acceptors catalyzed by using variety of transition metal catalysts. Acceptorless dehydrogenation of alcohol is a green and atom-economic alternative, which provides aldehyde (or ketone) without the use of sacrificial acceptor molecules and the side product is molecular hydrogen. Catalytic acceptorless dehydrogenation reactions are very important for the synthesis of various organic compounds. Although ADC offers considerable benefits with respect to atom economy and environmental impact because of the avoidance of stoichiometric oxidants, it has been much less used in the synthesis of fine chemicals, pharmaceuticals, and agrochemicals. In spite of sacrificial hydrogen acceptors and additives are frequently used, ADC of alcohols have been realized with metal complexes in recent years.⁵



Scheme 2. ADC of alcohols by Co-Complex catalyst

Even though there is no use of oxidant and no by-product were produced but the system is homogeneous, additives were used, showed lower turnover number, difficulties in catalyst/product separation and no reusability of catalyst. To overcome these issues the green and sustainable new approach should be introduced. For this aspect, several heterogeneous catalysts have been developed for dehydrogenation of alcohols into their corresponding dehydrogenated products using various oxidizing agents. The previous reported methodologies were mostly involved in over oxidation of the dehydrogenated product and other functional groups on the substrate due to high reaction temperatures which inhibit its utility for a wide substrate scope. Moreover, the formation of byproduct water, produced during dehydrogenation could lead to catalyst deactivation and reusability problems. Alternatively, several precious metal-based heterogeneous catalysts have been developed to overcome these limitations and to achieve an efficient oxidant-free dehydrogenation of wide range of alcohols.

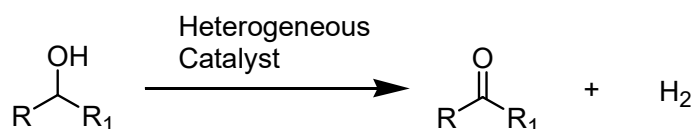
1.1.2 Acceptorless dehydrogenative coupling (ADC) reaction by heterogeneous catalyst

Heterogeneous catalysis for the one-pot synthesis of added-value chemicals is a growing area in green and sustainable chemistry. Among various types of organic transformations that are accessible by this approach, acceptorless dehydrogenative coupling (ADC) reactions have been established as efficient processes that generate various classes of organic compounds via the formation of C–O, C–N, C–S, C–C, and C=C bonds. Recent developments of our group, on the one-pot synthesis of organic compounds that are driven by the dehydrogenation of alcohols promoted by supported transition-metal catalysts in the absence of hydrogen acceptors. A major feature of the design of such catalysts is the cooperation between the metal sites and the acid and/or base sites on the metal–oxide supports. Recent examples for the organometallic catalysis of ADC reactions of alcohols are presented and their efficiency is put into contrast with that of related reactions carried out using conventional supported transition-metal catalysts. Finally, aspects pertaining to the mechanism and catalyst design of these new ADC reactions are discussed in the context of directions for future developments in this area.

A series of dehydrogenative coupling reactions of alcohols with nucleophiles have been demonstrated by our group (Scheme 3). And these reactions are acceptorless and showed high yields and higher TON than the complex molecular catalysis. With this background we plan to demonstrate more challenging multistep dehydrogenative coupling reactions. Pt nanocluster-loaded metal oxides, in situ pre-reduced under H₂ at 500 °C, were tested for the

dehydrogenation of aliphatic secondary alcohols in the liquid phase. According to the report, activity for dehydrogenation of 2-octanol depended strongly on the acid–base character of the support oxide, and amphoteric oxides, especially γ -Al₂O₃, which gave high activity for this reaction. Al₂O₃ supported Pt acted as reusable heterogeneous catalyst for dehydrogenation of aliphatic secondary alcohols to the corresponding ketones. Pt/Al₂O₃ showed higher activity than other M/Al₂O₃ (Co, Ni, Cu, Ru, Rh, Pd, Ag, Re, Ir, Au) catalysts and showed two orders of magnitude higher turnover number (TON) than previously reported Pt catalysts for dehydrogenation of alcohol to ketones.⁶

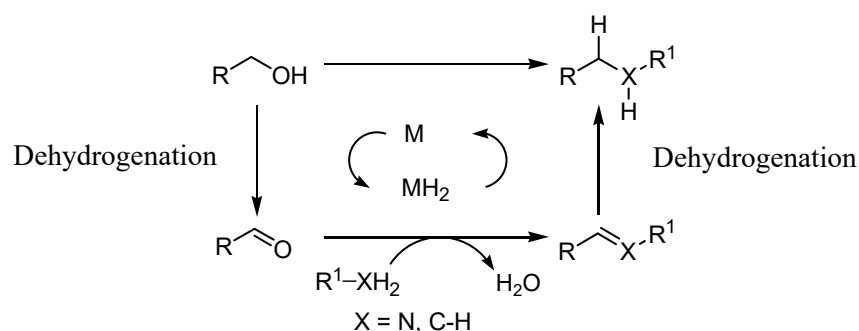
Another report, SnO₂-supported Pt (Pt/SnO₂) represents a reusable heterogeneous catalyst for the ADC of various primary alcohols to form esters under additive- and solvent-free conditions. Pt/SnO₂ displays a higher activity than various other SnO₂-supported transition metals such as Ir, Re, Ru, Rh, Pd, Ag, Co, Ni and Cu. The catalytic activity of Pt thereby depends on the nature of the support, whereby SnO₂ exhibits a superior performance relative to ZrO₂, CeO₂, Nb₂O₅, TiO₂, carbon, Al₂O₃, SiO₂, H-beta zeolite, and MgO.⁷



Scheme 3. Acceptorless dehydrogenative coupling reaction of alcohols by using heterogeneous catalysts by our group

1.1.3 Synthesis of heterocycles by ADC of alcohols using heterogeneous catalyst

Heterocycles can be synthesized by acceptorless dehydrogenative coupling of alcohols. First, metal accept hydrogen from alcohols and convert it to aldehyde and ketone. Then another molecule of alcohol combines with aldehyde and ketone and an intermediate is formed. This intermediate convert to heterocycle by losing another molecule of hydrogen.



Scheme 4. Catalytic acceptorless dehydrogenative coupling of alcohols

Very recently, efficient and clean synthetic homogeneous catalytic method have been developed for the acceptorless dehydrogenative coupling reactions of alcohols.⁸⁻¹⁴ But the method suffers from several drawbacks such as: low turnover number, difficult in catalyst/product separation and non-reusability of catalyst. So the atom economic sustainable heterogeneous catalytic methods are needed for the synthesis of heterocycles by ADC of alcohols.

Recently our group developed, Carbon supported Pt-Nanoparticle (Pt/C) shows effectiveness for the synthesis of pyrroles in the presence of KO^tBu and affords a wide range of pyrroles. The method has the advantage that the catalyst, which displays a high TON, can be prepared by a simple impregnation method and that it can be reused without significant loss of activity. This method generates pyrroles from 2-amino-1-butanol and various secondary alcohols such as 1-phenylethanols, as well as cyclic and acyclic aliphatic alcohols.¹⁵

Another report, for the synthesis of 2-quinazolines and 2-benzimidazoles from diamines and alcohols as an additive- and acceptor free heterogeneous catalytic system has been developed. These efforts revealed that Pt/CeO₂ is an excellent catalyst for the 2-quinazoline-forming reactions between primary alcohols and 2-aminomethyl-phenylamine.¹⁶

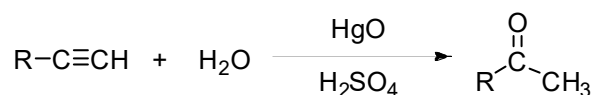
1.2 Hydrophobic substrates (alkynes, epoxides, and glycerol) in polar solvent (water)

The term 'hydrophobic' is derived from *hydro-* (water) and *phobos* (fear). However, it is not so much that hydrophobic molecules 'fear' water as water 'fears' the hydrophobic molecules. The polar character of water makes an excellent solvent for polar and ionic materials, which are therefore said to be hydrophilic. Nonpolar substances are virtually insoluble in water and are consequently described as being hydrophobic. The use of water as an inexpensive and benign reagent in organic synthesis is an important topic, and the hydration of hydrophobic substrates are a typical example of such use. It is one of the most useful methods for the functionalization of unactivated hydrophobic substrates, and has found numerous synthetic uses.^{17,18} But the transformation of hydrophobic substrates to important chemicals are more attractive in organic synthesis. Therefore, atom economic, green sustainable methods are required for the hydration of hydrophobic substrates. Development of a heterogeneous catalyst for the transformation of hydrophobic substrates in polar solvent is a great challenge. From this viewpoint, hydrophobic Bronsted acid catalyst can be a good choice. Hydrophobic catalyst can easily activate the hydrophobic substrates to transform into product in polar

environment.

Hydration of alkynes and epoxides

Hydration of alkynes forms carbonyl compounds as key intermediates for both bulk- and fine- chemical industries. With the addition of water, alkynes can be hydrated to form enols that spontaneously tautomerize to ketones. The addition of water to alkynes with Hg(II) salts to form carbonyl compounds was first reported by Berthelot in 1862, and since then, it is a classical textbook reaction. [M. Berthelot, C. R. Hebd. Seances Acad. Sci. 1862, 50, 805] Mercury (II) salts combined with acids, such as HgO/H₂SO₄ and HgO/BF₃, are reliable catalysts for the hydration of alkynes and these catalysts were extensively used in high-scale industrial processes until the discovery of the corrosion of reactor and toxicity of mercury salts.

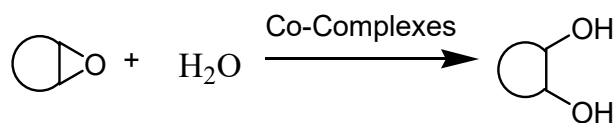


Scheme 5. Hydration of alkynes in conventional method

In homogeneous system, use of concentrated solution of strong acids (H₂SO₄, CF₃SO₃H and PTSA) is known to promote the alkyne hydration process. Transition metal catalysts (Fe, Ir, Ag, Co and Au), mineral acids are used as homogeneous catalysts.^{17,19,20} The hydration of phenylacetylene and other alkynes in an acidic, aqueous medium catalyzed by various water-soluble organometallic complexes was investigated. Nevertheless, it not always fruitful for large scale preparations. Even this method has more or less drawbacks such as low turnover number, difficulties in catalyst/product separation, non-reusability of catalyst.

Glycol is widely used as intermediates for the manufacture of polyester resins, antifreezes, cosmetics, medicines, and other products. Glycol is produced predominantly by non-catalytic liquid-phase hydration of epoxides with di-ol and tri-ol as byproducts. Thus, a large excess of water (up to 20 M equiv) required for obtaining high glycol selectivity in a hydration of epoxide makes it one of the most cost and energy intense processes in chemical industry. Various acids and bases (e.g., cation- and anion-exchange resins, quaternary phosphonium halides, polymeric organosilane ammonium salts, macrocyclic chelating compounds, cyclic amine, and supported metal oxides) have been developed to catalyze the ring-opening hydration of epoxides. However, a high H₂O/epoxide molar ratio (i.e. >10) is still required for high glycol selectivity. Typically, acid catalysts are used for the hydration of epoxides. In

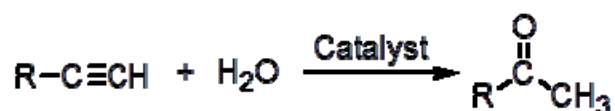
homogeneous catalytic system, metal salts, cyclic amines and Co-complexes have been explored.



Scheme 6. Hydration of epoxides by homogeneous catalysts

1.2.1 Hydration of alkynes and epoxides by heterogeneous catalysts

Alternative metallic catalysts have been searched over the years, mainly transition metal-based catalysts, such as Pt, Fe, Pd, Ir, Ag, Os and Au. Whereas, most of these metal catalysts have shortcomings, such as lower reactivity, recovery and reuse of (expensive) catalysts and prohibit their frequent use for laboratory as well as industrial purpose. Transition metal containing heterogeneous catalysts generally produce contaminated products. In recent years, green and economic considerations have raised strong attention to redesign commercially important processes to avoid the use of harmful reagents and the generation of toxic waste. In this respect, the development of easily recyclable and recoverable heterogeneous catalysts can solve the problems of the homogeneous systems and has received particular research interest by synthetic organic chemists.²¹⁻²⁴



Scheme 7. Hydration of alkynes by heterogeneous catalysts

The development of an efficient and environmentally benign process for the hydration of epoxides with an H₂O/epoxide molar ratio approaching the stoichiometric value of the chemical reaction is still a huge challenge. More recently, many heterogeneous catalytic methods have been developed for the ring opening hydration of epoxides.^{18,25,26} Resins, Mo-V oxides, Nb-based oxides, immobilized transition metal complexes have been explored. However, these catalysts are potential to solve the previous problems, but still there are some problems including low reusability due to their instability. So, the development of a more

atom economic environmentally friendly, transition metal-free heterogeneous catalyst for the hydration of epoxides is highly challenging.



Scheme 8. Hydration of epoxides by heterogeneous catalysts

Acetalization of glycerol

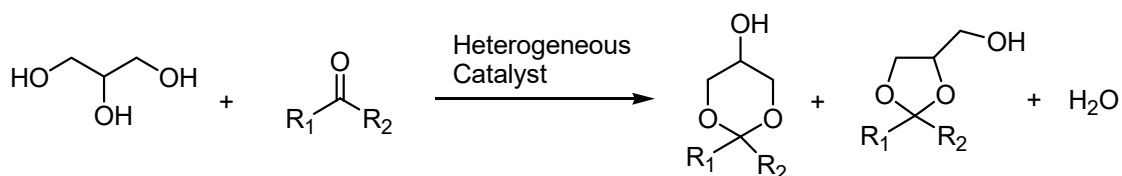
Biodiesel production is accompanied by the formation of glycerol as a by-product. The use of glycerol is limited now, being mainly, confined to pharmaceuticals and cosmetics. Hence, the development of effective and environmentally friendly approaches for efficient conversion of GL to value-added chemicals is a challenging and demanding task.²⁷ The development of improved protocols and strategies for the efficient construction of carbon-carbon bonds continues to be a challenge in organic synthesis. Typically, classical methods make use of electrophilic alkylating agents like alkyl halides and result in the formation of undesired salts as by-products. The condensation of glycerol with carbonyl compounds to synthesize acetals (acetalization) have attracted much attention for the usefulness of cyclic acetals for diesel fuels and flavor compounds.²⁸

In homogeneous catalytic system, the synthesis of acetals is the reaction of carbonyl compounds with alcohol or orthoester in the presence of acid catalyst. The general method for acetal synthesis involves reaction of carbonyl compounds with an alcohol or an ortho-ester in the presence of protic acid or Lewis acid catalysts. Protic acids such as PTSA, HCl, H₃PO₄, H₂SO₄ and Lewis acids such as AlCl₃, FeCl₃, ZnCl₂, SnCl₂ and metal complex catalysts are largely used in homogeneous system to produce acetal.^{29,30} However, these catalysts have some defects, such as low thermal stability, low surface area, the problem of separating them from the reaction mixture.

1.2.2 Acetalization of glycerol by heterogeneous catalyst

To overcome these issues heterogeneous catalysts Brønsted acidity, such as sulfonic mesostructured silicas, molybdenum and tungsten promoted SnO₂ solid acids and Lewis acid mesoporous substituted silicates (Zr- and Hf-TUD-1, and Sn-MCM41) have been reported to be active in this reaction. Some transition metal catalysts, heteropoly acid catalysts, metal organic frameworks have been developed.³¹⁻³⁴ The main drawback of glycerol acetalization is the production of water, which has to be removed in order to hinder the reversibility of this

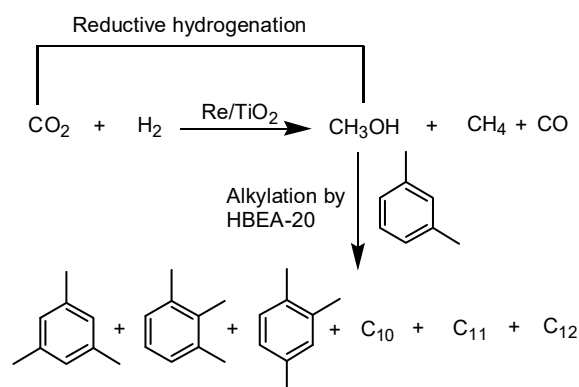
reaction and catalyst deactivation. To solve the problem, various water-tolerant catalysts such as zeolites, periodic mesoporous organo-silicas (PMO), heteropoly acid salts and oxides were used for glycerol acetalization.³⁵⁻⁴⁰ These heterogeneous catalysts show higher yield, high turnover number and reusability of catalysts.



Scheme 9. Acetalization of glycerol by heterogeneous catalysts

1.3 Combination of metal nanoparticle and Brønsted acid catalysts

In previous study ADC reaction by heterogeneous supported transition metal (Pt/C) catalysts were developed for the synthesis of N-containing heterocycles, pyrimidines and pyridines. Another target was to develop Brønsted acidic zeolite catalyst for the hydration of hydrophobic substrates in a polar environment. These two catalytic methods showed different syntheses of organic compounds. According to the concept of previous study, a new heterogeneous mix catalyst was developed for the activation of C-H bonds of aromatic rings for the conversion of CO₂ to fuels, rather than organic chemicals, is expected to play a major role in CO₂ emission management strategies.



Scheme 10. Combination of metal catalyst and zeolite to methylation of *m*-xylene

1.3.1 Chemical utilization of CO₂

Scientists have been aware of the potential economic and environmental benefits of using CO₂ as a feedstock for the synthesis of commodity chemicals and fuels for decades. It is a generally inexpensive waste product, which contributes significantly to global warming.⁴³ Nevertheless, despite the large amount of fundamental research that has been performed

regarding the conversion of CO₂ into more valuable products there are relatively few examples of industrially viable processes. The challenges associated with the conversion of CO₂ are primarily related to both its kinetic and thermodynamic stability. CO₂ cannot be converted into commodity chemicals or fuels without significant inputs of energy and contains strong bonds that are not particularly reactive. In this chapter we provide a general idea of the current state of research into chemical pathways for the conversion of CO₂ into valuable chemicals and fuels. CO₂ hydrogenation is the easiest path for the direct CO₂ conversion into valuable chemicals. Wide attention has been paid to CO₂ hydrogenation to basic chemicals, such as CO, CH₃OH, HCOOH, and CH₄.⁴⁴ However, the inertness of CO₂ and high kinetic barriers for C–C bond formation hamper opportunities for long-carbon-chain growth. It is still a challenge to synthesize long-chain hydrocarbons directly from CO₂.

1.3.2 Hydrogenation of CO₂ to value added chemicals

Efficient utilization of carbon dioxide (CO₂), a major component of greenhouse gases, as a C1 source in organic synthesis has always been a topic of interest among scholars. Not only does the use of CO₂ as a chemical feedstock is a way to reduce atmospheric CO₂ concentration, it is also abundant, nontoxic, and easily available. Therefore, the valorization of CO₂ is advantageous from both environmental and economical point of view. So far, much attention has been directed towards the catalytic transformation of CO₂ via hydrogenation to produce value-added chemicals, especially CH₃OH, due to the popularity of “methanol economy”.⁴⁵ CH₃OH, one of the most important commodity chemicals in the world, is widely used as a C1 building block for industrial purpose, especially for the formation of C-N and C-C bond. In recent years, several studies on the direct methylation of C-N and C-H bonds by employing using CO₂/H₂ has been reported. Although these studies are highly impactful, the substrate scope are mostly limited to molecules which contain activated C-N or C-H bonds such as amines, imines and heteroarenes.

1.3.3 Catalytic methylation of *m*-xylene with CO₂/H₂

Methylation of organic compounds are fundamental reactions in organic synthesis. In chemical industry, methylation of aromatic compounds is of particular importance in the production of poly-methylated compounds. Methylation of xylene forms poly methylated products have been also extensively used in petrochemical industries for the production of plastics, polymers, solvents, pesticides, dyes and adhesives.²⁸ As is well-known, syngas (H₂/CO) obtained from shale gas, natural gas, biomass and coal can be a potential source for

producing hydrocarbons. Most previous studies on syngas to aromatics have been based on modified Fischer-Tropsch (FT) synthesis or an indirect process starting from methanol synthesis.⁴¹ However, in both cases there are some limitations that hamper the efficiency of syngas to aromatics. The efficient conversion of CO₂ to useful chemicals is a promising way to reduce atmospheric CO₂ concentration and also reduce reliance on fossil-based resources. Although much progress has been made toward the production of basic chemicals, like methanol, through CO₂ hydrogenation, the direct conversion of CO₂ to value added aromatic compounds. Recently, a direct CO₂ conversion route was developed to synthesize gasoline-range hydrocarbons, in which CO₂ was first reduced to CO via a reverse water-gas shift (RWGS) reaction, and then the formed CO was hydrogenated into hydrocarbons via a Fischer-Tropsch synthesis (FTS) process. Furthermore, bifunctional catalysts composed of methanol synthesis catalyst and acidic zeolite were also proposed for the efficient conversion of CO₂ to C₅+ hydrocarbons.⁴²

A variety of reports on the catalytic methylation of C-H bonds for aromatic hydrocarbons, by using fossil-based methylation agents such as methanol, dimethyl ether, methane, and syngas are widely available. These reactions are mainly carried out by using a bifunctional catalyst system which includes a methanol synthesis catalyst coupled with acidic zeolite, which act as a methanol conversion catalyst. The methylation of aromatic hydrocarbons is of great importance as aromatics such as BTX (benzene, toluene, and xylenes) are one of the most important platform molecules for the petrochemical industry.⁴⁶ Therefore, the direct methylation of aromatic hydrocarbons by using CO₂/H₂ is highly attractive.

1.4 Summary

In this study, Various heterogenous catalytic methods were investigated for the synthesis of various useful organic chemicals. Acceptorless dehydrogenative coupling of alcohols to heterocycles (pyrimidines, pyridines) using heterogeneous carbon supported Pt nanoparticles is a new approach according to the concept of green chemistry. The Bronsted acid site of zeolite is much attractive for the different organic reaction. In this study, the hydration of alkynes and epoxides is important to produce ketones and diols respectively. This hydration chemistry was mainly focused on the acid site and hydrophobic nature of zeolite. By the continuation of this study, another organic reaction named acetalization was developed. Acetalization of glycerol to acetal is not the new reaction in organic chemistry but the new concept on catalytic method depends on the acid site and hydrophobic nature of zeolite. Even though, Synthesis of different organic reactions with different heterogeneous catalysts is not

the new approach, but the combination of different catalytic method can be introduced for the new atom economic ideal synthesis of organic chemistry.

1.5 Outline of thesis

This thesis focuses on development of heterogeneous catalysts for acceptorless dehydrogenative coupling of alcohols to overcome the critical issues of previous methods. The objectives of thesis are to develop new heterogeneous catalyst for ADC of alcohols and Bronsted acid catalysts for transformations of hydrophobic substrates in a polar environment is another important target in modern synthetic catalysis. The thesis will show two classes of heterogeneous catalysts for these two issues: supported Pt nanoparticles (NPs) for ADC reactions (Chapters 2,3) and high-silica Beta zeolites for hydration of epoxides and alkynes in water and acetalization of glycerol to acetal (Chapters 4,5) in a batch reactor. Combining these methods, a new catalytic method for methylation of xylenes with CO₂/H₂ is developed (Chapters 6). Studies on structure-activity relationship and reaction mechanism are also described in order to propose design concept of effective heterogeneous catalysis for clean organic synthesis.

Chapter 2 demonstrates the first example of the heterogeneous catalysis for the synthesis of 2,4,6-trisubstituted pyrimidines by ADC reaction of secondary and primary alcohols and amidines using a carbon-supported Pt catalyst (Pt/C) with KO^tBu. Pt/C showed higher yield than Pt-loaded metal oxides ZrO₂, Al₂O₃, CeO₂, TiO₂, SiO₂, MgO, zeolite, Nb₂O₅. Pt/C promotes a higher yielding reaction than do other transition metal NPs supported on carbon (Ir/C, Ni/C, Pd/C, Rh/C, Ru/C, Re/C, Cu/C, and Ag/C). The reaction takes place efficiently for a wide range of substrates (32 examples). The Pt/C catalyst that promotes this process is reusable and has a higher turnover number (TON) than previously methods using homogeneous catalysts. The results of mechanistic studies suggest that the process takes place through a pathway that begins with Pt-catalyzed acceptorless dehydrogenation of the alcohol, which is followed by sequential condensation, cyclization, and dehydrogenation. Measurements of the turnover frequency (TOF) combined with the results of density functional theory calculations on different metal surfaces suggest that the adsorption energy of H on the Pt surface is optimal for the acceptorless dehydrogenation process, which causes the higher catalytic activity of Pt over those of other metals.

Chapter 3 shows the first heterogeneous catalytic method for the synthesis of pyridine derivatives by ADC reaction of amino alcohols and secondary alcohols using the Pt/C catalyst. The reaction involves nucleophilic attack by the amine group of a α -amino alcohol

molecule on the ketone can produce an imine intermediate, followed by dehydrogenation of the resulting imine-alcohol intermediate and C-C bond formation by condensation under basic reaction conditions, eventually leading to a dihydropyridine derivative which is further dehydrogenated to the desired pyridine.

Chapter 4 is the catalytic study for the hydration of hydrophobic epoxides and alkynes in water using proton-exchanged *BEA zeolite (HBeta). Among 24 types of heterogeneous and homogeneous catalysts tested, HBeta zeolite with a relatively high Si/Al ratio (Si/Al = 75), HBeta-75, is an effective catalyst for both of the reactions in water. HBeta-75 showed wide substrate scope, good reusability, and applicability in gram-scale synthesis for both types of reactions. The effects of hydrophobicity, acidity, and the size of zeolite pores were also comprehensively studied through the hydration of hydrophilic and hydrophobic epoxides and alkynes with different molecular sizes using two types of zeolite (HBeta and HZSM5). Hydrophobicity and acidity of different zeolites were studied by various characterization methods, including TPD, adsorption experiments in water, and IR spectroscopy. It is concluded that the high catalytic activity of HBeta-75 are attributed to the three important factors: 1) hydrophobic interaction between zeolite pores with the substrates; 2) large pore size; 3) Brønsted acidity. The larger pore size of HBeta-75 compared to HZSM5-75 played an important role in achieving high yields. The higher Si/Al ratio results in the higher TOF, which is caused by larger adsorption capacity of hydrophobic substrate in water.

Chapter 5 shows that HBeta-75 is effective for the acetalization of glycerol with carbonyl compounds. This catalyst system was amenable to a wide substrate scope and exhibited good reusability. The TOF, based on Brønsted acid site concentration, increased as a function of Si/Al ratio, monotonically increases with increasing Si/Al ratio, which is similar to the dependency of hydrophobicity on the Si/Al ratio. The results indicate that hydrophobic nature of the HBeta catalysts accelerate the acetalization reaction. On the hydrophobic inner pore surface, the generated H₂O molecule, as a co-product, easily desorbs, thus accelerating the acetalization reaction. The results in Chapters 4,5 show that HBeta-75, having the Brønsted acid sites at the hydrophobic inner surface of large pore zeolite, is general and versatile catalyst for organic reactions in water or in the presence of water as a byproduct.

Chapter 6 shows development of new catalytic reaction, methylation of xylenes with CO₂/H₂, by combining the two catalytic materials studied in this thesis: supported metal nanoparticles and hydrophobic zeolites. Screening study showed that TiO₂-supported Re (Re/TiO₂) with HBeta-20 (Si/Al=20) is the best combination for achieving high activity for this reaction. Under the optimized reaction conditions (PCO₂ = 1 MPa; PH₂ = 5 MPa; T =

513 K), this catalytic system achieved high performance for the synthesis of polymethyl benzenes with high yield. Re metal NPs catalyze a hydrogenation step, while the HBeta-20 zeolite catalyzes alkylation step.

Chapter 7 is the general summary. Chapters 2,3 show the first examples of heterogeneous catalysis for the synthesis of heterocycles via ADC reactions of alcohols based on dehydrogenation-condensation and cyclization-dehydrogenation steps with elimination of water and liberation of H₂ as byproduct. Pt metal NPs play an important role in the dehydrogenation step. Chapters 4,5 conclude that HBeta-75, having the Brønsted acid sites at the hydrophobic inner surface of large pore zeolite, is general and versatile catalyst for organic reactions in water or in the presence of water as a byproduct. Chapter 6 shows development of a new catalytic reaction for methylation of xylenes with CO₂/H₂ combination of metal NPs catalysts and acidic zeolites. The developed catalyst (Re/TiO₂ with HBeta-20) gave polymethyl benzenes in high yield. Re metal NPs catalyze for the hydrogenation step, while the HBeta-20 zeolite catalyzes alkylation step. These three types of heterogeneous catalytic methods will be useful in sustainable synthesis of chemicals. Conceptual conclusions from structure-activity relationship and mechanistic studies will be useful for designing more effective heterogeneous catalysts.

References

- (1) Corma, A.; Garcia, H. *Chem. Soc. Rev.* **2008**, *37* (9), 2096–2126.
- (2) Muzart, J. *Chem. Rev.* **1992**, *92* (1), 113–140.
- (3) Punniyamurthy, T.; Velusamy, S.; Iqbal, J. *Chem. Rev.* **2005**, *105* (6), 2329–2364.
- (4) Hu, Z.; Kerton, F. M. *Org. Biomol. Chem.* **2012**, *10* (8), 1618–1624.
- (5) Choi, J.; MacArthur, A. H. R.; Brookhart, M.; Goldman, A. S. *Chem. Rev.* **2011**, *111* (3), 1761–1779.
- (6) Kon, K.; Hakim Siddiki, S. M. A.; Shimizu, K. I. *J. Catal.* **2013**, *304*, 63–71.
- (7) Moromi, S. K.; Hakim Siddiki, S. M. A.; Ali, M. A.; Kon, K.; Shimizu, K. I. *Catal. Sci. Technol.* **2014**, *4* (10), 3631–3635.
- (8) Allais, C.; Grassot, J. M.; Rodriguez, J.; Constantieux, T. *Chem. Rev.* **2014**, *114* (21), 10829–10868.
- (9) Deibl, N.; Ament, K.; Kempe, R. *J. Am. Chem. Soc.* **2015**, *137* (40), 12804–12807.
- (10) Guo, B.; Yu, T.-Q.; Li, H.-X.; Zhang, S.-Q.; Braunstein, P.; Young, D. J.; Li, H.-Y.; Lang, J.-P. *ChemCatChem* **2019**.
- (11) Pan, B.; Liu, B.; Yue, E.; Liu, Q.; Yang, X.; Wang, Z.; Sun, W. H. *ACS Catal.* **2016**, *6*

- (2), 1247–1253.
- (12) Chai, H.; Wang, L.; Liu, T.; Yu, Z. *Organometallics* **2017**, *36* (24), 4936–4942.
- (13) Wang, R.; Fan, H.; Zhao, W.; Li, F. *Org. Lett.* **2016**, *18* (15), 3558–3561.
- (14) Srimani, D.; Ben-David, Y.; Milstein, D. *Chem. Commun.* **2013**, *49* (59), 6632.
- (15) Siddiki, S. M. A. H.; Touchy, A. S.; Chaudhari, C.; Kon, K.; Toyao, T.; Shimizu, K. I. *Org. Chem. Front.* **2016**, *3* (7), 846–851.
- (16) Chaudhari, C.; Hakim Siddiki, S. M. A.; Tamura, M.; Shimizu, K. I. *RSC Adv.* **2014**, *4* (95), 53374–53379.
- (17) Chen, D.; Wang, D.; Wu, W.; Xiao, L. *Appl. Sci.* **2015**, *5* (2), 114–121.
- (18) Zhong, M.; Zhao, Y.; Yang, Q.; Li, C. *J. Catal.* **2016**, *338*, 184–191.
- (19) Cabrero-Antonino, J. R.; Leyva-Pérez, A.; Corma, A. *Chem. - A Eur. J.* **2012**, *18* (35), 11107–11114.
- (20) Tachinami, T.; Nishimura, T.; Ushimaru, R.; Noyori, R.; Naka, H. *ChemInform* **2013**, *44* (24), no-no.
- (21) Venkateswara Rao, K. T.; Sai Prasad, P. S.; Lingaiah, N. *Green Chem.* **2012**, *14* (5), 1507–1514.
- (22) Mamede, N.; Peraka, S.; Marri, M. R.; Kodumuri, S.; Chevella, D.; Gutta, N.; Nama, N. *Appl. Catal. A Gen.* **2015**, *505*, 213–216.
- (23) Veer, S. D.; Pathare, S. P.; Akamanchi, K. G. *Arkivoc* **2016**, *2016* (4), 59–66.
- (24) Xu, S.; Yun, Z.; Feng, Y.; Tang, T.; Fang, Z.; Tang, T. *RSC Adv.* **2016**, *6* (74), 69822–69827.
- (25) Ogawa, H.; Miyamoto, Y.; Fujigaki, T.; Chihara, T. *Catal. Letters* **1996**, *40* (3–4), 253–255.
- (26) Tang, B.; Dai, W.; Wu, G.; Guan, N.; Li, L.; Hunger, M. *ACS Catal.* **2014**, *4*, 2801–2810.
- (27) Han, X.; Zhu, G.; Ding, Y.; Miao, Y.; Wang, K.; Zhang, H.; Wang, Y.; Liu, S. Bin. *Chem. Eng. J.* **2019**.
- (28) Rueping, M.; Phapale, V. B. *Green Chem.* **2012**, *14* (1), 55–57.
- (29) Li, X.; Zheng, L.; Hou, Z. *Fuel* **2018**, *233* (January), 565–571.
- (30) Scamardella, C.; Cucciolito, M. E.; Ruffo, F.; Raucci, U.; Rega, N.; Esposito, R.; Di Guida, R. *ACS Omega* **2019**, *4* (1), 688–698.
- (31) Konwar, L. J.; Samikannu, A.; Mäki-Arvela, P.; Boström, D.; Mikkola, J. P. *Appl. Catal. B Environ.* **2018**, *220* (July 2017), 314–323.

- (32) Arias, K. S.; Garcia-Ortiz, A.; Climent, M. J.; Corma, A.; Iborra, S. *ACS Sustain. Chem. Eng.* **2018**, *6* (3), 4239–4245.
- (33) Wang, K.; Wang, Y.; Zhang, H.; Ding, Y.; Zhu, G.; Miao, Y.; Han, X.; Liu, S.-B. *Chem. Eng. J.* **2018**, *359* (April 2018), 733–745.
- (34) Bakuru, V. R.; Churipard, S. R.; Maradur, S. P.; Kalidindi, S. B. *Dalt. Trans.* **2019**, *48* (3), 843–847.
- (35) Fonseca, A. M.; Ferreira, C.; Rombi, E.; Araujo, A.; Cutrufello, M. G.; Calvino-Casilda, V.; Bañares, M. A.; Neves, I. C. *Microporous Mesoporous Mater.* **2018**, *271* (February), 243–251.
- (36) Sonar, S. K.; Shinde, A. S.; Asok, A.; Niphadkar, P. S.; Mayadevi, S.; Joshi, P. N.; Bokade, V. V. *Environ. Prog. Sustain. Energy* **2018**, *37* (2), 797–807.
- (37) Ammaji, S.; Rao, G. S.; Chary, K. V. R. *Appl. Petrochemical Res.* **2018**, *8* (2), 107–118.
- (38) Venkatesha, N. J.; Bhat, Y. S.; Jai Prakash, B. S. *RSC Adv.* **2016**, *6* (23), 18824–18833.
- (39) Nair, G. S.; Adrijanto, E.; Alsalmeh, A.; Kozhevnikov, I. V.; Cooke, D. J.; Brown, D. R.; Shiju, N. R. *Catal. Sci. Technol.* **2012**, *2* (6), 1173–1179.
- (40) Neves, T. M.; Fernandes, J. O.; Lião, L. M.; Deise da Silva, E.; Augusto da Rosa, C.; Mortola, V. B. *Microporous Mesoporous Mater.* **2019**, *275* (September 2018), 244–252.
- (41) Zhou, W.; Shi, S.; Wang, Y.; Zhang, L.; Wang, Y.; Zhang, G.; Min, X.; Cheng, K.; Zhang, Q.; Kang, J.; Wang, Y. *ChemCatChem* **2019**.
- (42) Wei, J.; Ge, Q.; Yao, R.; Wen, Z.; Fang, C.; Guo, L.; Xu, H.; Sun, J. *Nat. Commun.* **2017**.
- (43) Aresta, M.; Dibenedetto, A.; Angelini, A. *J. CO₂ Util.* **2013**, *3–4*, 65–73.
- (44) Wang, Y.; Tan, L.; Tan, M.; Zhang, P.; Fang, Y.; Yoneyama, Y.; Yang, G.; Tsubaki, N. *ACS Catal.* **2019**, *9* (2), 895–901.
- (45) Kar, S.; Kothandaraman, J.; Goeppert, A.; Prakash, G. K. S. *J. CO₂ Util.* **2018**, *23* (October 2017), 212–218.
- (46) Adebajo, M. O.; Howe, R. F.; Long, M. A. *Catal. Today* **2000**, *63* (2–4), 471–478.

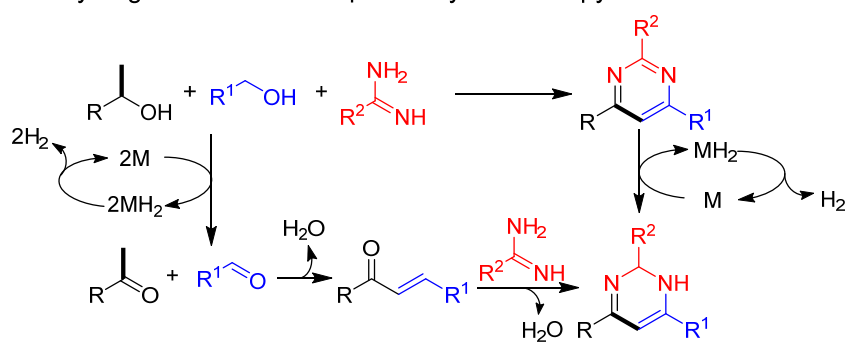
Chapter 2

Acceptorless Dehydrogenative Synthesis of Pyrimidine from Alcohols and Amidines Catalyzed by Supported Platinum Nanoparticles

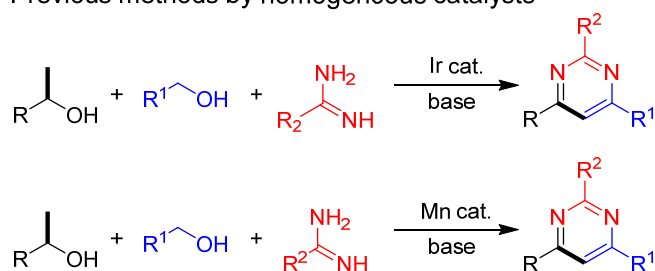
2.1 Introduction

Heterogeneous catalysts that promote one-pot reactions leading to value-added chemicals have attracted much attention.^{1,2} Among various types of organic transformations that fall in this category, H₂ evolving, acceptorless dehydrogenation (AD) reactions have been developed to synthesize various types of organic compounds.³ AD reactions have advantages not shared by traditional reactions employing stoichiometric amounts of inorganic substances or O₂ as oxidants, because they do not require the use of oxidants or sacrificial hydrogen acceptors.⁴⁻⁶ As a result, AD reactions do not generate stoichiometric amounts of waste.⁷ Gaseous H₂ generated in these processes is also valuable and can potentially be utilized as an energy source. Because homogeneous catalysts normally suffer from product separation and catalysts recycling issues, their heterogeneous counterparts are typically better suited for AD reactions.^{3,8} However, the development of heterogeneous catalysts for reactions that produce value-added chemicals is challenging because of the empirical approaches that are used in their development.⁹ Also, the complexity of surface reactions makes predicting catalyst performance a formidable task.¹⁰ Consequently, an important target in the development of environmentally friendly, atom-efficient AD reactions is the design of heterogeneous catalysts showing high activities, stabilities, and recyclability in the absence of hydrogen acceptors. Selective catalytic transformation of alcohols, which are readily available and sustainable substrates, to fine chemicals is a growing area of interest in catalysis, organic synthesis, and green sustainable chemistry.^{5,11-18} One representative example of the transformation of alcohols to fine chemicals is the catalytic one-pot synthesis of nitrogen-containing heterocycles (indoles,¹⁹⁻²¹ quinolines,^{22,23} pyrroles,²⁴⁻³² pyridines,³³⁻³⁶ pyrimidines,³⁷⁻³⁹ and quinazolines⁴⁰), which have broad applications as pharmaceutical and flavoring agents, agrochemicals, and other functional chemicals.^{41,42} The methods are based on AD reactions of alcohols that initially form carbonyl compounds, which are then transformed to products through multiple condensation/dehydrogenation reactions occurring

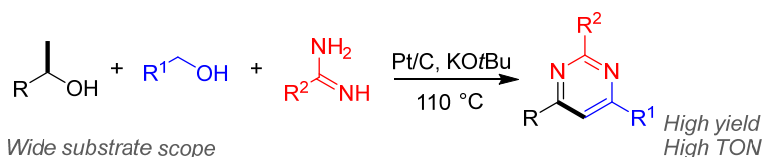
Dehydrogenative three component synthesis of pyrimidines



Previous methods by homogeneous catalysts



This work: reusable heterogeneous catalyst with high TON



Scheme 1. Pyrimidine synthesis using AD reactions

in the same vessel. A recent advance made in this area is the synthesis of 2,4,6-trisubstituted-pyrimidines from primary and secondary alcohols, along with amidines using homogeneous transition metal catalysts with a basic additive (KOtBu). Following the first report by Kempe et al. describing the use of a homogeneous Ir catalyst to promote this process,³⁷ Kirchner et al.³⁸ and Kempe et al.³⁹ individually developed new methods using less expensive Mn complexes as homogeneous catalysts. These catalytic methods for the preparation of 2,4,6-trisubstituted-pyrimidines are more atom-efficient and sustainable than their conventional counterparts, exemplified by reactions of amidines with α,β -unsaturated ketones,⁴³ α,α -dibromo oxime ethers with Grignard reagents,⁴⁴ alkynes, and nitriles using TfOH,⁴⁵ and the cascade synthesis of pyrimidines from propargylic alcohols and amidines using the transition metal catalysts BaMnO₄.⁴⁶ Although the catalytic method for synthesis of pyrimidines from alcohols and amidines is attractive, it suffers from low turnover number (TON) and difficulties with catalyst/product separation and catalyst recycling.^{37–39} Consequently, the development of a highly efficient heterogeneous catalyst for this reaction,

which has a wide scope, could overcome these problems. To date, however, only homogeneous catalysts have been used to promote this process. Our group recently reported a series of studies of AD reactions and acceptorless dehydrogenative coupling (ADC) reactions of alcohols that are promoted by heterogeneous carbon-supported Pt catalysts (Pt/C).^{21,32,40,47-49} This approach has advantages associated with the use of a recyclable heterogeneous catalyst and the facility of catalyst preparation. It is anticipated that this catalytic system would find applications to other challenging reactions that produce value-added chemicals in a one-pot manner. In studies described below, targeted at uncovering these applications, we developed a new heterogeneous catalytic system to promote AD reactions that form 2,4,6-trisubstitutedpyrimidines from diverse combinations of primary and secondary alcohols, along with amidines. The Pt/C catalyst developed for these processes has reusability and displays a higher turnover number (TON) than previously used homogeneous catalysts.³⁷⁻³⁹ In addition, the results of fundamental studies have led to elucidate a plausible mechanism for the process and to an understanding of factors that affect the catalytic activities of various metal nanoparticle catalysts.

2.2 Experimental

2.2.1 General

Commercially available organic and inorganic compounds, except for the amidine-hydrochlorides, (from Tokyo Chemical Industry, Wako Pure Chemical Industries, and Sigma-Aldrich, Kishida Chemical, or Mitsuwa Chemicals) were used without purification. Amidines were extracted twice from commercially available amidine-hydrochlorides (0.1 mol) using 0.33 mol KOH, 70 mL H₂O, and 50 mL CH₂Cl₂, and dried using a rotary evaporator before use in reactions. Benzyl- α,α -d₂ alcohol (BzCD₂OH, 99.5 atom %D) and 1-phenylethan- 1-d₁-ol (C₆H₅CD(OH)CH₃, 98 atom %D) were obtained from Sigma-Aldrich. GC (Shimadzu GC-14B and GC-2014), and GCMS (Shimadzu GCMS-QP2010) analyses were performed with an Ultra ALLOY capillary column UA+-1 (Frontier Laboratories Ltd.) using He or N₂ as the carrier gas. ¹H and ¹³C NMR measurements were performed with JEOLCX 600 operating at 600.17 and 150.92 MHz, respectively. Tetramethylsilane was used as the internal standard.

2.2.2 Catalyst preparation

Carbon was obtained commercially from Kishida Chemical. SiO₂ (Q-10) was supplied by Fuji Silysia Chemical Ltd. CeO₂ (JRC-CEO3), TiO₂ (JRC-TIO-4), MgO (JRC-MGO-3), and

H⁺-exchanged β zeolite (H β , SiO₂/ Al₂O₃ = 25 \pm 5, JRC-Z-HB25) were obtained from the Catalysis Society of Japan. ZrO₂ was synthesized by hydrolysis of zirconium oxynitrate 2-hydrate in an aqueous solution of NH₄OH, followed by filtration, washing with distilled water, drying at 100 °C for 12 h, and finally calcination at 500 °C for 3 h. γ -Al₂O₃ was prepared by calcining γ -AlOOH (Catapal B Alumina, Sasol) at 900 °C for 3 h. Nb₂O₅ was prepared by calcining Nb₂O₅·nH₂O (Companhia Brasileira de Metallurgia e Mineração (CBMM)) at 500 °C for 3 h. The Pt/C precursor was prepared by the impregnation method as follows. A mixture of carbon (10 g) and an aqueous HNO₃ solution of Pt(NH₃)₂(NO₃)₂ containing 4.96 wt % of Pt (10.62 g) and 50 mL of ion-exchanged water was added to a round-bottom flask (500 mL). The mixture was stirred for 15 min at room temperature (200 rpm). The mixture was evaporated to dryness at 50 °C. This was followed by drying at 90 °C under ambient pressure for 12 h. Prior to each experiment, a Pt/C catalyst (5 wt % Pt loading) was prepared by reducing the precursor in a Pyrex tube under a H₂ flow (20 cm³ min⁻¹) at 300 °C for 0.5 h. Other supported Pt catalysts (5 wt % Pt loadings) were prepared in the same manner. In addition, M/C (M = Rh, Ir, Ru, Pd, Re, Cu, Ni, Ag) catalysts were prepared in a similar method using aqueous HNO₃ solutions of Rh(NO₃)₃ or Pd(NH₃)₂(NO₃)₂ or aqueous solutions of metal nitrates (for Ni, Cu), IrCl₃·nH₂O, RuCl₃, or NH₄ReO₄. Metal loadings were adjusted to 5 wt %. Platinum oxides-loaded carbon (PtO_x/C) was prepared by calcining the Pt(NH₃)₂(NO₃)₂- loaded carbon at 300 °C for 0.5 h in air.

2.2.3 Catalyst characterization

X-ray diffraction (XRD; Rigaku Miniflex) measurements were conducted using Cu K α radiation. N₂ adsorption measurements were carried out by using AUTOSORB 6AG (Yuasa Ionics Co.). The sizes of supported metal particles were estimated by using transmission electron microscopy (TEM) using a JEOL JEM-2100F TEM operated at 200 kV. CO adsorption experiments were carried out at room temperature by using BELCAT (MicrotracBEL). Prior to each CO adsorption experiment, a sample (0.1 g) was heated in a flow of 5% H₂/Ar (20 mL min⁻¹) at 300 °C for 10 min. Pt L₃-edge X-ray absorption near-edge structures (XANES) and extended X-ray absorption fine structures (EXAFS) were determined in a transmittance mode at the BL01B1 with a Si(111) double crystal monochromator in SPring-8 operated at 8 GeV (Proposal No. 2017B1279). The Pt/C catalyst following the recycle study in **Figure 1** was sealed in cells made of polyethylene under N₂, and then the spectrum was measured at room temperature. The EXAFS analysis was carried out using the REX ver. 2.5 program (RIGAKU). The parameters for Pt–O and Pt–Pt shells were provided by

the FEFF6.

2.2.4 Catalytic test

Pt/C (39 mg; 1 mol % Pt with respect to benzamidine 3a) was used as the standard catalyst. After reduction, the catalyst was placed in a closed glass tube sealed with a septum inlet and cooled to room temperature under H₂. Toluene (2 mL) was injected through the septum inlet into the glass tube containing the prereduced catalyst. Next, the septum was removed, and secondary alcohol 1 (1.25 mmol), primary alcohol 2, amidine 3 (1.0 mmol), KO^tBu (1.5 mmol), *n*-dodecane (0.25 mmol), and a magnetic stirrer bar were added to the tube followed by filling N₂ through the septum inlet. Then, the resulting mixture was magnetically stirred (400 rpm) under reflux conditions. For the standard catalyst screening reactions of 1-phenylethanol, benzyl alcohol, and benzamidine (Table 1), reaction optimizations (Table 2), kinetic studies, and control reactions, the conversions and yields of products were determined by using GC with *n*-dodecane as the internal standard. GC-sensitivities were estimated using isolated products or commercial compounds. In substrate scope studies (Schemes 1–4), products were isolated by using column chromatography on silica gel 60 (spherical, 40–100 μm, Kanto Chemical Co. Ltd.) using hexane/ethyl acetate (9:1, v/v) as the eluent, and yields of the isolated products were determined. Products were identified by using ¹H and ¹³C NMR spectroscopy in combination with GCMS, in which the mass spectrometer was equipped with the same column as that used for GC analyses. Analysis of the gaseous product (H₂) was carried out by using mass spectrometry (BELMASS).

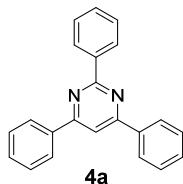
Recycling experiments were performed with the following procedure. After each catalytic run, 2-propanol (3 mL) was added to the mixture. The catalyst was separated by using centrifugation and washed with water (3 mL) and acetone (6 mL). Subsequently, the catalyst was dried at 110 °C for 3 h and reduced at 300 °C for 0.5 h under an atmosphere of H₂. Subsequently, the recovered Pt/C catalyst was placed in the reactor with a mixture of the substrate and KO^tBu. Note that the initial rates were obtained on the basis of product yields after a reaction time of 1 h where the product yields are below 30%.

2.2.5 NMR and GC-MS analysis

¹H and ¹³C NMR spectra of the products were assigned and reproduced to the corresponding literature. ¹H and ¹³C NMR spectra were recorded using at ambient temperature on JEOL-ECX 600 operating at 600.17 MHz and 150.92 MHz and JEOL-ECX 400-2 operating at 399.78 MHz and 100.52 MHz respectively with tetramethylsilane as an internal standard.

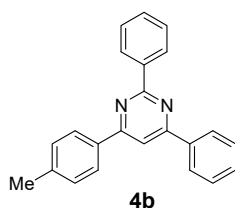
Abbreviations used in the NMR experiments: s, singlet; d, doublet; t, triplet; q, quartet; m, multiplet, br, broad singlet. GC-MS spectra were taken by SHIMADZU QP2010.

2,4,6-Triphenylpyrimidine:¹



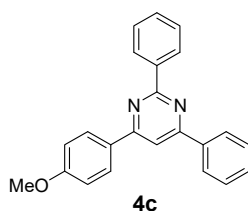
¹H NMR (600.17 MHz, CDCl₃, TMS): δ 8.73 (d, *J* = 7.56 Hz, 2H), 8.30 (d, *J* = 10.32 Hz, 4H), 8.02 (s, 1H), 7.61-7.50 (m, 9H), ¹³C NMR (150.92 MHz, CDCl₃): δ 164.75 (C×2), 164.50, 138.13, 137.54 (C×2), 130.77 (C×2), 130.62 (C×3), 128.91 (C×4), 128.45 (C×2), 127.27 (C×2), 125.57 (C×2), 110.30; GC-MS *m/e* 308.15.

2,4-Diphenyl-6-*p*-tolyl-pyrimidine:²



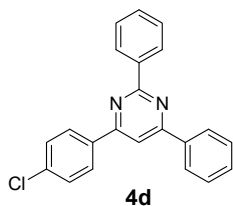
¹H NMR (600.17 MHz, CDCl₃, TMS): δ 8.72 (d, *J* = 6.84 Hz, 2H), 8.26 (d, *J* = 6.90 Hz, 2H), 8.17 (d, *J* = 7.50 Hz, 2H), 7.94 (s, 1H), 7.55-7.50 (m, 6H), 7.33 (d, *J* = 8.22 Hz, 2H), 2.43 (s, 3H), ¹³C NMR (150.92 MHz, CDCl₃): δ 164.59, 164.52, 164.35, 141.09, 138.22, 137.58 (C×2), 134.64, 130.64, 130.52, 129.59 (C×2), 128.83 (C×2), 128.42, 128.38(C×2), 127.22 (C×2), 127.13 (C×2), 109.87, 21.45; GC-MS *m/e* 322.15.

4-(4-Methoxyphenyl)-2,6-diphenylpyrimidine:³



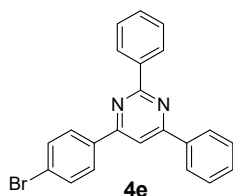
¹H NMR (600.17 MHz, CDCl₃, TMS): δ 8.72 (d, *J* = 7.56 Hz, 2H), 8.29-8.15 (m, 4H), 7.94 (s, 1H), 7.56-7.49 (m, 6H), 7.05 (d, *J* = 8.22 Hz, 2H), 3.89 (s, 3H), ¹³C NMR (150.92 MHz, CDCl₃): δ 164.44, 164.31, 164.16, 161.88, 138.25, 137.67, 130.61, 130.50, 129.91 (C×2), 128.84 (C×2), 128.76 (C×3), 128.38 (C×2), 127.21 (C×2), 114.21 (C×2), 109.39, 55.41; GC-MS *m/e* 338.15.

4-(4-Chloro-phenyl)-2,6-diphenyl-pyrimidine:¹



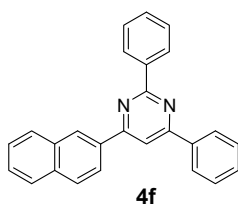
¹H NMR (600.17 MHz, CDCl₃, TMS): 8.70 (d, *J* = 11.04 Hz, 2H), 8.31-8.22 (m, 4H), 7.97 (s, 1H), 7.59-7.52 (m, 8H). ¹³C NMR (150.92 MHz, CDCl₃): 164.97, 164.54, 163.49, 137.92, 137.33, 136.93, 130.89, 130.75 (C×2), 129.13 (C×2), 128.93 (C×2), 128.54 (C×2), 128.46 (C×2), 128.43 (C×2), 127.26 (C×2), 109.96.; GC-MS m/e 342.10.

4-(4-Bromophenyl)-2,6-diphenylpyrimidine:⁴



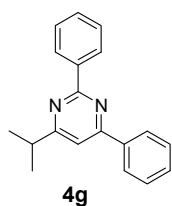
¹H NMR (600.17 MHz, CDCl₃, TMS): 8.70 (dd, *J* = 7.52 Hz, 2.70, 2H), 8.29-8.24 (m, 2H), 8.15 (d, *J* = 8.94 Hz, 2H), 7.94 (s, 1H), 7.68 (d, *J* = 7.56 Hz, 2H), 7.57-7.52 (m, 6H). ¹³C NMR (150.92 MHz, CDCl₃): 164.93, 164.53, 163.51, 137.89, 137.29, 136.35, 132.07 (C×2), 130.88, 130.74, 128.91 (C×2), 128.75 (C×2), 128.45 (C×2), 128.43 (C×2), 127.25 (C×2), 125.38, 109.87; GC-MS m/e 386.05.

4-Naphthalen-2-yl-2,6-diphenyl-pyrimidine:¹



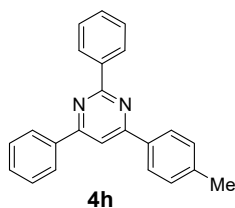
¹H NMR (600.17 MHz, CDCl₃, TMS): δ 8.78-8.74 (m, 3H), 8.37 (m, 3H), 8.15 (s, 1H), 8.04-7.89 (m, 3H), 7.60-7.51 (m, 8H), ¹³C NMR (150.92 MHz, CDCl₃): δ 164.80, 164.64, 164.56, 138.19, 137.57 (C×2), 134.84 (C×2), 134.59, 133.29, 130.79, 130.66, 129.02, 128.93 (C×2), 128.67, 128.51 (C×2), 128.47 (C×2), 127.78, 127.39 (C×2), 127.31, 126.57, 110.51; GC-MS m/e 358.15.

4-Isopropyl-2,6-diphenyl-pyrimidine:⁵



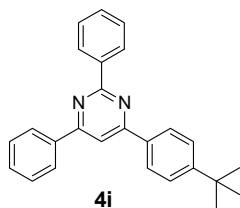
¹H NMR (600.17 MHz, CDCl₃, TMS): δ 8.56-8.52 (m, 2H), 8.13-8.09 (m, 2H), 7.43-7.38 (m, 6H), 7.35 (s, 1H), 3.06-2.99 (m, 1H), 1.32 (d, *J* = 6.84 Hz, 6H)¹³C NMR (150.92 MHz, CDCl₃): δ 176.26, 164.00, 163.90, 138.32, 137.58, 132.46, 130.48 (C×2), 130.34, 128.78 (C×2), 128.34 (C×2), 127.16 (C×2), 111.51, 36.30, 21.90 (C×2); GC-MS m/e 274.15.

2,4-Diphenyl-6-p-tolyl-pyrimidine:¹



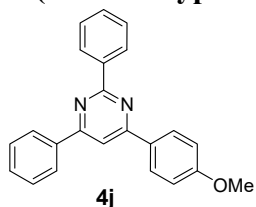
¹H NMR (600.17 MHz, CDCl₃, TMS): δ 8.71 (d, *J* = 8.22 Hz, 2H), 8.27 (d, *J* = 6.18 Hz, 2H), 8.18 (d, *J* = 8.22 Hz, 2H), 7.96 (s, 1H), 7.58-7.49 (m, 6H), 7.34 (d, *J* = 7.50 Hz, 2H), 2.44 (s, 3H), ¹³C NMR (150.92 MHz, CDCl₃): δ 164.62, 164.56, 164.37, 141.11, 138.22, 137.60 (C×2), 134.67, 130.65, 130.53, 129.60 (C×2), 128.85 (C×2), 128.43 (C×2), 128.39, 127.23 (C×2), 127.14 (C×2), 109.89, 21.46; GC-MS m/e 322.15.

4-(4-tert-Butyl-phenyl)-2,6-diphenyl-pyrimidine:³



¹H NMR (600.17 MHz, CDCl₃, TMS): δ 8.74-8.69 (m, 2H), 8.32-8.27 (m, 2H), 8.24-8.19 (m, 2H), 8.00 (s, 1H), 7.61-7.50 (m, 8H), 1.39 (s, 6H), 1.31 (s, 3H), ¹³C NMR (150.92 MHz, CDCl₃): δ 164.73, 164.57, 154.27, 138.25, 137.64, 134.77, 130.68, 130.55, 128.89 (C×2), 128.43 (C×2), 128.40 (C×2), 128.06 (C×2), 127.25 (C×2), 127.04 (C×2), 125.88 (C×2), 110.09, 34.89, 31.24 (C×2); GC-MS m/e 364.20.

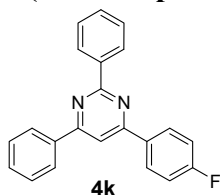
4-(4-Methoxyphenyl)-2,6-diphenylpyrimidine:¹



¹H NMR (600.17 MHz, CDCl₃, TMS): δ 8.71 (d, *J* = 8.22 Hz, 2H), 8.28-8.17 (m, 4H), 7.95 (s, 1H), 7.56-7.51 (m, 6H), 7.07 (d, *J* = 8.94 Hz, 2H), 3.90 (s, 3H), ¹³C NMR (150.92 MHz, CDCl₃): δ 164.48, 164.35, 164.19, 161.90, 138.28, 137.71, 130.63 (C×2), 130.52, 129.94

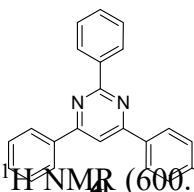
(C×2), 128.86, 128.78, 128.41 (C×2), 128.38 (C×2), 127.23(C×2), 114.23 (C×2), 109.42, 55.43; GC-MS m/e 338.15.

4-(4-Fluorophenyl)-2,6-diphenylpyrimidine:¹



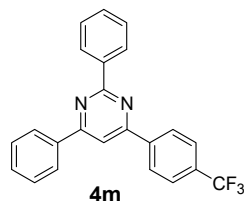
¹H NMR (600.17 MHz, CDCl₃, TMS): 8.70 (d, *J* = 7.50 Hz, 2H), 8.30-8.27 (m, 4H), 7.97(s, 1H), 7.57-7.52 (m, 6H), 7.26-7.23 (m, 2H). ¹³C NMR (150.92 MHz, CDCl₃): 164.96, 164.65, 164.62 (d, *J*_{CF} = 262.60), 163.73, 138.10, 137.60, 133.74 (d, *J*_{CF} = 2.82 Hz), 130.95, 130.82, 129.43 (d, *J*_{CF} = 8.66 Hz), 129.04 (C×4), 128.57 (C×2), 127.37 (C×4), 116.21 (d, *J* = 59.24 Hz), 110.04; GC-MS m/e 326.10.

4-(4-Chloro-phenyl)-2,6-diphenyl-pyrimidine:¹



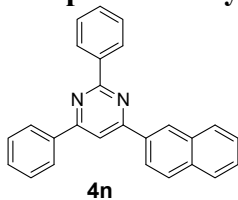
¹H NMR (600.17 MHz, CDCl₃, TMS): δ 8.75-8.71 (m, 2H), 8.31-8.28 (m, 4H), 8.02 (s, 1H), 7.59-7.51 (m, 8H), ¹³C NMR (150.92 MHz, CDCl₃): δ 164.75 (C×2), 164.49, 138.13 (C×2), 137.54 (C×3), 130.77 (C×2), 130.62, 128.91 (C×4), 128.44 (C×2), 127.27 (C×4), 110.30; GC-MS m/e 342.10.

2,4-Diphenyl-6-(4-trifluoromethyl-phenyl)-pyrimidine:



GC-MS m/e 376.10.

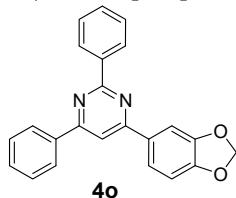
4-Naphthalen-2-yl-2,6-diphenyl-pyrimidine:²



¹H NMR (600.17 MHz, CDCl₃, TMS): δ 8.78 (d, *J* = 8.94 Hz, 3H), 8.41 (d, *J* = 9.60 Hz, 1H), 8.34 (d, *J* = 10.26 Hz, 2H), 8.16 (s, 1H), 8.06-8.00 (m, 2H), 7.94-7.90 (m, 1H), 7.60-7.53 (m,

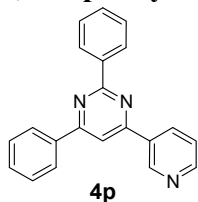
8H), ^{13}C NMR (150.92 MHz, CDCl_3): δ 164.79, 164.66, 164.56, 138.19, 137.57 (C \times 2), 134.82 (C \times 2), 134.59, 133.29, 130.80, 130.66, 129.02, 128.93 (C \times 2), 128.67, 128.51 (C \times 2), 128.47 (C \times 2), 127.79, 127.32 (C \times 2), 126.58, 124.24, 110.51; GC-MS m/e 358.15.

4-(Benzo [1,3] dioxol-5-yl)-2,6-diphenylpyrimidine:¹



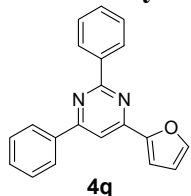
^1H NMR (600.17 MHz, CDCl_3 , TMS): δ : 8.70-8.66 (m, 2H), 8.29-8.22 (m, 2H), 7.92-7.88 (m, 2H), 7.84-7.82 (m, 1H), 7.59-7.51 (m, 6H), 6.98-6.94 (m, 1H), 6.06 (d, $J = 2.76\text{Hz}$, 1H). $^{13}\text{C}\{^1\text{H}\}$ NMR (δ , d_6 CD_2Cl_2 , 20°C): 164.55, 164.29, 163.95, 149.95, 148.44, 138.13, 137.57, 131.80, 130.68, 130.58, 128.86 (C \times 2), 128.40 (C \times 2), 127.22 (C \times 4), 121.80, 109.55, 108.52, 107.46, 101.60; GC-MS m/e 352.10.

2,4-Diphenyl-6-pyridin-3-yl-pyrimidine:¹



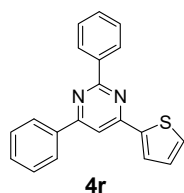
^1H NMR (600.17 MHz, CDCl_3 , TMS): δ 8.77-8.71 (m, 5H), 8.38 (d, $J = 7.56\text{ Hz}$, 2H), 7.92-7.89 (m, 1H), 7.57-7.51 (m, 6H), 7.45-7.41 (m, 1H), ^{13}C NMR (150.92 MHz, CDCl_3): δ 164.91, 163.99, 163.35, 154.43, 149.17, 137.82, 137.12, 136.87, 130.61, 130.42, 128.60 (C \times 2), 128.26 (C \times 2), 128.17 (C \times 2), 127.21 (C \times 2), 125.05, 121.70, 110.34; GC-MS m/e 309.15.

4-Furan-2-yl-2,6-diphenyl-pyrimidine:¹



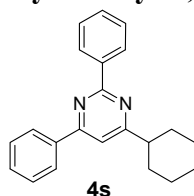
^1H NMR (600.17 MHz, CDCl_3 , TMS): δ 8.65 (dd, $J = 7.56, 1.86\text{ Hz}$, 2H), 8.29-8.21 (m, 2H), 7.94 (s, 1H), 7.64 (s, 1H), 7.56-7.50 (m, 6H), 7.44 (d, $J = 3.42\text{ Hz}$, 1H), 6.64-6.61 (m, 1H), ^{13}C NMR (150.92 MHz, CDCl_3): δ 164.59, 164.43, 156.30, 152.69, 144.74, 137.91, 137.30, 130.83, 130.62, 128.85 (C \times 2), 128.40 (C \times 2), 128.36 (C \times 2), 127.22 (C \times 2), 112.55, 112.05, 107.99; GC-MS m/e 298.10.

2,4-Diphenyl-6-thiophen-2-yl-pyrimidine:¹



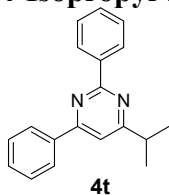
¹H NMR (600.17 MHz, CDCl₃, TMS): δ 8.59 (dd, *J* = 10.32 Hz, 8.22 Hz, 2H), 8.17 (dd, *J* = 10.32 Hz, 11.04 Hz, 2H), 7.82 (dd, *J* = 2.76 Hz, 3.42 Hz, 1H), 7.75 (s, 1H), 7.48-7.39 (m, 7H), 7.11 (t, *J* = 8.22 Hz, 1H), ¹³C NMR (150.92 MHz, CDCl₃): δ 164.52, 164.40, 159.65, 143.34, 137.72, 137.31, 130.80, 130.70, 129.76 (C×2), 128.87 (C×2), 128.41 (C×2), 128.28 (C×2), 127.21 (C×2), 127.02, 108.39; GC-MS *m/e* 314.10.

4-Cyclohexyl-2,6-diphenyl-pyrimidine:⁶



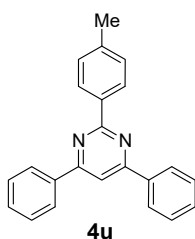
¹H NMR (600.17 MHz, CDCl₃, TMS): δ 8.61 (d, *J* = 7.56 Hz, 2H), 8.20 (d, *J* = 7.56 Hz, 2H), 7.50-7.45 (m, 6H), 7.44 (s, 1H), 2.81-2.72 (m, 1H), 2.05 (t, *J* = 10.29 Hz, 2H), 1.90 (d, *J* = 15.84 Hz, 2H), 1.79 (d, *J* = 13.02 Hz, 1H), 1.71-1.62 (m, 2H), 1.50-1.41 (m, 2H), 1.34-1.30 (m, 1H), ¹³C NMR (150.92 MHz, CDCl₃): δ 175.36, 164.00, 163.81, 138.38, 137.64, 130.46 (C×2), 130.30 (C×2), 128.78 (C×2), 128.33 (C×2), 127.16 (C×2), 111.85, 46.31, 32.17 (C×2), 26.32 (C×2), 26.01; GC-MS *m/e* 314.20.

4-Isopropyl-2,6-diphenyl-pyrimidine:⁵



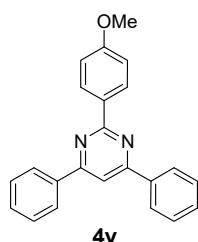
¹H NMR (600.17 MHz, CDCl₃, TMS): δ 8.66-8.61 (m, 2H), 8.25-8.19 (m, 2H), 7.55-7.48 (m, 6H), 7.46 (s, 1H), 3.18-3.09 (m, 1H), 1.42 (d, *J* = 8.22 Hz, 6H) ¹³C NMR (150.92 MHz, CDCl₃): δ 176.29, 164.03, 163.92, 138.34, 137.62, 130.51 (C×2), 130.35 (C×2), 128.80 (C×2), 128.36 (C×2), 127.19 (C×2), 111.53, 36.33, 21.92 (C×2); GC-MS *m/e* 274.15.

4,6-Diphenyl-2-p-tolyl-pyrimidine:³



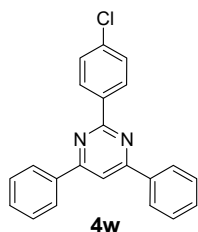
^1H NMR (600.17 MHz, CDCl_3 , TMS): δ 8.61 (d, $J = 8.22$ Hz, 2H), 8.28 (d, $J = 7.56$ Hz, 4H), 7.99 (s, 1H), 7.56-7.49 (m, 6H), 7.33 (d, $J = 8.28$ Hz, 2H), 2.45 (s, 3H), ^{13}C NMR (150.92 MHz, CDCl_3): δ 164.68 (C \times 2), 164.59, 140.83, 137.65 (C \times 2), 135.45, 130.70, 129.20 (C \times 4), 128.89, 128.41 (C \times 2), 127.99 (C \times 4), 127.27 (C \times 2), 110.06, 21.56; GC-MS m/e 322.15.

2-(4-Methoxyphenyl)-4,6-diphenylpyrimidine:⁶



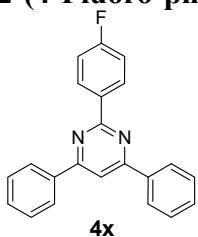
^1H NMR (600.17 MHz, CDCl_3 , TMS): δ 8.69 (d, $J = 8.22$ Hz, 2H), 8.28-8.21 (m, 4H), 7.93 (s, 1H), 7.56-7.51 (m, 6H), 7.04 (d, $J = 8.92$ Hz, 2H), 3.89 (s, 3H), ^{13}C NMR (150.92 MHz, CDCl_3): δ 164.58, 164.24 (C \times 2), 161.78, 137.65 (C \times 2), 130.86 (C \times 2), 130.64 (C \times 2), 130.07 (C \times 4), 128.84 (C \times 2), 127.21 (C \times 4), 113.70, 109.60, 55.41; GC-MS m/e 338.15.

2-(4-Chloro-phenyl)-4,6-diphenyl-pyrimidine:⁶



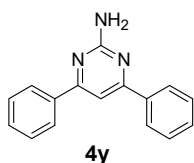
^1H NMR (600.17 MHz, CDCl_3 , TMS): δ 8.65 (d, $J = 8.28$ Hz, 2H), 8.25 (d, $J = 9.60$ Hz, 4H), 7.99 (s, 1H), 7.58-7.53 (m, 6H), 7.48 (d, $J = 7.56$ Hz, 2H), ^{13}C NMR (150.92 MHz, CDCl_3): δ 164.80 (C \times 2), 163.46, 137.31 (C \times 2), 136.77, 136.62, 130.86 (C \times 2), 129.79 (C \times 2), 128.93 (C \times 4), 128.61 (C \times 2), 127.24 (C \times 4), 110.41; GC-MS m/e 342.10.

2-(4-Fluoro-phenyl)-4,6-diphenyl-pyrimidine:³



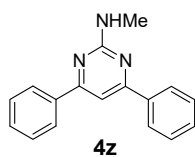
^1H NMR (600.17 MHz, CDCl_3 , TMS): δ 8.73-8.70 (m, 2H), 8.26-8.24 (m, 4H), 7.97 (s, 1H), 7.60-7.51 (m, 6H), 7.22-7.18 (m, 2H), ^{13}C NMR (150.92 MHz, CDCl_3): δ 164.80 (C \times 3), 163.51 (d, $J = 193.60$ Hz), 140.83, 137.31 (C \times 2), 136.77, 136.61 (d, $J = 24.14$ Hz), 130.87 (C \times 2), 129.79 (C \times 2), 128.93 (d, $J = 46.22$ Hz) (C \times 3), 128.62 (C \times 2), 127.24 (C \times 3), 110.42; GC-MS m/e 326.10.

4,6-Diphenyl-pyrimidin-2-ylamine:⁶



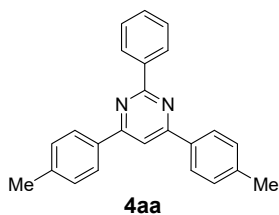
^1H NMR (600.17 MHz, CDCl_3 , TMS): δ 8.05-8.03 (m, 4H), 7.50-7.47 (m, 6H), 7.44 (s, 1H), 5.41 (br. s, 2H), ^{13}C NMR (150.92 MHz, CDCl_3): δ 166.21 (C \times 2), 163.64, 163.42, 137.73, 130.39 (C \times 2), 128.72 (C \times 4), 127.08 (C \times 4), 104.26; GC-MS m/e 247.10.

(4,6-Diphenyl-pyrimidin-2-yl)-methyl-amine:



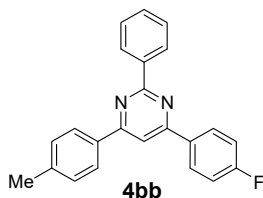
GC-MS m/e 261.15.

2-Phenyl-4,6-di-p-tolyl-pyrimidine:²



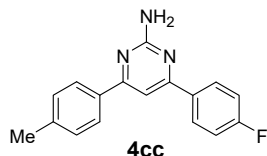
^1H NMR (600.17 MHz, CDCl_3 , TMS): δ 8.72-8.71 (m, 2H), 8.19 (d, $J = 8.28$ Hz, 4H), 7.95 (s, 1H), 7.54-7.49 (m, 3H), 7.35 (d, $J = 8.28$ Hz, 4H), 2.45 (s, 6H), ^{13}C NMR (150.92 MHz, CDCl_3): δ 164.50 (C \times 2), 164.24, 141.01, 138.32, 134.80 (C \times 2), 130.46, 129.59 (C \times 4), 128.42 (C \times 3), 128.37 (C \times 3), 127.14 (C \times 4), 109.56, 21.47; GC-MS m/e 336.15.

4-(4-Fluoro-phenyl)-2-phenyl-6-p-tolyl-pyrimidine:²



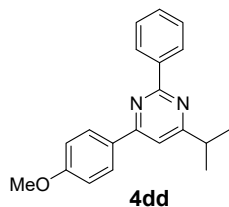
^1H NMR (600.17 MHz, CDCl_3 , TMS): δ 8.71-8.69 (m, 2H), 8.30-8.27 (m, 2H), 8.18 (d, $J = 10.32$ Hz, 2H), 7.93 (s, 1H), 7.55-7.51 (m, 3H), 7.35 (d, $J = 7.50$ Hz, 2H), 7.24-7.21 (m, 2H), 2.45 (s, 3H), ^{13}C NMR (150.92 MHz, CDCl_3): δ 165.44, 164.71, 164.36, 163.72, 163.46 (d, $J = 187.84$ Hz), 141.23, 138.09, 134.58, 133.63 (d, $J = 143.05$ Hz), 130.63 (C \times 2), 129.65 (C \times 2), 129.29 (d, $J = 8.67$ Hz) (C \times 2), 128.44 (C \times 2), 127.15 (C \times 2), 115.96, 115.82 (d, $J = 21.67$ Hz), 109.51, 21.49; GC-MS m/e 340.15.

4-(4-Fluoro-phenyl)-6-p-tolyl-pyrimidin-2-ylamine:⁷



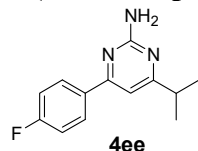
^1H NMR (600.17 MHz, CDCl_3 , TMS): δ 8.08-8.04 (m, 2H), 7.95 (d, $J = 8.28$ Hz, 2H), 7.40 (s, 1H), 7.30 (d, $J = 7.56$ Hz, 2H), 7.17 (t, $J = 8.22$ Hz, 2H), 5.16 (s, 2H), 2.42 (s, 3H), ^{13}C NMR (150.92 MHz, CDCl_3): δ 166.23, 164.87 (d, $J = 205.16$ Hz), 163.43, 140.86, 134.73, 133.92 (d, $J = 4.33$ Hz), 129.49 (C \times 2), 129.10 (d, $J = 11.55$ Hz, C \times 2), 129.02, 126.98 (C \times 2), 115.78 (d, $J = 21.67$ Hz), 115.64, 103.57, 21.42; GC-MS m/e 279.10.

4-Isopropyl-6-(4-methoxy-phenyl)-2-phenyl-pyrimidine:²



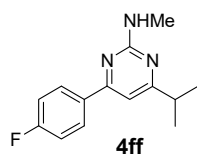
^1H NMR (600.17 MHz, CDCl_3 , TMS): δ 8.63-8.59 (m, 2H), 8.22-8.18 (m, 2H), 7.51-7.47 (m, 2H), 7.39 (s, 1H), 7.06-7.01 (m, 3H), 3.89 (s, 3H), 3.11-3.09 (m, 1H), 1.40 (d, $J = 6.84$ Hz, 6H), ^{13}C NMR (150.92 MHz, CDCl_3): δ 176.40, 163.88, 163.42, 161.67, 138.48, 130.24, 130.05, 128.65 (C \times 2), 128.33 (C \times 2), 128.31 (C \times 2), 114.13 (C \times 2), 110.58, 55.39, 36.30, 21.92 (C \times 2); GC-MS m/e 304.15.

4-(4-Fluoro-phenyl)-6-isopropyl-pyrimidin-2-ylamine:¹



^1H NMR (600.17 MHz, CDCl_3 , TMS): δ 8.00-7.96 (m, 2H), 7.16-7.11 (m, 2H), 6.87 (s, 1H), 5.25 (s, 2H), 2.89-2.82 (m, 1H), 1.29 (d, $J = 7.56$ Hz, 6H), ^{13}C NMR (150.92 MHz, CDCl_3): δ 177.72, 165.00, 164.39, 163.34 (d, $J=177.73$ Hz), 163.22, 133.88, 129.02, 128.97 (d, $J = 8.67$ Hz), 115.54 (d, $J = 21.6$ Hz), 104.21, 36.11, 21.71 (C \times 2); GC-MS m/e 231.10.

4-(4-Fluoro-phenyl)-6-isopropyl-pyrimidin-2-yl-methyl-amine:¹



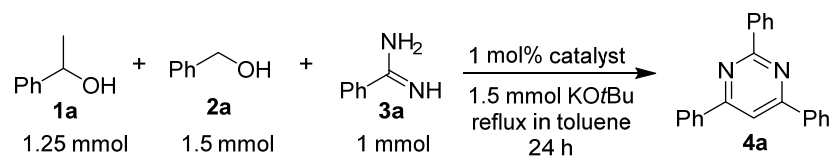
¹H NMR (400.17 MHz, CDCl₃, TMS): δ 8.09-7.97 (m, 2H), 7.18-7.08 (m, 2H), 6.80 (s, 1H), 5.26 (br, s, 1H), 3.05 (d, *J* = 4.55 Hz, 3H), 2.88-2.79 (m, 1H), 1.28 (d, *J* = 8.23 Hz, 6H), ¹³C NMR (100.52 MHz, CDCl₃): δ 177.71, 165.31 (d, *J* = 173.48 Hz), 163.59, 163.20, 162.83, 134.22, 128.94 (d, *J* = 7.67 Hz), 128.86, 115.35 (d, *J* = 21.09 Hz), 102.82, 36.13, 28.35, 21.71 (C×2); GC-MS *m/e* 245.15.

2.3- Results and discussion

Optimization of the Catalyst and Reaction Conditions

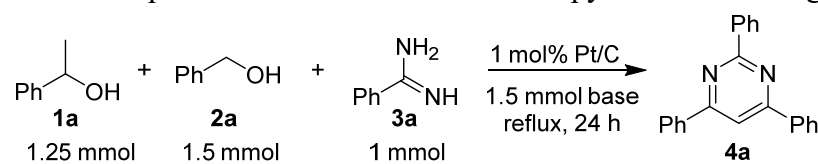
In the initial phase of studies aimed at developing a heterogeneous catalytic system to promote 2,4,6-trisubstituted-pyrimidine forming AD reactions, catalyst screening was performed using the reaction of 1-phenylethanol (**1a**, 1.25 mmol), benzyl alcohol (**2a**, 1.5 mmol) and benzamidine (**3a**, 1.0 mmol) and KO^tBu (1.5 mmol) in refluxing toluene for 24 h. **Table 1** shows the yields of 2,4,6-triphenylpyrimidine (**4a**), based on benzamidine, for various AD reactions promoted by Pt nanoparticles on different support materials and various metal nanoparticles on carbon containing 0.01 mmol (1 mol%) of the active metal. Under these conditions, reactions do not take place in the absence of the catalyst (entry 1). The results show that platinum oxides-loaded carbon (PtO_x/C, entry 2) does not promote the reaction. In contrast, metallic Pt-loaded carbon (Pt/C), reduced with H₂ at 300 °C, catalyzes a reaction that occurs in 95% yield (entry 3), while use of pre-reduced, air-exposed Pt/C (Pt/C-air in entry 4) leads to a lower yield (57%). The yields of AD reactions promoted by Pt/C are higher than those catalyzed by Pt-loaded metal oxides (ZrO₂, Al₂O₃, CeO₂, TiO₂, SiO₂, MgO, H-β zeolite, Nb₂O₅, entries 5-12). Moreover, the Pt/C catalyst promotes a higher yielding reaction than do other transition metal nanoparticles supported on carbon (Ir/C, Ni/C, Pd/C, Rh/C, Ru/C, Re/C, Cu/C, and Ag/C) shown in entries 13-20.

Table 1. Catalyst screening for synthesis of pyrimidine **4a** from 1-phenylethanol **1a**, benzyl alcohol **2a** and benzamidine **3a**.



Entry	Catalyst	Yield (%) ^a
1	None	0
2	PtO _x /C	0
3	Pt/C	95
4	Pt/C-air	57
5	Pt/ZrO ₂	70
6	Pt/Al ₂ O ₃	67
7	Pt/CeO ₂	65
8	Pt/TiO ₂	63
9	Pt/SiO ₂	61
10	Pt/MgO	53
11	Pt/Hβ	43
12	Pt/Nb ₂ O ₅	38
13	Ir/C	45
14	Ni/C	36
15	Pd/C	34
16	Rh/C	31
17	Ru/C	26
18	Re/C	19
19	Cu/C	15
20	Ag/C	11

^a GC yield.

Table 2. Optimization of the conditions for pyrimidine forming reaction of **1a**, **2a** and **3a**.

Entry	Base	Solvent	Yield (%) ^a
1	KOtBu	toluene	95
2	KOtBu	<i>n</i> -octane	66
3	KOtBu	<i>o</i> -xylene	69
4	KOtBu	mesitylene	71
5	KOtBu	<i>tert</i> -amyl alcohol	78
6	NaOtBu	toluene	65
7	NaOH	toluene	70
8	KOH	toluene	61
9	none	toluene	0

^a GC yield.

Using the most effective catalyst, Pt/C, we conducted a study targeted at finding optimal conditions for the reaction of **1a**, **2a**, and **3a** (**Table 2**). Inspection of the results arising from reactions promoted by Pt/C and KOtBu in various solvents at reflux (entries 1-5) showed that reaction in toluene (entry 1) forms **4a** in the highest yield. A survey of reactions in refluxing toluene with different basic additives (entries 1, 6-8) showed that KOtBu (entry 1) leads to a higher yield than with the other basic additives (NaOtBu, NaOH, KOH). It was also demonstrated that the reaction hardly proceeds in the absence of a base (entry 9). Consequently, we adopted refluxing toluene using Pt/C and KOtBu as the standard conditions for reaction of **1a**, **2a**, and **3a**.

Catalytic Properties and Scope of the Reaction

The heterogeneous nature and reusability of the catalytic system developed for the AD reactions were confirmed by the results of the recycling test shown in **Figure 1**. After carrying out the standard AD reaction for 24 h, the catalyst was separated from the mixture by using filtration, dried at 110 °C for 3 h and then reduced in a H₂ atmosphere at 300 °C for 0.5 h. The recovered catalyst was found to promote an AD reaction to form **4a** in high yields (88-95%) that gradually decrease over five cycles. In a separate series of experiments, the

initial rates of **4a** formation were determined for each cycle. The results (gray bars in **Figure 1**) show that the initial rates also gradually decrease with increasing number of cycles.

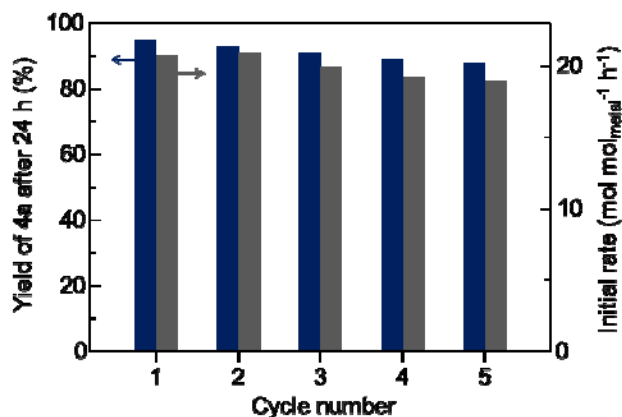


Figure 1. Catalyst reuse for the synthesis of **4a** from **1a**, **2a**, and **3a** promoted by Pt/C and KO^tBu under the standard conditions shown in Table 2 (entry 1): (navy bars) **4a** yields after 24 h and (gray bars) initial rates of **4a** formation.

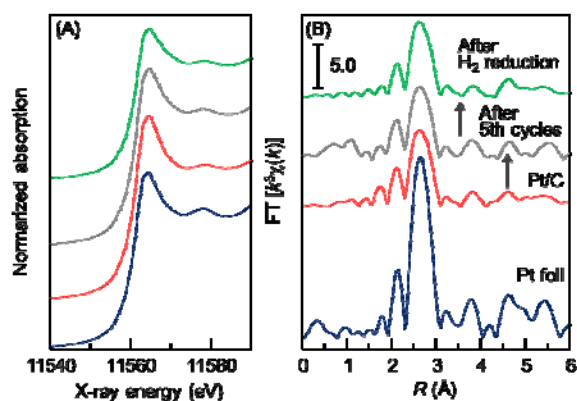


Figure 2. Pt L₃-edge (A) XANES spectra and (B) EXAFS Fourier transforms of Pt/C before and after the catalyst recycling.

To assess possible reasons for the gradual catalyst deactivation in the recycling processes described above, structural characterization was carried out on the recovered Pt/C catalyst following the 5th cycle of reactions by using X-ray absorption near-edge structural (XANES) and extended X-ray absorption fine structure (EXAFS) analysis **Figure 2**, and TEM analysis (**Figure 3**).

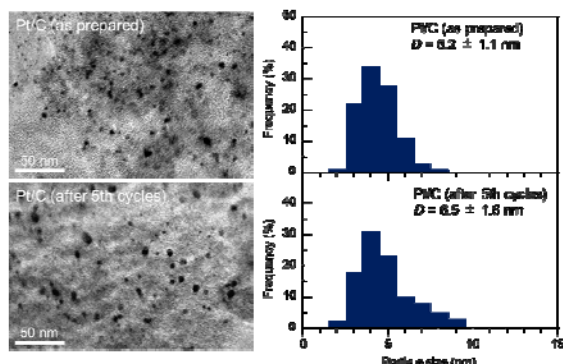


Figure 3. Typical TEM images and Pt particle size distributions of Pt/C before and after recycling.

The results of EXAFS curve fitting analysis are shown in **Table 3**. Note, characterization of freshly prepared Pt/C was reported in our previous study.⁴⁹ The XANES feature of the recycled Pt/C catalyst is similar to those of Pt foil and fresh Pt/C. This finding indicates that the oxidation states of Pt in the Pt/C catalyst are the same before and after recycling, and that the Pt species are metallic. The EXAFS of Pt/C after the fifth catalytic cycle consists of 8.3 Pt–Pt bonds at 2.74 Å, a distance that is close to that of Pt foil (2.76 Å). This observation shows that Pt in the catalyst after the fifth cycle exist in the metallic state, which is consistent with the XANES result. However, the particle size distribution, estimated by using TEM analysis (**Figure 3**), shows that the fraction of Pt metal particles with diameters above 7 nm increases during recycling. The volume-area mean diameter (D)⁵⁰ of Pt particles in the recycled Pt/C (6.5 ± 1.6 nm) is larger than that in fresh Pt/C (5.2 ± 1.1 nm), an increase that is likely responsible for the slight decrease in the catalytic activity seen after the 5th cycle. The coordination number for the catalyst after recycling was found to be 10.1, and this result is in accordance with these observations.

Table 3. Curve-fitting analysis of Pt L₃-edge EXAFS of Pt/C.

Sample	Shell	N ^a	R (Å) ^b	σ (Å) ^c	R _f (%) ^d
Pt/C	Pt	9.9	2.75	0.079	3.9
Pt/C (after 5th cycles)	Pt	10.1	2.74	0.074	3.8

^a Coordination numbers. ^b Bond distance. ^c Debye-Waller factor. ^d Residual factor.

This catalytic system is applicable to gram scale synthesis of pyrimidines. This capability was demonstrated by reaction of 12.5 mmol of **1a**, 15 mmol of **2a**, 10 mmol of **3a** and 15 mmol of KO^tBu using 0.05 mol% of Pt/C catalyst for 120 h, which produces **4a** in 89% yield corresponding to a TON of 1780. As the data in **Table 4** demonstrate, the new

method has two advantages over those previously developed including a more than 10 times higher TON and reusability of the catalyst.

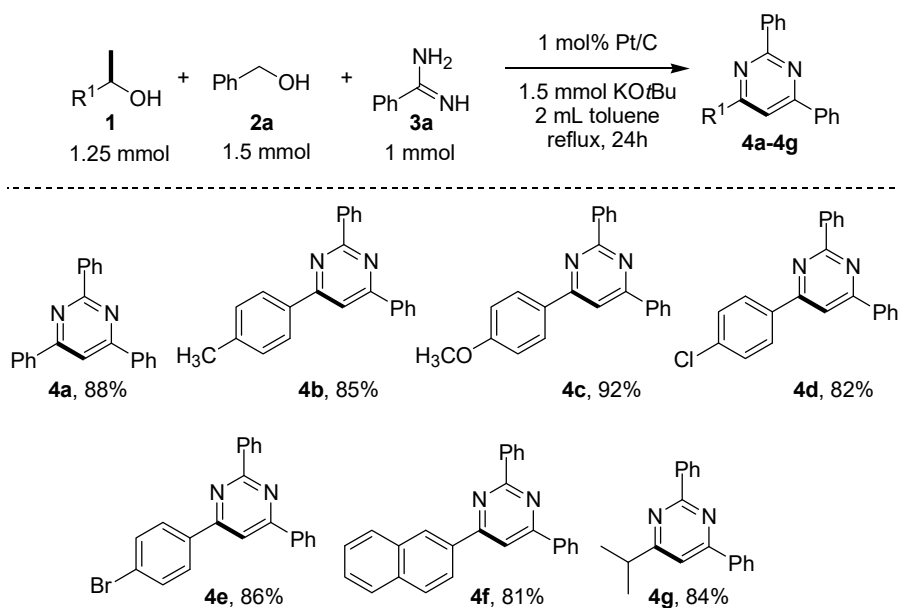
Table 4. TON and catalyst reusability for synthesis of **4a** from **1a**, **2a** and **3a**.

Catalyst	TON	Catalyst reuse	Ref.
Ir complex	158	no	37
Mn complex	172	no	39
Mn complex	48	no	38
Pt/C	1780	5th cycles	This study

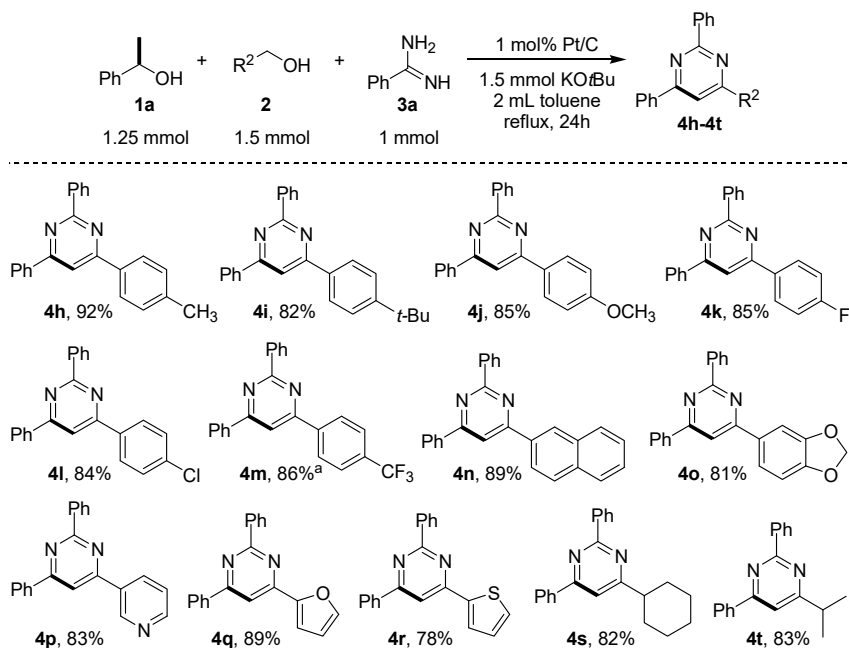
The substrate scope of the Pt/C-catalyzed process was explored next. The results show that the catalytic system is effective in promoting AD reactions of various primary alcohols (benzylic and heterocyclic), secondary alcohols (aliphatic, 1-phenylethanol) and amidines. In these processes, pyrimidines are generated in high yields (78-92%) (**Scheme 2-5**). The scope of secondary alcohols **1** in this process is seen by viewing the results in **Scheme 2**, which show that high yields of isolated pyrimidines attend AD reactions of various secondary alcohols **1** with benzylalcohol **2a** and benzamide **3a**. Reactions of 1-phenylethanol and its derivatives with electron-withdrawing and -donating groups at *para*-positions produce the corresponding pyrimidines (**4a** to **4e**) with good to excellent yields (82-92%). AD reaction of 1-(naphthalen-2-yl)ethan-1-ol with **2a** and **3a** also generates the corresponding pyrimidine **4f** in 81% yield. Finally, AD reaction with 3-methyl butan-2-ol gave the pyrimidine **4g** occurring in 84% yield, demonstrates the applicability of the method to aliphatic secondary alcohols.

The results in **Scheme 3** show the scope of primary alcohols **2**, including aromatic, heterocyclic and aliphatic alcohols, in the new AD reaction. Benzyl alcohols with different substituents at *para*-positions react with 1-phenylethanol **1a** and benzamide **3a** to produce the corresponding pyrimidines (**4h-4m**) in good to high isolated yields (82-92%). 2-Naphthylmethanol also forms pyrimidine analogue **4n** in an acceptable 89% yield. Primary alcohols containing heterocycles groups, such as piperonyl, pyridyl, furyl and thiophenyl, are converted to the corresponding pyrimidines (**4o-4r**) in high isolated yields (78-89 %). Also,

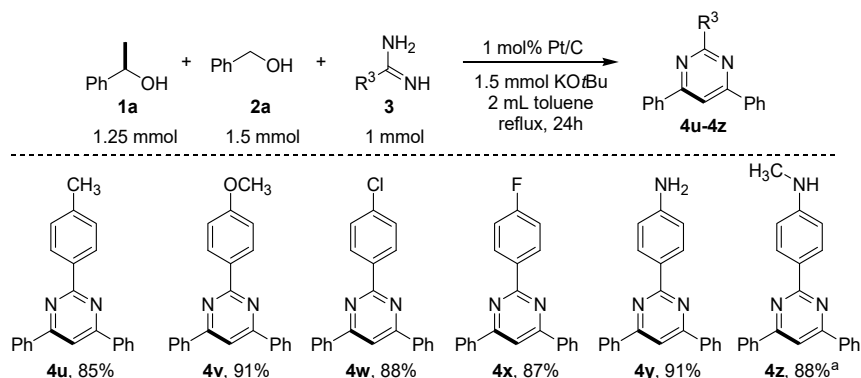
AD reactions of aliphatic primary alcohols, cyclohexylmethanol and iso-butyl alcohol with **2a** and **3a** yield the corresponding pyrimidines (**4s**, **4t**) in high isolated yields. Significantly, (4-(trifluoromethyl) phenyl) methanol, 2-naphthylmethanol and 2-furylmethanol are the first examples of primary alcohols that undergo reactions with 1-phenylethanol and benzamidine to form trisubstituted-pyrimidines.



Scheme 2. Synthesis of pyrimidines from, **2a** and **3a**, and secondary alcohols. Isolated yields are shown.



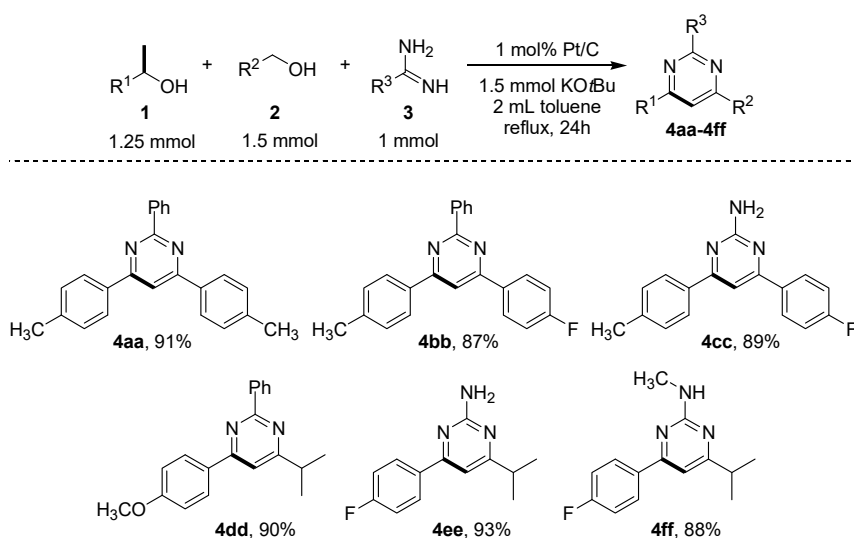
Scheme 3. Synthesis of pyrimidines from **1a**, primary alcohols and **3a**. Isolated yields are shown. ^a GC yield.



Scheme 4. Synthesis of pyrimidines from **1a**, **2a** and different amidines. Isolated yields are shown, ^a GC yield.

The results of pyrimidine forming AD reaction of different benzamidines with 1-phenylethanol and benzyl alcohol are displayed in **Scheme 4**. Benzamidines possessing strongly (*p*-methoxyphenyl), weakly (*p*-methylphenyl) electron donating groups, and a weakly electron withdrawing (*p*-chlorophenyl, *p*-fluorophenyl) groups react with **1a** and **2a** to produce the corresponding pyrimidines (**4u-4x**) in excellent yields (85-91%). Guanidine and methylguanidine also react with **1a** and **2a** to form the corresponding pyrimidines (**4y** and **4z**) in excellent respective 91% and 88% yields.

Scheme 5 shows the results of AD reactions of *para*-substituted 1-phenylethanols, various primary alcohols, including *p*-substituted benzylalcohols (**4aa-4cc**) and 2-butanol (**4dd-4ff**), with various amidines (benzamidine and guanidine). The observations demonstrate that the new process is applicable to various combinations of substrates, and it generates the corresponding pyrimidines (**4aa-4ff**) in excellent isolated yields (87-93%). It should be noted that products **4ee** and **4ff** are important intermediates in the total synthesis of rosuvastatin, which is used as a pharmaceutical drug for treatment of patients with high levels of cholesterol.⁵¹ Compared to those previously devised, the new heterogeneous catalytic system is characterized by the higher isolated yields of pyrimidine forming reactions.



Scheme 5. Synthesis of pyrimidines from various secondary alcohols, primary alcohols and amidines. Isolated yields are shown.

Mechanistic Study

The mechanism of the AD reaction was not discussed in reports of pioneering studies probing the use of homogeneous catalysts owing to the lack of experimental information.³⁷⁻³⁹ In the current effort, we carried out kinetic studies and control reactions, summarized in equations (1)-(6), which provide observations that enable us to propose a possible mechanistic pathway for the reaction (**Scheme 6**). First, the time course of AD reaction of **3a** under the standard conditions was monitored (**Figure 4**). The results show that initially ($t = 0.5$ h), the amount of acetophenone **1a'** and benzaldehyde **2a'** increases and then decreases as the reaction time is increased. Simultaneously, the amount of benzylideneacetophenone (**5a**) increases with time until 2 h, after which it decreases along with a corresponding increase in the amount of product, triphenylpyrimidine **4a**. A measurement of the evolution of H₂ (eqn. 1) shows that an almost

theoretical amount of this gas is formed at $t = 0.5$ h, demonstrating the occurrence of acceptorless dehydrogenation.

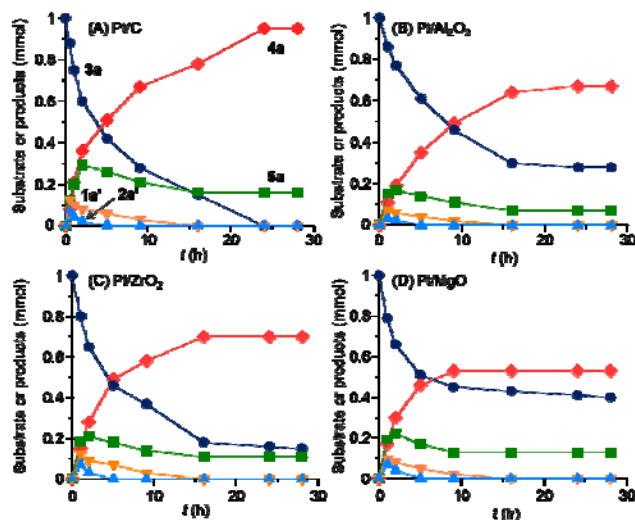
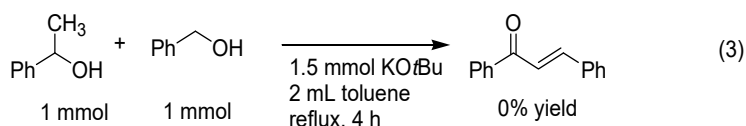
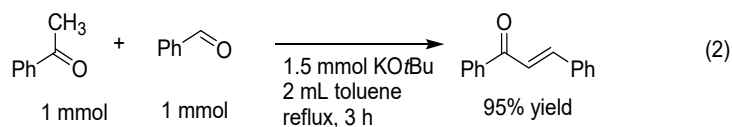
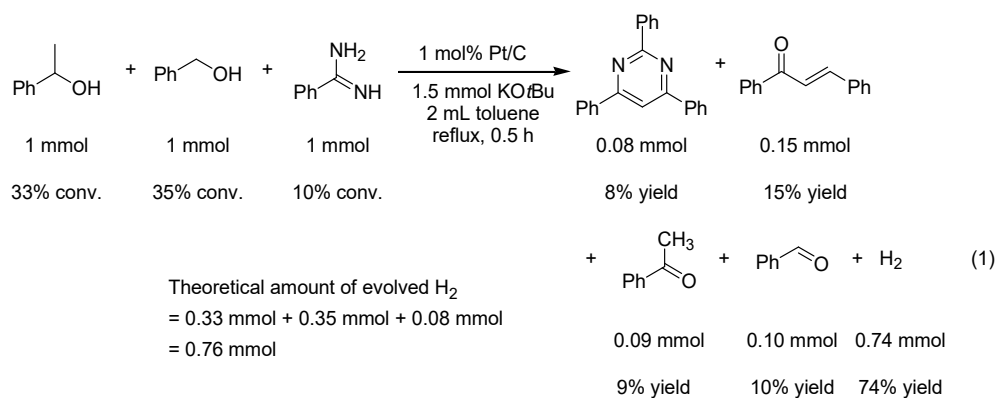
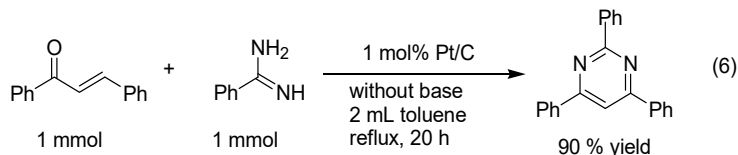
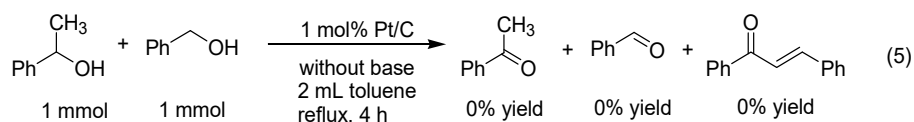
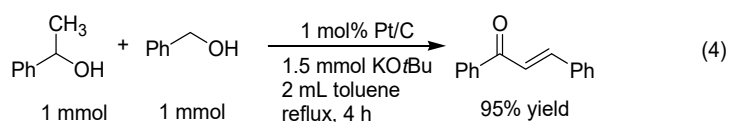


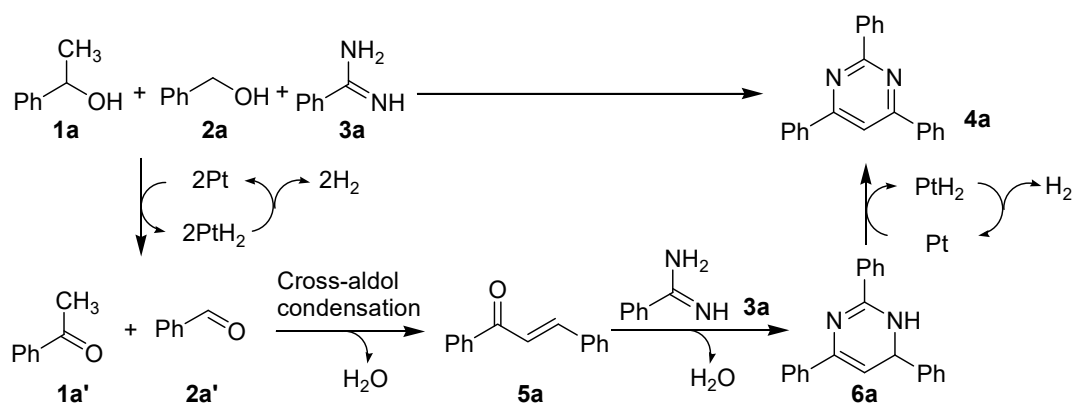
Figure 4. Plots of the amounts of benzamidine **3a**, acetophenone **1a'**, benzaldehyde **2a'**, chalcone **5a** and triphenylpyrimidine **4a** versus reaction time over (A) Pt/C, (B) Pt/Al₂O₃, (C) Pt/ZrO₂, and (D) Pt/MgO catalysts.

Equation.





The above results suggest that the mechanistic pathway for the process, shown in **Scheme 6**, begins with a step in which acceptorless dehydrogenations of primary and secondary alcohols take place to form the corresponding aldehydes and ketones. The second step of the process involves base-catalyzed Claisen-Schmidt condensation of acetophenone with benzaldehyde to form chalcones. The roles played by Pt and KOtBu (base) is evidenced by the results of the control reaction of acetophenone **1a'** and benzaldehyde **2a'** with KOtBu, which produces chalcone **5a** in 95% yield (eqn. 2), and by the observation that this reaction is not catalyzed by Pt/C in the absence of KOtBu (result not shown) nor does reaction of 1-phenylethanol **1a** and benzyl alcohol **2a** with KOtBu in refluxing toluene for 4 h yield chalcone **5a** (eqn. 3). Moreover, in the presence of Pt/C and KOtBu, reaction of 1-phenylethanol **1a** and benzyl alcohol **2a** generates chalcone **5a** in 95% yield (eqn. 4), while Pt/C does not catalyze the dehydrogenation reaction when base is absent (eqn. 5). These results indicate that the dehydrogenation step catalyzed by Pt is assisted by KOtBu, which likely promotes deprotonation of alcohols, and that the second condensation step is catalyzed by KOtBu. The third step, involving condensation of **5a** with benzamidine **3a**, is followed by dehydrogenation of the formed intermediate 2,4,6-triphenyl-1,6-dihydropyrimidine **6a** that produces the final product **4a**. In the presence of Pt/C, reaction of **5a** with **3a** forms triphenylpyrimidine **4a** in 90% yield (eqn. 6).



Scheme 6. Plausible mechanism for AD reaction of 1-phenylethanol, benzyl alcohol and benzamidine that generates 2,4,6-triphenylpyrimidine.

In order to gain additional insight into the mechanism of the AD reaction, kinetic isotope effect (KIE) studies were conducted using **1a** (PhCH(OH)CH_3 or PhCD(OH)CH_3), **2a** (PhCH_2OH or PhCD_2OH) and **3a** (**Figure 5**). Because the plots of the initial amounts of **4a** formed versus time are linear, the slopes of the lines correspond to zero-order rate constants. The results show that the rate constant for reaction of PhCH(OH)CH_3 , PhCH_2OH , and **3a** (k_{HH}) is larger than that for the reaction of PhCD(OH)CH_3 , PhCD_2OH , and **3a** (k_{DD}). The difference corresponds to a KIE ($k_{\text{HH}}/k_{\text{DD}}$) of 2.8 (**Figure 5B**). Also, the KIE for the reaction of **1a** and **2a** to **5a** was found to be 1.5 (**Figure 5A**), which is smaller than that for reaction of **1a**, **2a**, and **3a** to form **4a**. Based on these results, we suggest that step involving dehydrogenation of **6a** to form **4a** is kinetically more important than dehydrogenation of **1a** and **2a**. This proposal is supported by a comparison that show that the initial rate of the reaction in the 4th step is about 6-times smaller than that of the 1st and 2nd steps (**Scheme 7**).

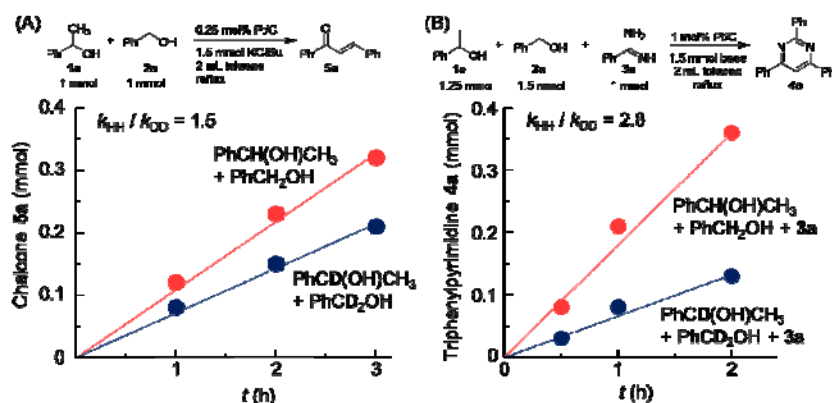
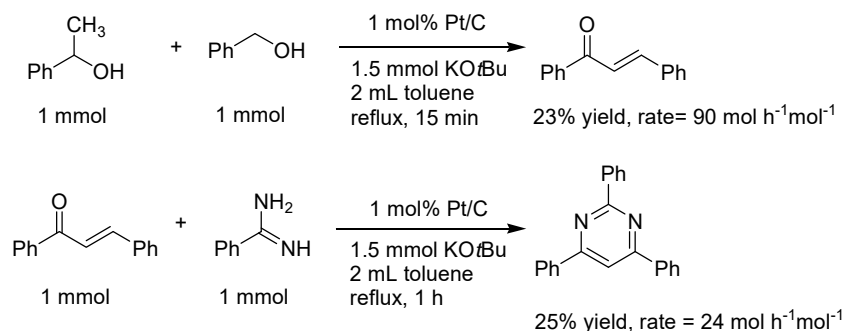


Figure 5. Kinetic isotopic effect analysis (A) for chalcone (**5a**) formation and (B) for triphenylpyrimidine (**4a**) formation under the conditions shown in Table 2 (entry 1).



Scheme 7. Comparison of the initial rates of reactions corresponding to the 1st and 2nd steps (**1a** and **2a** to **5a**) with that of the 4th step (**5a** and **3a** to **4a**).

Origin of the High Catalytic Activity of Pt

The results of the kinetic studies described above show that dehydrogenation of **6a** to **4a** is a kinetically important step in the AD reaction. In addition, the KIE value of 1.5 for reaction of **1a** with **2a** to form **5a** suggests that the first step involving dehydrogenation of alcohols also contributes to the rate of the overall process. Generally, dehydrogenation activities of metal surfaces depend on metal-hydrogen (M–H) bond energies or adsorption energies of a H atom on the surface, which can be assessed theoretically by using density functional theory (DFT).^{52,53} The first elementary step for the dehydrogenation processes on a metal surface forms a surface adsorbed H atom. Metals with low H adsorption energy are not efficient promoters of this step, while metals with very large H adsorption energies are not effective for the promoting the subsequent step, namely removal of H₂ from the surface via M–H bond dissociation. Considering the Brønsted–Evans–Polanyi (BEP) relation and the Sabatier principle,^{54–56} it is reasonable to suggest that the new one-pot reaction described above is most effectively catalyzed by a metal that has a moderate H adsorption energy. In an attempt to verify this hypothesis, we conducted a quantitative analysis of the activity trends for the standard reaction of **1a**, **2a** and **3a** catalyzed by various transition metals loaded carbon catalysts.

To evaluate catalytic activity, initial rates of the product (**4a**) formation over various transition metals loaded carbon catalysts were measured under the conditions where conversion of **1a**, **2a** and **3a** are below 50%. **Table 5** lists the initial rates per total metal atoms in the catalyst (N_T). Volume-area mean diameter (D) of metal particles were estimated using particle size distributions using results of TEM analysis of the catalysts (See **Fig. S1-S10** in the Supporting Information for more details). The D values of the catalysts were

Table 5. Summary of characterization and catalytic results for supported Pt catalysts.

Catalyst	$S_{\text{BET}}^{\text{a}}$ ($\text{m}^2 \text{g}^{-1}$)	$\text{CO}_{\text{ads}}^{\text{b}}$ ($\mu\text{mol g}^{-1}$)	$\text{CO}_{\text{ads after}}^{\text{c}}$ ($\mu\text{mol g}^{-1}$)	D^{d} (nm)	V_0^{e} ($\text{mol mol}_{\text{Pt}}^{-1} \text{h}^{-1}$)	TOF^{f} (h^{-1})
Pt/C	924	62.3	64.3	4.6	21	86.4
Pt/ZrO ₂	91	46.3	<0.1	6.2	14.4	79.8
Pt/Al ₂ O ₃	149	126.1	2.8	2.3	10.8	21.9
Pt/CeO ₂	104	98.5	<0.1	2.9	9.7	25.2
Pt/TiO ₂	52	139.5	0.1	2.1	8.9	16.4
Pt/SiO ₂	318	58.5	0.5	4.9	7.8	34.2
Pt/MgO	24	38.6	18.3	7.5	16.5	109.4
Pt/H β	511	148.4	10.7	1.9	7.7	13.3
Pt/Nb ₂ O ₅	74	44.8	1.3	6.5	5.8	33.2

^a Determined from N₂ adsorption isotherm.

^b Number of CO adsorbed on the catalysts.⁵⁰

^c Number of CO adsorbed on the catalysts after reaction.

^d Average particle size of the supported Pt before catalytic reactions estimated by CO adsorption experiments.⁵⁰

^e Initial rate of **4a** formation (mol h^{-1}) divided by total metal atoms in the catalyst, N_{T} (mol).

^f TOF per surface metal atom defined as $\text{TOF} = V_0 (\text{mol mol}_{\text{Pt}}^{-1} \text{h}^{-1}) \times N_{\text{S}}/N_{\text{T}}$. N_{S} is the number of surface metal atoms derived from CO adsorption experiments for fresh catalysts.

Table 6. Summary of characterization, catalytic results and details of analysis for various carbon supported metal catalysts.

Supported metal	D^{a} (nm)	Phase ^b	Crystal plane ^b	N^{c} (nm^{-2})	$N_{\text{S}}/N_{\text{T}}^{\text{d}}$	V_0^{e} ($\text{mol mol}_{\text{metal}}^{-1} \text{h}^{-1}$)	TOF^{f} (h^{-1})	$E_{\text{Had}}^{\text{g}}$ (eV)
Pt	4.4	fcc	111	14.6	0.31	21.0	66.9	-2.81
Ir	4.9	fcc	111	14.6	0.26	8.0	30.9	-2.74
Re	3.9	hcp	0001	15.1	0.35	2.4	6.8	-3.17
Pd	8.3	fcc	111	14.8	0.17	6.5	39.6	-2.99
Rh	3.8	fcc	111	15.6	0.35	12.7	36.2	-2.91
Ru	6.4	hcp	0001	16.3	0.21	4.5	21.2	-2.99
Ag	31.7	fcc	111	13.3	0.045	0.5	10.1	-2.21
Cu	9.3	fcc	111	17.7	0.14	2.0	15.3	-2.6
Ni	7.0	fcc	111	18.8	0.17	7.3	41.9	-2.92

^a Volume mean diameter of supported metal particles estimated by TEM analysis.

^b Crystal plane of the metal surface for calculation of dispersion and DFT study.

^c Number of metal atoms per unit area (nm^2) on the assumed surface.

^d Dispersion of supported metals, $N_{\text{S}}/N_{\text{T}}$, where N_{S} is the number of surface metal atoms and N_{T} is the total number of metal atoms in the supported metals.

^e Initial rate of **4a** formation (mol h⁻¹) divided by total metal atoms in the catalyst, N_T (mol).

^f TOF per surface metal atom defined as $\text{TOF} = V_0 (\text{mol mol}_{\text{metal}}^{-1} \text{h}^{-1}) \times N_s/N_T$.

^g Adsorption energy of a H atom on the assumed metal surface.⁵⁹

found to have similar sizes in the range of 3.8-7.0 nm except for Ag/C (31.7 nm). It is known that dispersion (fraction of the exposed metal atoms) of metal nanoparticles correlates with the D value owing to the fact that D values estimated by TEM agrees with mean particle diameters estimated from the number of surface atoms on the spherical particles.⁵⁰ Considering the fact that the fraction of low coordination surface atoms is relatively low for the metal particles above 3.8 nm,⁵⁷ we employed the most stable and common planes for each metal to obtain volume-area mean diameters in order to estimate the dispersion from D and density of metal. Namely, the (111) surface was used for metals having a face-centered-cubic (fcc) structure, while the (0001) surface was used for metals having a hexagonal-close-packed (hcp) structure. Finally, the multiple of initial rates and dispersion yields gives the turnover frequency (TOF) per surface metal atoms given in **Table 5**. In our recent study, we theoretically estimated the adsorption energies of a H atom on Pt(111), Ir(111), Pd(111), Rh(111), Cu(111), Ni(111), Ru(0001), and Re(0001) surfaces by using DFT calculations.⁵⁸ **Figure 6** shows the TOF per surface metal atoms for various metal catalysts as a function of the adsorption energy of a H atom as well as the d-band center, which is a well-known descriptor of catalytic activities.⁵⁹⁻⁶¹

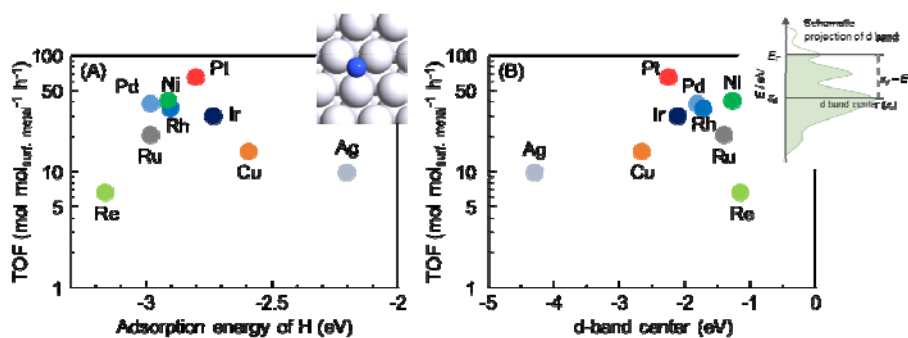


Figure 6. TOF (per surface metal atoms) for the standard reaction promoted by metal-loaded carbon catalysts as a function of (A) the adsorption energy of hydrogen on the metal surface and (B) the d-band center.

The plot shows the existence of a volcano-type dependence of the catalytic activity on both the H adsorption energy and the d-band center, and that Pt catalyst display the highest catalytic activities. The result suggests that Pt catalysts that have an optimum strength of the Pt-H bond and the d-band center are suitable for promoting AD reactions, resulting in higher

catalytic activity of Pt than the other metals. This conceptual finding might be useful for the rational design of new catalytic systems for similar types of metal nanoparticle catalyzed organic reactions without the need to conduct extensive trial-and-error studies.

2.4 Conclusion

In the effort described above, we developed a new catalytic system for the one-pot synthesis of 2,4,6-trisubstitutedpyrimidines by AD reaction of secondary and primary alcohols with amidines, promoted by a Pt/C catalyst and KO^tBu. The catalyst used in this process is heterogeneous and, thus, recyclable. Compared with previously devised catalytic AD reactions, the new process has the following advantages: (1) easy catalyst/product separation, (2) catalyst recyclability, (3) higher TON; and (4) higher isolated yields of pyrimidines even in reactions of challenging substrates such as guanidine. The results of kinetic studies and DFT calculations on various metal surfaces suggest that the higher activity of the Pt catalyst as compared to those of other metal catalysts is a consequence of the optimum strength of the Pt-hydrogen bond, which is required for efficient operation of the acceptorless dehydrogenation steps. The results should be a useful guide to rationalizing the properties of catalytic systems and the design of new catalysts.

References

- (1) Climent, M. J.; Corma, A.; Iborra, S. Heterogeneous Catalysts for the One-Pot Synthesis of Chemicals and Fine Chemicals. *Chem. Rev.* **2011**, *111*, 1072–1133.
- (2) Miyamura, H.; Kobayashi, S. Tandem Oxidative Processes Catalyzed by Polymer-Incarcerated Multimetallic Nanoclusters with Molecular Oxygen. *Acc. Chem. Res.* **2014**, *47*, 1054–1066.
- (3) Siddiki, S. M. A. H.; Toyao, T.; Shimizu, K. Acceptorless Dehydrogenative Coupling Reactions with Alcohols over Heterogeneous Catalysts. *Green Chem.* **2018**, *20*, 2933–2952.
- (4) Kallmeier, F.; Kempe, R. Manganese Complexes for (De)Hydrogenation Catalysis: A Comparison to Cobalt and Iron Catalysts. *Angewandte Chemie-International Edition.* **2018**, *57*, 46–60.
- (5) Gunanathan, C.; Milstein, D. Applications of Acceptorless Dehydrogenation and Related Transformations in Chemical Synthesis. *Science* **2013**, *341*, 249–260.
- (6) Sawama, Y.; Asai, S.; Monguchi, Y.; Sajiki, H. Versatile Oxidation Methods for Organic and Inorganic Substrates Catalyzed by Platinum-Group Metals on Carbons.

- Chem. Rec.* **2016**, *16*, 261–272.
- (7) Crabtree, R. H. Homogeneous Transition Metal Catalysis of Acceptorless Dehydrogenative Alcohol Oxidation: Applications in Hydrogen Storage and to Heterocycle Synthesis. *Chem. Rev.* **2017**, *117*, 9228–9246.
 - (8) Taniguchi, K.; Jin, X.; Yamaguchi, K.; Nozaki, K.; Mizuno, N. Versatile Routes for Synthesis of Diarylamines through Acceptorless Dehydrogenative Aromatization Catalysis over Supported Gold–palladium Bimetallic Nanoparticles. *Chem. Sci.* **2017**, *8*, 2131–2142.
 - (9) Corma, A.; Iborra, S.; Velty, A. Chemical Routes for the Transformation of Biomass into Chemicals. *Chem. Rev.* **2007**, *107*, 2411–2502.
 - (10) Calle-Vallejo, F.; Loffreda, D.; Koper, M. T. M.; Sautet, P. Introducing Structural Sensitivity into Adsorption–energy Scaling Relations by Means of Coordination Numbers. *Nat. Chem.* **2015**, *7*, 403–410.
 - (11) Nixon, T. D.; Whittlesey, M. K.; Williams, J. M. J. Transition Metal Catalysed Reactions of Alcohols Using Borrowing Hydrogen Methodology. *Dalt. Trans.* **2009**, 753–762.
 - (12) Yamaguchi, R.; Fujita, K.; Zhu, M. Recent Progress of New Catalytic Synthetic Methods for Nitrogen Heterocycles Based on Hydrogen Transfer Reactions. *Heterocycles* **2010**, *81*, 1093–1140.
 - (13) Guillena, G.; Ramón, D. J.; Yus, M. Hydrogen Autotransfer in the N-Alkylation of Amines and Related Compounds Using Alcohols and Amines as Electrophiles. *Chem. Rev.* **2010**, *110*, 1611–1641.
 - (14) Obora, Y. Recent Advances in α -Alkylation Reactions Using Alcohols with Hydrogen Borrowing Methodologies. *ACS Catal.* **2014**, *4*, 3972–3981.
 - (15) Shimizu, K. Heterogeneous Catalysis for the Direct Synthesis of Chemicals by Borrowing Hydrogen Methodology. *Catal. Sci. Technol.* **2015**, *5*, 1412–1427.
 - (16) Yang, Q.; Wang, Q.; Yu, Z. Substitution of Alcohols by N-Nucleophiles via Transition Metal-Catalyzed Dehydrogenation. *Chem. Soc. Rev.* **2015**, *44*, 2305–2329.
 - (17) Nandakumar, A.; Midya, S. P.; Landge, V. G.; Balaraman, E. Transition-Metal-Catalyzed Hydrogen-Transfer Annulations: Access to Heterocyclic Scaffolds. *Angew. Chemie-Int. Ed.* **2015**, *54*, 11022–11034.
 - (18) Kozłowski, J. T.; Davis, R. J. Heterogeneous Catalysts for the Guerbet Coupling of Alcohols. *ACS Catal.* **2013**, *3*, 1588–1600.
 - (19) Tsuji, Y.; Huh, K.; Yokoyama, Y. Ruthenium Catalysed N-Heterocyclisation: Lndoles

- from 2-Aminophenethyl Alcohols. *J. Chem. Soc. Chem. Commun.* **1986**, 1575–1576.
- (20) Fujita, K.; Yamamoto, K.; Yamaguchi, R. Oxidative Cyclization of Amino Alcohols Catalyzed by a Cp*Ir Complex. Synthesis of Indoles, 1,2,3,4-Tetrahydroquinolines, and 2,3,4,5-Tetrahydro-1-Benzazepine. *Org. Lett.* **2002**, *4*, 2691–2694.
- (21) Moromi, S. K.; Touchy, A. S.; Siddiki, S. M. A. H.; Ali, M. A.; Shimizu, K. Synthesis of Indoles via Dehydrogenative N-Heterocyclization by Supported Platinum Catalysts. *RSC Adv.* **2015**, *5*, 1059–1062.
- (22) Taguchi, K.; Sakaguchi, S.; Ishii, Y. Synthesis of Quinolines from Amino Alcohol and Ketones Catalyzed by [IrCl(Cod)]₂ or IrCl₃ under Solvent-Free Conditions. *Tetrahedron Lett.* **2005**, *46*, 4539–4542.
- (23) Mierde, H. Vander; Van Der Voort, P.; De Vos, D.; Verpoort, F. A Ruthenium-Catalyzed Approach to the Friedlander Quinoline Synthesis. *European J. Org. Chem.* **2008**, *9*, 1625–1631.
- (24) Schley, N. D.; Dobereiner, G. E.; Crabtree, R. H. Oxidative Synthesis of Amides and Pyrroles via Dehydrogenative Alcohol Oxidation by Ruthenium Diphosphine Diamine Complexes. *Organometallics* **2011**, *30*, 4174–4179.
- (25) Michlik, S.; Kempe, R. A Sustainable Catalytic Pyrrole Synthesis. *Nat. Chem.* **2013**, *5*, 140–144.
- (26) Srimani, D.; Ben-David, Y.; Milstein, D. Direct Synthesis of Pyrroles by Dehydrogenative Coupling of β -Aminoalcohols with Secondary Alcohols Catalyzed by Ruthenium Pincer Complexes. *Angew. Chemie-Int. Ed.* **2013**, *52*, 4012–4015.
- (27) Iida, K.; Miura, T.; Ando, J.; Saito, S. The Dual Role of Ruthenium and Alkali Base Catalysts in Enabling a Conceptually New Shortcut to N-Unsubstituted Pyrroles through Unmasked α -Amino Aldehydes. *Org. Lett.* **2013**, *15*, 1436–1439.
- (28) Zhang, M.; Neumann, H.; Beller, M. Selective Ruthenium-Catalyzed Three-Component Synthesis of Pyrroles. *Angew. Chemie-Int. Ed.* **2013**, *52*, 597–601.
- (29) Zhang, M.; Fang, X.; Neumann, H.; Beller, M. General and Regioselective Synthesis of Pyrroles via Ruthenium-Catalyzed Multicomponent Reactions. *J. Am. Chem. Soc.* **2013**, *135*, 11384–11388.
- (30) Emayavaramban, B.; Sen, M.; Sundararaju, B. Iron-Catalyzed Sustainable Synthesis of Pyrrole. *Org. Lett.* **2017**, *19*, 6–9.
- (31) Forberg, D.; Obenauf, J.; Friedrich, M.; Hühne, S.-M.; Mader, W.; Motz, G.; Kempe, R. The Synthesis of Pyrroles via Acceptorless Dehydrogenative Condensation of Secondary Alcohols and 1,2-Amino Alcohols Mediated by a Robust and Reusable

- Catalyst Based on Nanometer-Sized Iridium Particles. *Catal. Sci. Technol.* **2014**, *4*, 4188–4192.
- (32) Siddiki, S. M. A. H.; Touchy, A. S.; Chaudhari, C.; Kon, K.; Toyao, T.; Shimizu, K. Synthesis of 2,5-Disubstituted Pyrroles via Dehydrogenative Condensation of Secondary Alcohols and 1,2-Amino Alcohols by Supported Platinum Catalysts. *Org. Chem. Front.* **2016**, *3*, 846–851.
- (33) Michlik, S.; Kempe, R. Regioselectively Functionalized Pyridines from Sustainable Resources. *Angew. Chemie-Int. Ed.* **2013**, *52*, 6326–6329.
- (34) Srimani, D.; Ben-David, Y.; Milstein, D. Direct Synthesis of Pyridines and Quinolines by Coupling of γ -Amino-Alcohols with Secondary Alcohols Liberating H₂ Catalyzed by Ruthenium Pincer Complexes. *Chem. Commun.* **2013**, *49*, 6632–6634.
- (35) Pan, B.; Liu, B.; Yue, E.; Liu, Q.; Yang, X.; Wang, Z.; Sun, W. H. A Ruthenium Catalyst with Unprecedented Effectiveness for the Coupling Cyclization of γ -Amino Alcohols and Secondary Alcohols. *ACS Catal.* **2016**, *6*, 1247–1253.
- (36) Hille, T.; Irrgang, T.; Kempe, R. Synthesis of Meta-Functionalized Pyridines by Selective Dehydrogenative Heterocondensation of β - and γ -Amino Alcohols. *Angew. Chemie - Int. Ed.* **2017**, *56*, 371–374.
- (37) Deibl, N.; Ament, K.; Kempe, R. A Sustainable Multicomponent Pyrimidine Synthesis. *J. Am. Chem. Soc.* **2015**, *137*, 12804–12807.
- (38) Mastalir, M.; Glatz, M.; Pittenauer, E.; Allmaier, G.; Kirchner, K. Sustainable Synthesis of Quinolines and Pyrimidines Catalyzed by Manganese PNP Pincer Complexes. *J. Am. Chem. Soc.* **2016**, *138*, 15543–15546.
- (39) Deibl, N.; Kempe, R. Manganese-Catalyzed Multicomponent Synthesis of Pyrimidines from Alcohols and Amidines. *Angew. Chemie-Int. Ed.* **2017**, *56*, 1663–1666.
- (40) Chaudhari, C.; Siddiki, S. M. A. H.; Tamura, M.; Shimizu, K. Acceptorless Dehydrogenative Synthesis of 2-Substituted Quinazolines from 2-Aminobenzylamine with Primary Alcohols or Aldehydes by Heterogeneous Pt Catalysts. *RSC Adv.* **2014**, *4*, 53374–53379.
- (41) Rachwal, S.; Katritzky, A. R. *Comprehensive Heterocyclic Chemistry III*; 2008.
- (42) Joule, J. A.; Mills, K. *Heterocyclic Chemistry*; 2010; Vol. 66.
- (43) Agarwal, A.; Srivastava, K.; Puri, S. K.; Chauhan, P. M. S. Antimalarial Activity of 2,4,6-Trisubstituted Pyrimidines. *Bioorganic Med. Chem. Lett.* **2005**, *15*, 1881–1883.
- (44) Müller, T. J.; Braun, R.; Ansorge, M. A Novel Three-Component One-Pot Pyrimidine Synthesis Based upon a Coupling-Isomerization Sequence. *Org. Lett.* **2000**, *2*,

- 1967–1970.
- (45) Kakiya, H.; Yagi, K.; Shinokubo, H.; Oshima, K. Reaction of α,α -Dibromo Oxime Ethers with Grignard Reagents: Alkylative Annulation Providing a Pyrimidine Core. *J. Am. Chem. Soc.* **2002**, *124*, 9032–9033.
 - (46) Bagley, M. C.; Lin, Z.; Pope, S. J. A. Barium Manganate in Microwave-Assisted Oxidation Reactions: Synthesis of Solvatochromic 2,4,6-Triarylpyrimidines. *Tetrahedron Lett.* **2009**, *50*, 6818–6822.
 - (47) Kon, K.; Siddiki, S. M. A. H.; Shimizu, K. Size- and Support-Dependent Pt Nanocluster Catalysis for Oxidant-Free Dehydrogenation of Alcohols. *J. Catal.* **2013**, *304*, 63–71.
 - (48) Moromi, S. K.; Siddiki, S. M. A. H.; Kon, K.; Toyao, T.; Shimizu, K. Acceptorless Dehydrogenation of N-Heterocycles by Supported Pt Catalysts. *Catal. Today* **2017**, *281*, 507–511.
 - (49) Siddiki, S. M. A. H.; Touchy, A. S.; Kon, K.; Shimizu, K. Direct Olefination of Alcohols with Sulfones by Using Heterogeneous Platinum Catalysts. *Chem. - A Eur. J.* **2016**, *22*, 6111–6119.
 - (50) Shimizu, K.; Onodera, W.; Touchy, A. S.; Siddiki, S. M. A. H.; Toyao, T.; Kon, K. Lewis Acid-Promoted Heterogeneous Platinum Catalysts for Hydrogenation of Amides to Amines. *ChemistrySelect* **2016**, *1*, 736–740.
 - (51) Kunimori, K.; Uchijima, T.; Yamada, M.; Matsumoto, H.; Hattori, T.; Murakami, Y. Percentage Exposed of Supported Pt, Pd and Rh Catalysts Studied by Gas Adsorption, Tpr and Tem Methods. *Appl. Catal.* **1982**, *4*, 67–81.
 - (52) Andrushko, N.; Andrushko, V.; König, G.; Spannenberg, A.; Börner, A. A New Approach to the Total Synthesis of Rosuvastatin. *European J. Org. Chem.* **2008**, *5*, 847–853.
 - (53) Nørskov, J. K.; Bligaard, T.; Rossmeisl, J.; Christensen, C. H. Towards the Computational Design of Solid Catalysts. *Nat. Chem.* **2009**, *1*, 37–46.
 - (54) Loffreda, D.; Delbecq, F.; Vigné, F.; Sautet, P. Fast Prediction of Selectivity in Heterogeneous Catalysis from Extended Brønsted-Evans-Polanyi Relations: A Theoretical Insight. *Angew. Chemie-Int. Ed.* **2009**, *48*, 8978–8980.
 - (55) Santen, R. A. Van; Neurock, M.; Shetty, S. G. Reactivity Theory of Transition-Metal Surfaces: A Brønsted-Evans-Polanyi Linear Activation Energy: Free-Energy Analysis. *Chem. Rev.* **2010**, *110*, 2005–2048.
 - (56) Medford, A. J.; Vojvodic, A.; Hummelshøj, J. S.; Voss, J.; Abild-Pedersen, F.; Studt,

- F.; Bligaard, T.; Nilsson, A.; Nørskov, J. K. From the Sabatier Principle to a Predictive Theory of Transition-Metal Heterogeneous Catalysis. *J. Catal.* **2015**, *328*, 36–42.
- (57) Toyao, T.; Suzuki, K.; Kikuchi, S.; Takakusagi, S.; Shimizu, K.; Takigawa, I. Toward Effective Utilization of Methane: Machine Learning Prediction of Adsorption Energies on Metal Alloys. *J. Phys. Chem. C* **2018**, *122*, 8315–8326.
- (58) Umpierre, A. P.; DeJesús, E.; Dupont, J. Turnover Numbers and Soluble Metal Nanoparticles. *ChemCatChem* **2011**, *3*, 1413–1418.
- (59) Siddiki, S. M. A. H.; Touchy, A. S.; Jamil, M. A. R.; Toyao, T.; Shimizu, K. C-Methylation of Alcohols, Ketones, and Indoles with Methanol Using Heterogeneous Platinum Catalysts. *ACS Catal.* **2018**, *8*, 3091–3103.
- (60) Ruban, A.; Hammer, B.; Nørskov, J. K. Surface Electronic Structure and Reactivity of Transition and Noble Metals. *J. Mol. Catal. A, Chem.* **1997**, *115*, 421–429.
- (61) Takigawa, I.; Shimizu, K.; Tsuda, K.; Takakusagi, S. Machine-Learning Prediction of the d-Band Center for Metals and Bimetals. *RSC Adv.* **2016**, *6*, 52587–52595.
- (62) Shen, X.; Pan, Y.; Liu, B.; Yang, J.; Zeng, J.; Peng, Z. More Accurate Depiction of Adsorption Energy on Transition Metals Using Work Function as One Additional Descriptor. *Phys. Chem. Chem. Phys.* **2017**, *19*, 12628–12632.

Chapter 3

Acceptorless Dehydrogenative Synthesis of Pyridine from Alcohols and Amidines Catalyzed by Supported Platinum Nanoparticles

3.1 Introduction

Apart from the fossil source derived chemical feedstocks renewable lignocellulosic biomass can be transformed to alcohols or polyols and these oxidized hydrocarbons possess unique chemical properties than from the cracking products of crude oil.¹ The development of new reactions that utilize these oxidized hydrocarbons is a direct way to convert alcohols into useful chemicals. Organic transformation borrowing hydrogen (BH) or hydrogen autotransfer (HA) has attract much attention and extensively studied to use alcohol as an alkylating agent in C-C and C-N, C-S or C-O coupling tractions. Where dehydrogenation of alcohols followed by condensation with nucleophiles in acceptorless dehydrogenative coupling (ADC) manner afford the synthesis of diverse heterocyclic compounds with the liberation of hydrogen and water.^{2,3} Acceptorless dehydrogenation (AD) reactions are progressed without employing any oxidants or sacrificial hydrogen acceptors. However, traditional reactions suffer with production of stoichiometric amounts of waste due to use of stoichiometric amounts of oxidants or hydrogen acceptors.⁴ Conventional homogeneous catalysts for these AD reactions have difficulties in catalyst-product separation and reusability. Demonstration of heterogeneous catalysts for AD reaction has already been studied with high activities, stabilities and recyclabilities.^{5,6}

Direct and sustainable catalytic access to nitrogen containing heterocycles (pyrroles, quinolines, quinazolines, indoles, pyridines, pyrimidines) adopting simple alcohols is an expanding area of interest in green sustainable chemistry and organic synthesis.⁷⁻¹³ AD reactions of alcohols enable these hererocyclization through multistep reaction in a one-pot system. Where alcohols dehydrogenate to reactive carbonyl compounds, then condensation/dehydrogenation with nucleophile to form the products over formation of consecutive and selective C-N and C-C bond.¹⁴ These N-heterocycles are abundant in natural products and have wide applications in pharmaceuticals, bioactive molecules, agrochemicals, and optoelectronic materials.^{15,16} Among these N-heterocycles pyridine scaffold exists in many of herbicides, fungicides, thousands of drugs and pyridine based polymers.⁹

Synthesis of pyridines from γ -amino-alcohols and secondary alcohols using homogeneous transition metal catalysts in presence of basic additive followed by ADC methodology have been demonstrated by several research group. The first report of this process was showed by Milstein et al. using Ru complex.⁸ Ir complex catalyzed a new development was demonstrated by Kempe et al.^{9,10} Less expensive Co and Cu complex catalyzed pyridines synthesis was exhibited separately by Balaraman et al. and Lang et al.^{3,17} Recent

improvement in Ru catalyzed homogeneous ADC systems also enables for pyridine synthesis.^{18,19} Compared to conventional pyridine synthesis methods (aldol-condensation, Michael addition) these homogeneous catalytic systems are more atom efficient and sustainable. Regardless of advantages, these catalytic methods suffer from difficulties in catalyst/product separation, reusability and low turnover number (TON). To overcome these difficulties an efficient heterogeneous catalytic system is highly desirable. Recently our group exhibited a series of heterocyclization reactions from alcohols under ADC methodology using recyclable carbon supported Pt catalysts (Pt/C) This Pt/C catalytic system could be effective for some other difficult reaction to generate heterocycles in a direct aspect.²⁰

Here we developed a novel heterogeneous catalytic system (Pt/C) to synthesize pyridine derivatives under ADC reactions from secondary alcohols and γ -amino-alcohols. The developed catalyst is reusable and displays a higher turnover number (TON) than previously used homogeneous catalysts.^{8,10,21} A plausible reaction pathway and factor that affect the catalytic activities exemplified by kinetic studies.

3.2 Experimental

3.2.1 General

Commercially available organic and inorganic compounds, (from Tokyo Chemical Industry, Wako Pure Chemical Industries, and Sigma Aldrich, Kishida Chemical, or Mitsuwa Chemicals) were used without purification. 1-phenylethan-1-d1-ol (C₆H₅CD(OH)CH₃, 98 atom %D) were purchased from Sigma- Aldrich. GC (Shimadzu GC-14B) and GCMS (Shimadzu GCMS-QP2010) analyses were carried out with an Ultra ALLOY capillary column UA+-1 (Frontier Laboratories Ltd.) using nitrogen or He as the carrier gas. 1H and 13C NMR measurements were performed at ambient temperature with JEOL-ECX 600 operating at 600.17 and 150.92 MHz, respectively with tetramethylsilane as the internal standard.

3.2.2 Catalyst preparation

Standard carbon (296 m² g⁻¹, Kishida Chemical) and SiO₂ (Q-10, 300 m² g⁻¹, Fuji Silysia Chemical Ltd.) supports were obtained commercially. CeO₂ (JRC-CEO3, 81 m² g⁻¹), MgO (JRC-MGO-3), TiO₂ (JRC-TIO-4), and H⁺-exchanged β zeolite (H β , SiO₂/Al₂O₃ = 25 \pm 5, JRC-Z-HB25) were supplied by the Catalysis Society of Japan. γ -Al₂O₃ was prepared by calcination of γ -AlOOH (Catapal B Alumina, Sasol) at 900 °C for 3 h. ZrO₂ was prepared by hydrolysis of zirconium oxynitrate 2-hydrate in an aqueous solution of NH₄OH, followed by

filtration, washing with distilled water, drying at 100 °C for 12 h and finally calcination at 500 °C for 3 h. Nb₂O₅ was prepared by calcination of Nb₂O₅·*n*H₂O (CBMM) at 500 °C for 3 h. The Pt/C precursor was prepared by the following impregnation method. A mixture of carbon (10 g) and an aqueous HNO₃ solution of Pt(NH₃)₂(NO₃)₂ that contained 4.96 wt% of Pt (10.62 g) and 50 mL of ion-exchanged water was added to a round-bottom flask (500 mL). The mixture was then stirred (200 rpm) for 15 min at room temperature. Subsequently, the mixture was evaporated to dryness at 50 °C, followed by drying at 90 °C under ambient pressure for 12 h. Prior to each experiment, a Pt/C sample with 5 wt% Pt loading was prepared by pre-reduction of the precursor in a Pyrex tube under a H₂ flow (20 cm³ min⁻¹) at 300 °C for 0.5 h. Other supported Pt catalysts (5 wt% Pt loadings) were prepared by using the same method. M/C (M = Rh, Ir, Ru, Pd, Re, Cu, Ni) catalysts with 5 wt% metal loadings were prepared in a similar manner using aqueous HNO₃ solutions of Rh(NO₃)₃ or Pd(NH₃)₂(NO₃)₂, or aqueous solutions of metal nitrates (for Ni, Cu), IrCl₃·*n*H₂O, RuCl₃, or NH₄ReO₄. Platinum oxides-loaded carbon (PtOx/C) was prepared by calcination of the Pt(NH₃)₂(NO₃)₂-loaded carbon at 300 °C for 0.5 h in air.

3.2.3 Catalyst characterization.

The sizes of supported metal particles were estimated by using transmission electron microscopy (TEM) using a JEOL JEM-2100F TEM operated at 200 kV. Pt L₃-edge X-ray absorption near-edge structures (XANES) and extended X-ray absorption fine structures (EXAFS) were determined in a transmittance mode at the BL01B1 with a Si (111) double crystal monochromator in SPring-8 operated at 8 GeV (Proposal No. 2017B1279). The Pt/C catalyst following the recycle study in **Figure 1** was sealed in cells made of polyethylene under N₂, and then the spectrum was measured at room temperature. The EXAFS analysis was performed using the REX ver. 2.5 program (RIGAKU). The parameters for Pt–O and Pt–Pt shells were provided by the FEFF6.

3.2.4 Catalytic test

Pt/C (39 mg; 1 mol% Pt with respect to α -amino alcohol) was used as the standard catalyst. After reduction, the catalyst was placed in a closed glass tube sealed with a septum inlet and cooled to room temperature under H₂. Toluene (2 mL) was injected through the septum inlet into the glass tube containing the pre-reduced catalyst. Next, the septum was removed, and amino alcohol (1.0 mmol), primary alcohol or secondary alcohol (1.5 mmol), KO^{*t*}Bu (1.1 mmol), *n*-dodecane (0.25 mmol) and a magnetic stirrer bar were added to the tube exposed to

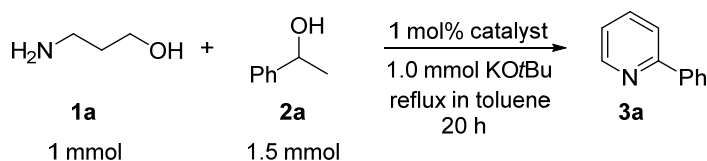
air, which was then placed in a stainless-steel autoclave (28 cm³). After sealing, the autoclave was charged with 1 bar N₂ and stirred (500 rpm) at reflux. For the standard catalyst screening reactions of 1-phenylethanol, α -amino alcohol and KO^tBu (**Table 1**), reaction optimizations (Table 2), kinetic studies and control reactions, the conversions and yields of products were determined by using GC with *n*-dodecane as the internal standard. GC-sensitivities were estimated using commercial compounds or isolated products. In substrate scope studies, products were isolated by using column chromatography on silica gel 60 (spherical, 40–100 μ m, Kanto Chemical Co. Ltd.) using hexane/ethyl acetate (9:1, v/v) as the eluent, and yields of the isolated products were determined. Products were identified by using ¹H and ¹³C NMR spectroscopy in combination with GCMS, in which the mass spectrometer was equipped with the same column as that used for GC analyses. Analysis of the gaseous product (H₂) was carried out by using mass spectrometry (BELMASS).

In the recycling experiments, after each catalytic cycle, 2-propanol (3 mL) was added to the mixture. The catalyst was separated by using centrifugation and washed with water (3 mL) and acetone (6 mL). The catalyst was then dried at 100 °C for 3 h and reduced at 300 °C for 0.5 h under an atmosphere of H₂. Subsequently, the reactor was charged with a mixture of the substrate and KO^tBu and the recovered Pt/C catalyst. It should be noted that the initial rates of product formation for reactions with yields below 30% were obtained based on product yields after a reaction time of 1 h.

3.3 Results and discussion

Initially, 2-phenyl-pyridine was synthesized by the reaction of aminopropanol and 1-phenylethanol as in the previous literature. This reaction was investigated as a model reaction system for the dehydrogenative cross-coupling of alcohols to form pyridines. Refluxing an equimolar amount of aminopropanol (1 mmol), 1 phenyl ethanol (1.5 mmol), and KO^tBu (1.1 mmol) in 2 mL toluene for 24 h in the presence of 1 mol% of Pt/C catalyst gave 88% yield of 2-phenyl-pyridine (Table 1, entry 3). Catalyst screening was performed using the reaction of aminopropanol (1.0 mmol), 1-phenylethanol (1.5 mmol) and KO^tBu (1.1 mmol) in refluxing toluene for 24 h. **Table 1** shows the yields of 2-phenyl-pyridine, based on aminopropanol, for various AD reactions promoted by Pt nanoparticles on different support materials and various metal nanoparticles on carbon containing 0.01 mmol (1 mol%) of the active metal. Under these conditions, reactions do not take place in the absence of the catalyst (entry 1). The results show that platinum oxides-loaded carbon (PtO_x/C, entry 2) does not promote the reaction. In contrast, metallic Pt-loaded carbon (Pt/C), reduced with H₂ at

Table 1. Catalyst screening for synthesis of pyridine derivatives 2-phenylpyridine **3a** from 3-aminopropanol **1a** and 1-phenylethanol **2a**



Entry	Catalysts	Conv. (%) ^(a)	GC yield (%) ^(a)
1	none	0	0
2	PtO _x /C	8	0
3	Pt/C	100	88
4	Pt/C-air	76	65
5	Pt/C _{KB}	100	84
6	Pt/C _{VX}	95	81
7	Pt/C _{SA}	100	84
8	Pt/C	75	63 ^(b)
9	Pt/C	91	77 ^(c)

10	Pt/Al ₂ O ₃	73	60
11	Pt/CeO ₂	64	53
12	Pt/MgO	66	48
13	Pt/ZrO ₂	64	47
14	Pt/Nb ₂ O ₅	61	47
15	Pt/TiO ₂	56	46
16	Pt/SiO ₂	45	31
17	Pt/HBEA	41	29

18	Rh/C	74	63
19	Ir/C	73	61
20	Ru/C	67	59
21	Pd/C	58	48
22	Re/C	41	31
23	Cu/C	27	19
24	Ni/C	26	17
25	Co/C	20	16

^(a) GC yield

300 °C, catalyzes a reaction that occurs in 88% yield (entry 3), while use of pre-reduced, air-exposed Pt/C (Pt/C-air in entry 4) leads to a lower yield (47%). The yields of AD reactions

promoted by Pt/C are higher than those catalyzed by Pt-loaded metal oxides Al₂O₃, CeO₂, MgO, ZrO₂, Nb₂O₅, TiO₂, SiO₂, H β zeolite, entries (5-12). The Pt-loaded metal oxides catalysts were characterized by XRD, N₂ adsorption, and CO adsorption measurements as well as TEM and XAFS measurements as previously reported.²² Moreover, the Pt/C catalyst promotes a higher yielding reaction than do other transition metal nanoparticles supported on carbon (Rh/C, Ir/C, Ru/C, Pd/C, Re/C, Cu/C, Ni/C, and Ag/C) shown in entries 13-20.

Table 2. Optimization of the reaction conditions for synthesis of pyridine derivatives 2-phenylpyridine **3a** from 3-aminopropanol **1a** and 1-phenylethanol **2a** by Pt/C catalyst

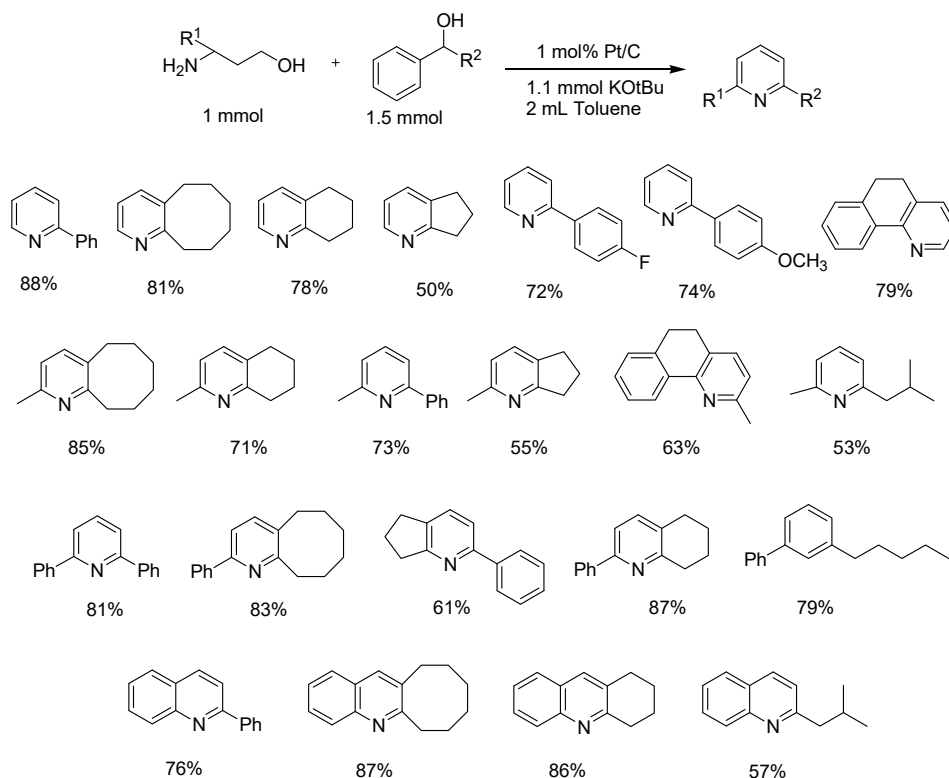
NCCCO (**1a**, p mmol) + CC(O)c1ccccc1 (**2a**, q mmol) $\xrightarrow[24\text{ h}]{\substack{x\text{ mol\% Pt/C} \\ y\text{ mmol base} \\ 2\text{ mL solvent, reflux}}}$ c1ccc(cc1)c2ccncc2 (**3a**)

Entry	Pt/C (x mol%)	1a (p mmol)	2a (q mmol)	Base (y)	Solvent	GC yield (%) ^(a)
1	1	1	1	none	toluene	0
2	1	1	1	KOtBu (0.5)	toluene	39
3	1	1	1	KOtBu (1.0)	toluene	66
4	1	1	1	KOtBu (1.5)	toluene	65
5	1	1	1	KOtBu (2.0)	toluene	58
6	0.5	1	1	KOtBu (1.0)	toluene	49
7	1.5	1	1	KOtBu (1.0)	toluene	67
8	2.0	1	1	KOtBu (1.0)	toluene	68
9	1	1.25	1	KOtBu (1.0)	toluene	67
10	1	1.50	1	KOtBu (1.0)	toluene	69
11	1	1	1.25	KOtBu (1.0)	toluene	77
12	1	1	1.50	KOtBu (1.0)	toluene	88
13	1	1	2	KOtBu (1.0)	toluene	83
14	1	1	1.5	KOtBu (1.0)	<i>n</i> -octane	54
15	1	1	1.5	KOtBu (1.0)	<i>n</i> -nonane	57
16	1	1	1.5	KOtBu (1.0)	mesitylene	65
17	1	1	1.5	KOtBu (1.0)	<i>o</i> -xylene	72
18	1	1	1.5	KOtBu (1.0)	diglyme	69
19	1	1	1.5	KOtBu (1.0)	<i>t</i> -amyl alcohol	77
20	1	1	1.5	K ₂ CO ₃ (1.0)	toluene	11
21	1	1	1.5	Cs ₂ CO ₃ (1.0)	toluene	29
22	1	1	1.5	NaOH (1.0)	toluene	57
23	1	1	1.5	KOH (1.0)	toluene	62
24	1	1	1.5	NaOCH ₃ (1.0)	toluene	34
25	1	1	1.5	KOtBu (1.0)	toluene	88

^(a)GC yield

Using the most effective catalyst, Pt/C, we conducted a study targeted at finding optimal conditions for the reaction of **1a**, and **2a** (Table 2). Inspection of the results arising from reactions promoted by Pt/C and KOtBu in various solvents at reflux (entries 14-19) showed that reaction in toluene (entry 12) forms **3a** in the highest yield. A survey of reactions in refluxing toluene with different basic additives (entries 17-23) showed that KOtBu (entry 12) leads to a higher yield than with the other basic additives (NaOtBu, NaOH, KOH, K₂CO₃, Cs₂CO₃, NaOCH₃, Et₃N, DBU). It was also demonstrated that the reaction hardly proceeds in the absence of a base (entry 1). Consequently, we adopted refluxing toluene using Pt/C and KOtBu as the standard conditions for reaction of **1a**, and **2a**.

Under the optimized reaction conditions, we checked the reactivity of different aromatic and aliphatic amino alcohols in moderate to good isolated yields (Scheme 1). The reaction with different secondary alcohols resulted in the formation of the corresponding pyridines with good to excellent yields. Refluxing the equimolar amount of aminopropanol (1 mmol), 1 phenyl ethanol (1.5 mmol), and KOtBu (1.1 mmol) in 2 mL toluene for 24 h in the presence of 1 mol% of Pt/C catalyst and then reaction was cooled to the room temperature. Then the reaction mixture was extracted with ethylacetate and analysed in GC and GC-MS using dodecane (0.25 mmol) as an internal standard.



Scheme 1. Synthesis of pyridines from amino alcohols and secondary alcohols. Yields are shown.

Then, we confirmed the heterogeneous nature and reusability of this catalytic system by the following results. **Figure 1** shows the result of catalyst recycle test. After the standard reaction for 24 h, the catalyst was separated from the reaction mixture by filtration and was dried at 110 °C for 3 h and then reduced in H₂ at 300 °C for 0.5 h. The recovered catalyst showed high yield (86-88%) at least 4 cycles.

Furthermore, this catalytic system was applicable for the gram scale synthesis of pyridines. The reaction of 5 mmol of amino alcohol, 10 mmol of 1-phenylethanol was carried out by using small amount of Pt/C catalyst in this process.

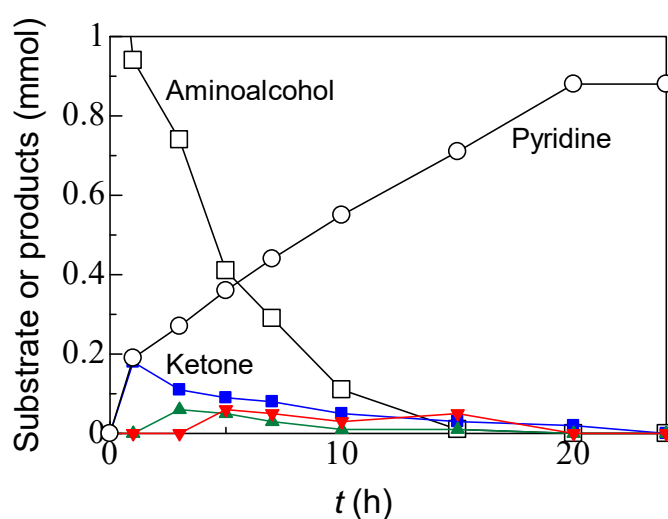


Figure 2. Time course plot for the synthesis of pyrimidine **3a** from amino alcohol **1a** and secondary alcohol **2a**

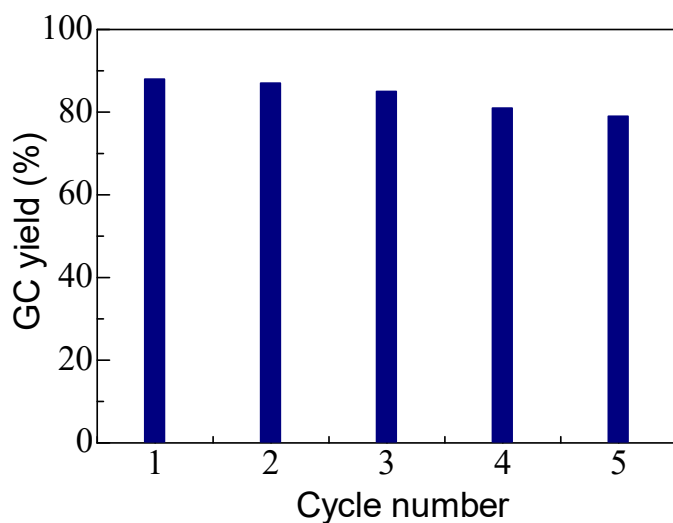


Figure 1. Catalyst reuse for the synthesis of **3a** from **1a**, and **2a** promoted by Pt/C and KO_tBu under

the standard conditions shown in Table 2 (entry 12).

3.4 Conclusion

We have developed a new catalytic system one-pot synthesis of pyridines from amino alcohols and secondary alcohols by a Pt/C catalyst. This system serves as a heterogeneous and recyclable catalytic process to realize pyridine synthesis from amino alcohols and secondary alcohols through acceptorless dehydrogenative mechanism. Considering the facts that the previous homogeneous catalytic systems have difficulties in catalyst/product separation and need expensive organic ligands, toxic solvent or excess amount of reductant and the previous heterogeneous systems show no catalyst reuse and quite limited scope, the present method can be the most atom-efficient method for the synthesis of pyridine. Compared with previous catalytic methods with the dehydrogenation mechanism, our method has the following advantages: (1) easy catalyst/product separation, (2) catalyst recyclability, (3) two orders of magnitude higher TON and (4) wide substrate scope.

References

- (1) Michlik, S.; Kempe, R. *Nat. Chem.* **2013**, *5* (2), 140–144.
- (2) Daw, P.; Kumar, A.; Espinosa-Jalapa, N. A.; Diskin-Posner, Y.; Ben-David, Y.; Milstein, D. *ACS Catal.* **2018**, *8* (9), 7734–7741.
- (3) Midya, S. P.; Landge, V. G.; Sahoo, M. K.; Rana, J.; Balaraman, E. *Chem. Commun.* **2017**, *54* (1), 90–93.
- (4) Vadagaonkar, K. S.; Kalmode, H. P.; Prakash, S.; Chaskar, A. C. *New J. Chem.* **2015**, *39* (5), 3639–3645.
- (5) Shimizu, K. I.; Kon, K.; Seto, M.; Shimura, K.; Yamazaki, H.; Kondo, J. N. *Green Chem.* **2013**, *15* (2), 418–424.
- (6) Sultana Poly, S.; Siddiki, S. M. A. H.; Touchy, A. S.; Ting, K. W.; Toyao, T.; Maeno, Z.; Kanda, Y.; Shimizu, K. I. *ACS Catal.* **2018**.
- (7) Desai, U. V.; Mitragotri, S. D.; Thopate, T. S.; Pore, D. M.; Wadgaonkar, P. P. *Arkivoc* **2007**, *2006* (15), 198–204.
- (8) Srimani, D.; Ben-David, Y.; Milstein, D. *Chem. Commun.* **2013**, *49* (59), 6632.
- (9) Hille, T.; Irrgang, T.; Kempe, R. *Angew. Chemie - Int. Ed.* **2017**, *56* (1), 371–374.
- (10) Michlik, S.; Kempe, R. *Angew. Chemie - Int. Ed.* **2013**, *52*, 6326–6329.
- (11) Deibl, N.; Ament, K.; Kempe, R. *J. Am. Chem. Soc.* **2015**, *137* (40), 12804–12807.

- (12) Deibl, N.; Kempe, R. *Angew. Chemie - Int. Ed.* **2017**, *56* (6), 1663–1666.
- (13) Mastalir, M.; Glatz, M.; Pittenauer, E.; Allmaier, G.; Kirchner, K. *J. Am. Chem. Soc.* **2016**, *138* (48), 15543–15546.
- (14) Gunanathan, C.; Milstein, D. *Science (80-.)*. **2013**, *341*, 249–260.
- (15) Rachwal, S.; Katritzky, A. R. *Comprehensive Heterocyclic Chemistry III*; 2008.
- (16) Joule, J. a.; Mills, K. *Heterocyclic Chemistry*; 2010; Vol. 66.
- (17) Tan, D.-W.; Li, H.-X.; Zhu, D.-L.; Li, H.-Y.; Young, D. J.; Yao, J.-L.; Lang, J.-P. *Org. Lett.* **2018**, *20* (3), 608–611.
- (18) Chai, H.; Wang, L.; Liu, T.; Yu, Z. *Organometallics* **2017**, *36* (24), 4936–4942.
- (19) Guo, B.; Yu, T.-Q.; Li, H.-X.; Zhang, S.-Q.; Braunstein, P.; Young, D. J.; Li, H.-Y.; Lang, J.-P. *ChemCatChem* **2019**.
- (20) Sultana Poly, S.; Siddiki, S. M. A. H.; Touchy, A. S.; Ting, K. W.; Toyao, T.; Maeno, Z.; Kanda, Y.; Shimizu, K. I. *ACS Catal.* **2018**, *8* (12), 11330–11341.
- (21) Pan, B.; Liu, B.; Yue, E.; Liu, Q.; Yang, X.; Wang, Z.; Sun, W. H. *ACS Catal.* **2016**, *6* (2), 1247–1253.
- (22) Shimizu, K.; Onodera, W.; Touchy, A. S.; Siddiki, S. M. A. H.; Toyao, T.; Kon, K. *ChemistrySelect* **2016**, *1*, 736–740.

Chapter 4

High-silica H-Beta Zeolites for Catalytic Hydration of Hydrophobic Epoxides and Alkynes in Water

4.1 Introduction

Hydrolysis and hydration of organic compounds are fundamental reactions in organic synthesis. In chemical industry, hydrolysis of esters and hydration of epoxides, alkenes, alkynes and nitriles are of importance in the production of oxygen-containing organic chemicals.^{1,2} Ring-opening hydration of epoxides¹⁻¹⁵ forms 1,2-diols as intermediates for the manufacture of polyester resins and other functional chemicals. Hydration of alkynes^{1,2,16-20} forms carbonyl compounds as key intermediates for both bulk- and fine-chemical industries. Conventionally, mineral acids such as sulfuric acid and hydrochloric acid have been used as catalysts in industrial hydration/hydrolysis process, but the current process has serious problems such as corrosion of reactor, toxicity, difficulty in catalyst reuse, and cost for neutralization of waste acid.^{1,2} Enormous studies have been reported for developing new catalytic hydration/hydrolysis methods which are environmentally more benign than the current process. For ring-opening hydration of epoxides, various heterogeneous catalysts (resins,⁸ Mo-V oxides,⁹ Nb-based oxides,¹⁰ immobilized transition metal complexes^{3-5,12,14,15,21}) and homogeneous catalysts (metal salts,¹ cyclic amines, Co-complexes⁶) have been explored. For hydration of alkynes, much effort has been devoted to explore for replacing toxic Hg(II)-base catalysts to alternatives including homogeneous transition metal catalysts (Fe,⁷ Ir,²⁰ Ag,¹⁷ Co,^{16,18,19} and Au²⁵), mineral acids in an ionic liquid²⁰ or in aqueous microemulsions,²⁷ and heterogeneous catalysts such as polymer-supported sulfonic acid,²² Sn-W mixed oxide,²³ and immobilized transition metals.²⁴⁻²⁶ However, homogeneous catalyst systems often suffer from difficulty in separation of the catalysts and transition metal-containing heterogeneous catalysts potentially produce contaminated products. These are disadvantageous from an environmental standpoint. Although organic heterogeneous catalysts, such as resins and polymer-supported sulfonic acids, have potentials to overcome these issues, there are still problems concerning low reusability due to their instability. Accordingly, the development of an inorganic and transition-metal free heterogeneous catalyst for hydration of epoxides and alkynes is highly demanded.

Brønsted acidic zeolite is promising for environmentally benign and practical catalyst system to produce contamination-free products because of stability, easy-handling, low-cost and no contamination of transition metals. It is known that hydrophilicity and hydrophobicity of aluminosilicate zeolites depend on Si/Al ratio and that zeolites with Si/Al > 5, so-called high-silica zeolite, have high hydrophobicity owing to nonpolar nature of the Si-O-Si

surface.^[38-46] The pore sizes of the zeolites are closer to organic molecules and the larger pore allows rapid diffusion of bulky organic molecules. To date, there are a few reports for hydration of epoxides and alkynes using aluminosilicate zeolites. Chihara et al. reported the effect of organic solvent on the catalysis in hydration of 1,2-epoxyhexane,⁹ but the other catalytic properties such as substrate scope and catalyst reusability were not investigated. As for the hydration of alkynes, Moreau et al. discussed the role of hydrophobic effect using dealuminated zeolites in hydration of phenylacetylene in EtOH solvent.²⁷ The zeolite-catalyzed hydration of alkynes without organic solvent was examined by Nama et al. and Tang et al., respectively.^{28,29} However, the comprehensive studies including the effects of acidity and pore size of zeolites on the catalysis were not investigated yet. Recently, our research group found that proton-exchanged *BEA zeolite (H β) with high Si/Al ratio and large pore catalyzed efficient hydrolysis of hydrophobic esters in water and studied comprehensively the roles of hydrophobicity, acidity, and pore size.³⁰ In this work, we report herein that hydration of hydrophobic epoxides and alkynes are smoothly catalyzed in water by the high-silica H β zeolite. Detailed catalytic studies show good reusability and wide substrate scope of our method. Furthermore, to elucidate the role of hydrophobicity, acidity, and pore size of zeolites, the hydration of hydrophilic/hydrophobic epoxides and alkynes with different molecular sizes using two-type of zeolites (H β and HZSM5) with different Si/Al ratio was carried out.

4.2 Experimental

4.2.1 General

Commercial compounds (Tokyo Chemical Industry or Sigma-Aldrich) were used without further purification. GC (Shimadzu GC-2014) and GCMS (Shimadzu GCMS-QP2010) analyses were carried out with Ultra ALLOY⁺-1 capillary column (Frontier Laboratories Ltd.) with N₂ and He as the carrier. Column chromatography was performed with silica gel 60 (spherical, 63-210 μ m, Kanto Chemical Co. Ltd.). Molecular sieves 4Å (MS4Å) was dehydrated at 100 °C.

4.2.2 Catalyst preparation.

The zeolites catalysts are designated as H β - x ; x denotes the Si/Al ratio of the H β zeolite. H β -75 (JRC-Z-HB150, originally supplied from Clariant), H β -12.5 (JRC-Z-HB25), HMOR-45 (JRC-Z-HM90, originally supplied from Clariant), TiO₂ (JRC-TIO-4), CeO₂ (JRC-CEO-3), amorphous SiO₂-Al₂O₃ (JRC-SAL-2, Al₂O₃ content = 13.75 wt%, surface area = 560 m² g⁻¹) were supplied from Catalysis Society of Japan. H β -20 (HSZ-940HOA), H β -255

(HSZ-980HOA), HZSM5-20 (HSZ-840HOA) and HY-50 (HSZ-385HUA) were commercially purchased from Tosoh Co. HZSM5-11 was prepared by calcination (550 °C, 3 h) of NH_4^+ -ZSM5 (Si/Al=11, HSZ-820NHA). HZSM5-75 and HZSM5-150 were supplied from N.E. CHEMCAT Co. Niobic acid (HY-340) was kindly supplied by CBMM, and Nb_2O_5 was prepared by calcination of the niobic acid at 500 °C for 3 h. SiO_2 (Q-10) was supplied from Fuji Silysia Chemical Ltd. ZrO_2 and SnO_2 were prepared by calcination (500 °C, 3 h) of $\text{ZrO}_2 \cdot n\text{H}_2\text{O}$ and H_2SnO_3 (Kojundo Chemical Laboratory Co., Ltd.). $\text{Cs}_{2.5}\text{H}_{0.5}\text{PW}_{12}\text{O}_{40}$ was prepared by titrating $\text{H}_3\text{PW}_{12}\text{O}_{40}$ (Nippon Inorganic Color and Chemicals Co.) by aqueous solution of Cs_2CO_3 (0.10 mol dm^{-3}) with vigorous stirring, followed by centrifuging and drying at 200 °C. Montmorillonite K10 clay and sulfonic resins (Amberlyst-15 and Nafion- SiO_2 composite) were purchased from Sigma-Aldrich. Scandium(III) trifluoromethanesulfonate, $\text{Sc}(\text{OTf})_3$, and *p*-toluenesulfonic acid (PTSA) were purchased from Tokyo Chemical Industry.

4.2.3 Catalytic characterization

IR measurements.

The NH_3 -adsorption IR (infrared) study was carried with JASCO FT/IR-4200 spectrometer equipped with an MCT detector using a flow-type IR cell connected to a flow reaction system. The IR disc of the sample (40 mg, 20 mm ϕ) was first dehydrated under He flow at 500 °C, and then a background spectrum was taken under He flow at 200 °C. Then, NH_3 (1%) was introduced to the sample, followed by purging by He, and by IR measurement of adsorbed NH_3 at 200 °C.

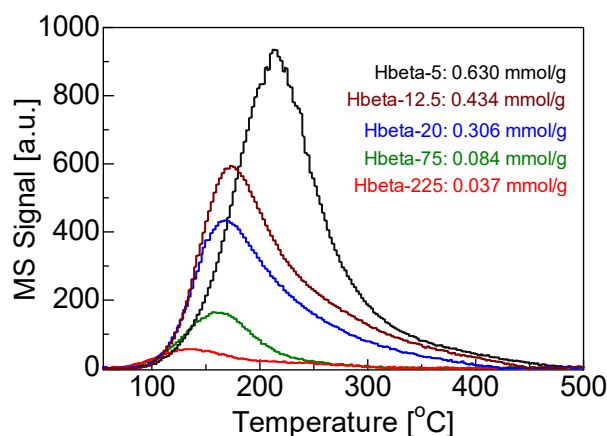


Figure 2. H_2O -TPD curves ($m/e = 18$) for $\text{H}\beta$ zeolites

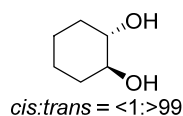
4.2.4 Catalytic tests.

The heterogeneous catalysts, stored under ambient conditions, were used for catalytic reactions without any pretreatment. Typically, ester (1 mmol), 1 mL H₂O and 10 mg of catalysts and a magnetic starter bar were added to a reaction vessel (Pyrex pressure tube, 13 mL), and the mixture was heated at 130 °C under air with stirring at 300 rpm. For the catalytic tests in **Table 1** and kinetic study, conversions and yields were determined by GC-FID using *n*-dodecane as an internal standard as follows. After completion of the reaction, acetone (7 mL) was added to the mixture, and the catalyst was separated by centrifugation. Then, *n*-dodecane (0.2 mmol) was added to the reaction mixture, and the mixture was analyzed by GC-FID and GC-MS. The GC-FID sensitivities of the products were determined using commercial carboxylic acids or the isolated products after the reaction. For some of the products in **Tables 2** and **3**, we determined isolated yields of the carboxylic acids as follows. After the filtration of the catalyst, followed by washing the catalyst with acetone (6 mL), and by evaporation, the product was isolated by column chromatography using silica gel 60 (spherical, 63-210 μm, Kanto Chemical Co. Ltd.) with hexane/ethylacetate (60/40 to 80/20) as the eluting solvent, followed by analyses by ¹H NMR, ¹³C NMR and GC-MS equipped with the same column as GC-FID.

4.2.5 NMR and GC/MS analysis

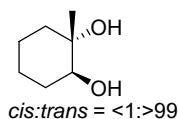
¹H and ¹³C NMR spectra for alcohols of **Table-2** and ketones of **Table-4** were assigned and reproduced to the corresponding literature. ¹H and ¹³C NMR spectra were recorded using at ambient temperature on JEOL-ECX 600 operating at 600.17 and 150.92 MHz, respectively with tetramethylsilane as an internal standard. Abbreviations used in the NMR experiments: s, singlet; d, doublet; t, triplet; q, quartet; m, multiplet; br, broad. GC-MS spectra were taken by SHIMADZU QP2010.

trans-Cyclohexane-1,2-diol: ^[1]



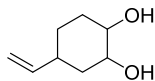
¹H NMR (600.17 MHz, CDCl₃, TMS): δ 3.35 (s, 2H), 2.36 (br s, 2H), 2.10-1.92 (m, 2H), 1.72-1.76-1.64 (m, 2H), 1.32-1.22 (m, 4H); ¹³C NMR (150.92 MHz, CDCl₃) δ 76.79 (C×2), 32.82 (C×2), 24.29 (C×2); GC-MS m/e 116.10.

trans-1-Methyl-cyclohexane-1,2-diol: ^[1]



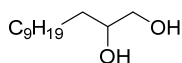
^1H NMR (600.17 MHz, CDCl_3 , TMS): δ 3.51-3.47 (m, 1H), 2.06 (s, 1H), 1.89-1.84 (m, 1H), 1.80 (s, 1H), 1.76-1.58 (m, 3H), 1.41-1.29 (m, 4H), 1.20 (s, 3H); ^{13}C NMR (150.92 MHz, CDCl_3) δ 76.63, 74.01, 38.61, 31.03, 24.07, 23.23, 19.48; GC-MS m/e 130.10.

4-Vinylcyclohexane-1,2-diol:



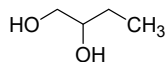
GC-MS m/e 142.15.

Dodecane-1,2-diol:



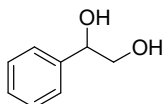
GC-MS m/e 202.20.

1,2 Butanediol: ^[2]



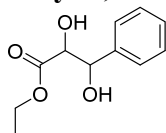
^1H NMR (600.17 MHz, CDCl_3 , TMS): δ 3.69-3.64 (m, 2H), 3.47-3.43 (m, 1H), 2.08 (d, $J = 4.14$ Hz, 1H), 1.94 (t, $J = 5.49$ Hz, 1H), 1.51-1.47 (m, 2H), 1.47 (s, 2H), 0.98 (t, $J = 7.56$ Hz, 3H); ^{13}C NMR (150.92 MHz, CDCl_3) δ 73.69, 66.41, 26.03, 9.89; GC-MS m/e 90.05.

1-Phenyl-ethane-1,2-diol: ^[2]



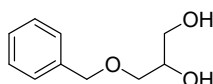
^1H NMR (600.17 MHz, CDCl_3 , TMS): δ 7.34-7.27 (m, 5H), 4.77-4.74 (m, 1H), 3.72-3.59 (m, 3H), 3.30 (br s, 1H); ^{13}C NMR (150.92 MHz, CDCl_3) δ 140.38, 128.45 (C \times 2), 127.88, 126.02 (C \times 2), 74.66, 67.97; GC-MS m/e 138.05.

Ethyl 2,3-dihydroxy-3-phenylpropanoate:



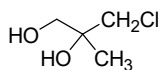
GC-MS m/e 210.10.

3-Benzyloxy-propane-1,2-diol: ^[3]



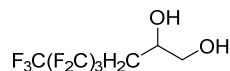
^1H NMR (600.17 MHz, CDCl_3 , TMS): δ 7.39-7.22 (m, 5H), 4.54 (s, 2H), 3.86 (s, 1H), 3.65 (d, $J = 7.56$ Hz, 2H), 3.58-3.49 (m, 2H), 2.89 (br s, 1H), 2.45 (br s, 1H); ^{13}C NMR (150.92 MHz, CDCl_3) δ 137.62, 128.48 (C \times 2), 127.89, 127.77 (C \times 2), 73.54, 71.73, 70.60, 64.02; GC-MS m/e 182.10.

3-Chloro-2-methyl-propane-1,2-diol: ^[4]



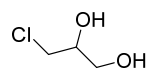
^1H NMR (600.17 MHz, CDCl_3 , TMS): δ 3.66-3.60 (m, 2H), 3.58-3.53 (m, 2H), 2.65 (br s, 2H), 1.27 (t, $J = 8.58$ Hz, 3H); ^{13}C NMR (150.92 MHz, CDCl_3) δ 72.57, 66.97, 50.29, 21.84; GC-MS m/e 124.05.

4,4,5,5,6,6,7,7,7-Nonafluoroheptane-1,2-diol:



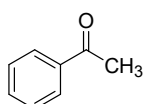
GC-MS m/e 294.05.

3-Chloropropane-1,2-diol:



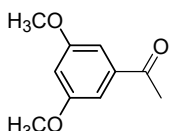
GC-MS m/e 110.05.

Phenylacetylene: ^[5]



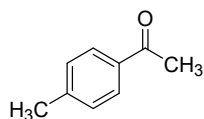
^1H NMR (600.17 MHz, CDCl_3 , TMS): δ 7.96 (d, $J = 8.28$ Hz, 2H), 7.56 (t, $J = 7.56$ Hz, 1H), 7.46 (t, $J = 6.87$ Hz, 2H), 2.60 (s, 3H); ^{13}C NMR (150.92 MHz, CDCl_3) δ 198.12, 137.08, 133.06, 128.53 (C \times 2), 128.26 (C \times 2), 26.57; GC-MS m/e 120.05.

1-(3,5-Dimethoxy-phenyl)-ethanone:



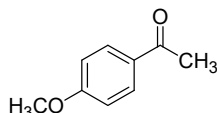
^1H NMR (600.17 MHz, CDCl_3 , TMS): δ 7.07 (d, $J = 7.56$ Hz, 2H), 6.65 (t, $J = 7.56$ Hz, 1H), 3.83 (s, 6H), 2.57 (s, 3H); ^{13}C NMR (150.92 MHz, CDCl_3) δ 197.74, 160.76 (C \times 2), 138.96, 106.06 (C \times 2), 105.23, 55.51 (C \times 2), 26.68; GC-MS m/e 180.10.

4-methylacetophenone: ^[5]



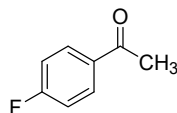
¹H NMR (600.17 MHz, CDCl₃, TMS): δ 7.80 (d, *J* = 7.56 Hz, 2H), 7.18 (d, *J* = 7.56 Hz, 2H), 2.50 (s, 3H), 2.34 (s, 3H); ¹³C NMR (150.92 MHz, CDCl₃) δ 197.06, 143.31, 134.30, 128.77 (C×2), 127.96 (C×2), 26.08, 21.08; GC-MS m/e 134.05.

4-methoxyacetophenone: ^[5]



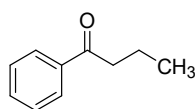
¹H NMR (600.17 MHz, CDCl₃, TMS): δ 7.94 (d, *J* = 8.94 Hz, 2H), 7.84 (d, *J* = 9.66 Hz, 2H), 3.87 (s, 3H), 2.56 (s, 3H); ¹³C NMR (150.92 MHz, CDCl₃) δ 196.73, 163.47, 130.57 (C×2), 130.36, 113.67 (C×2), 55.44, 26.31; GC-MS m/e 150.05.

4-Fluoroacetophenone: ^[5]



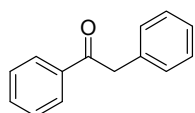
¹H NMR (600.17 MHz, CDCl₃, TMS): δ 8.10-7.92 (m, 2H), 7.09-7.18 (m, 2H), 2.59 (s, 3H); ¹³C NMR (150.92 MHz, CDCl₃) δ 196.44, 165.73 (d, *J* = 254.30 Hz), 133.55, 130.91 (d, *J* = 8.66 Hz, C×2), 115.62 ((d, *J* = 21.67 Hz, C×2)), 26.51; GC-MS m/e 138.05.

1-phenyl-1-butan-1-one: ^[6]



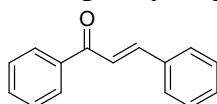
¹H NMR (600.17 MHz, CDCl₃, TMS): δ 7.95 (t, *J* = 7.80 Hz, 2H), 7.54 (t, *J* = 7.56 Hz, 1H), 7.45 (t, *J* = 7.89 Hz, 2H), 2.94 (t, *J* = 7.23 Hz, 2H), 1.79-1.75 (m, 2H), 1.00 (t, *J* = 7.56 Hz, 3H) ¹³C NMR (150.92 MHz, CDCl₃) δ 200.32, 137.01, 132.78, 128.46 (C×2), 127.95 (C×2), 40.42, 17.68, 13.81; GC-MS m/e 148.10.

Phenyl benzyl ketone: ^[7]



¹H NMR (600.17 MHz, CDCl₃, TMS): δ 8.01 (d, *J* = 7.56 Hz, 2H), 7.54 (t, *J* = 7.56 Hz, 1H), 7.45 (t, *J* = 7.89 Hz, 2H), 7.32 (t, *J* = 7.56 Hz, 2H), 7.29-7.22 (m, 3H), 4.28 (s, 2H); ¹³C NMR (150.92 MHz, CDCl₃) δ 197.59, 136.57, 134.51, 133.13, 129.44 (C×2), 128.64 (C×2), 128.61 (C×2), 128.58 (C×2), 126.85, 45.47; GC-MS m/e 196.10.

1,3-diphenyl-2-propyn-1-ol: ^{16]}

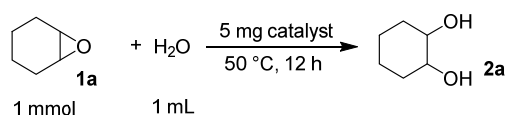


¹H NMR (600.17 MHz, CDCl₃, TMS): δ 8.02 (d, *J* = 7.56 Hz, 2H), 7.82 (d, *J* = 15.84 Hz, 1H), 7.65 (t, *J* = 7.56 Hz, 2H), 7.59 (t, *J* = 7.56 Hz, 1H), 7.55 (s, 1H), 7.51 (t, *J* = 8.25 Hz, 2H), 7.46- 7.40(m, 3H); ¹³C NMR (150.92 MHz, CDCl₃) δ 190.55, 144.84, 138.19, 134.87, 132.76, 130.53, 128.94 (C×2), 128.61 (CX2), 128.48 (C×2), 128.44 (C×2), 122.08; GC-MS *m/e* 208.10.

4.3 Results and Discussion

Catalyst Performance for Hydration of Epoxides

Ring-opening hydration of a model epoxide, 1,2-epoxycyclohexane (**1a**), was carried out in water. **Table 1** summarizes the conversion of **1a** and yields of 1,2-cyclohexanediol (**2a**) for the hydration of **1a** (1 mmol) with H₂O (1 mL) at 50 °C for 12 h in the presence of 5 mg of the catalysts. Before stirring and heating the mixture, the epoxide (oil droplet) was on water, and the solid catalysts were in water. The reaction without catalyst resulted in no conversion of **1a** (entry 1). We screened 21 types of heterogeneous catalysts (entries 2-22) and 3 types of homogeneous catalysts (entries 23-25). Proton-exchanged zeolites (entries 2-10) showed moderate to high yields (43-98%) of **2a**. Hβ catalysts (entries 5-8) showed higher yields than other zeolites such as HZSM5 (entries 2-4), HY (entry 9), and HMOR (entry 10). The yields for the Hβ catalysts depend on the Si/Al ratio, and the Hβ zeolite with intermediate Si/Al values, Hβ-75 (entry 7), gave the highest yield of 98%. Among various metal oxides (entries 11-27), ZrO₂ (entry 13), and Nb₂O₅ (entry 17) showed relatively high yields (70-77%). Niobic acid (entry 18)³¹, a heteropoly acid salt Cs_{2.5}H_{0.5}PW₁₂O₄₀ (entry 19) are well-known water-tolerant solid acids.² These catalysts showed lower yields (59-75%) than Hβ-75 (entry 7). Commercially available solid acids, montmorillonite K10 clay (entry 20), Nafion/SiO₂ composite (entry 21), and Amberlyst-15 (entry 22, acidic resins with sulfonic acid groups) also showed lower yields (32-74%) than Hβ-75. Homogeneous Brønsted acids, H₂SO₄ (entry 23) and *p*-toluenesulfonic acid (PTSA, entry 24), and a water-tolerant homogeneous Lewis acid, Sc (OTf)₃ (entry 25),³² showed lower yields (34-78%) than Hβ-75. It is noteworthy that Hβ-75 shows a higher yield than the conventional homogeneous catalysts under the same catalyst weight conditions. From the screening results, Hβ-75 is the most effective catalyst for the ring-opening hydration of the epoxide **1a** in water.

Table 1. Catalyst screening for hydration of 1,2-epoxycyclohexane (**1a**)

Entry	Catalyst	Yield (%) ^a
1	none	0
2	HZSM5-11	49
3	HZSM5-75	43
4	HZSM5-150	74
5	Hβ-12.5	82
6	Hβ-20	87
7	Hβ-75	98
8	Hβ-255	74
9	HY-50	56
10	HMOR-45	77

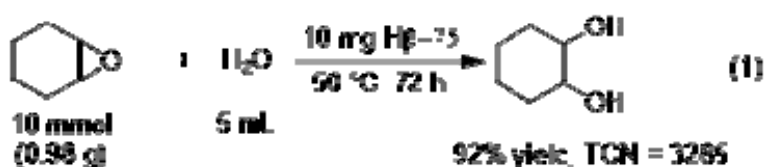
11	SiO ₂ -Al ₂ O ₃	19
12	SiO ₂	2
13	ZrO ₂	77
14	TiO ₂	1
15	SnO ₂	5
16	CeO ₂	2
17	Nb ₂ O ₅	70
18	Niobic acid	75
19	Cs _{2.5} H _{0.5} PW ₁₂ O ₄₀	59
20	Mont. K10	32
21	Nafion-SiO ₂	74
22	Amberlyst-15	71

23	H ₂ SO ₄	34
24	PTSA	78
25	Sc(OTf) ₃	31

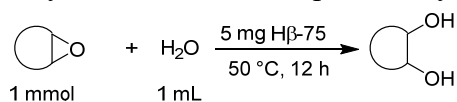
^aGC yield

Having established the optimized catalyst (Hβ-75), we investigated the catalytic performance of our method. The ring-opening hydration of a variety of epoxides was conducted. Table 2 lists the yields of the corresponding glycols. Hβ-75 smoothly catalyzed the hydration of and derivatives of cyclohexane oxide (entries 1-3), 1,2-epoxydodecane (entry 4), 1,2-epoxybutane

(entry 5), styrene oxides (entry 6) and its derivative (entry 7), benzyl glycidyl ether (entry 8), and halogenated epoxides (entries 9-11) including epichlorohydrin (entry 11) were hydrated to the corresponding glycols with good to high yields (73-98%). The epoxide groups were selectively transformed without changing other functional groups such as vinyl, ether, ester and halogen groups. After the first cycle for the hydration of **1a** to **2b** (Table 2, entry 1), the H β -75 was separated from the mixture by centrifugation, followed by washing with acetone, drying at 90 °C for 3 h, and then was reused. The yield for the fifth cycle (94%) is close to that for the first cycle, indicating that the H β -75 catalyst is recyclable. A gram scale reaction of **1a** (10 mmol) with a small amount of the catalyst for 72 h gave **2a** in 92% yield (eq. 1).



Adopting the number of Brønsted acid sites in H β -75 (0.28 mmol g⁻¹), the yield corresponds to the turnover number (TON) of 3300 (per number of acid sites), which is more than 3 times higher than that of the recently reported catalysts including Sn-zeolite (977)¹², mesoporous silica-supported Fe (314)¹³, and Co(salen)-OTs encapsulated in silica nanocages (345).³

Table 2. Hydration of various epoxides by H β -75

Entry	Epoxides	Products	<i>T</i> [°C]	Yield [%] ^[a]
1			50	98 (94)
2			50	98 (95)
3 ^[b]			50	97
4 ^[b]			50	73
5			50	76 (71)
6			50	82 (77)
7 ^[b]			100	77
8			50	91 (86)
9			50	97 (88)
10 ^[b]			100	67
11 ^[b]			50	97

[a] GC yield, isolated yield in parentheses [b] catalyst 25 mg

Catalyst Performance for Hydration of Alkynes

Adopting a relatively bulky alkyne, diphenylacetylene (**3a**), as a model substrate, we carried out catalyst screening for hydration of alkynes in water. **Table 3** compares the yields of benzyl phenyl ketone (**4a**) in the hydration of **3a** (1 mmol) with H₂O (1 mL) under refluxing conditions for 18 h in the presence of 30 mg of the catalysts. Note that the yields of **4a** were nearly close to the conversion of **3a** for all the catalytic tests in **Table 1**. As same as the case of hydration of epoxide **1a**, H β -75 (entry 7) showed the highest yield (98%) among 21 types of heterogeneous catalysts (entries 2-22) and 3 types of homogeneous catalysts (entries 23-25).

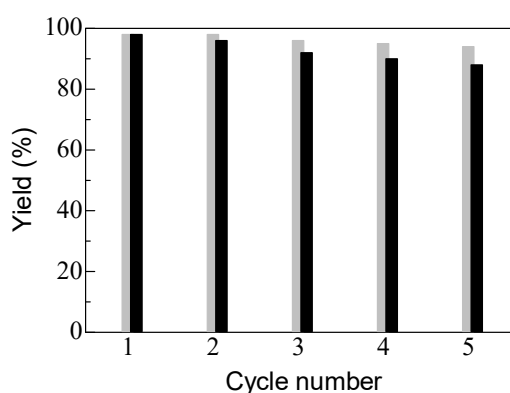
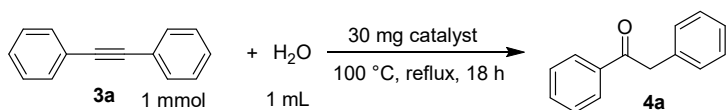
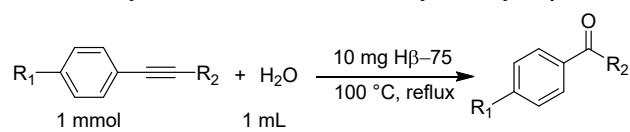


Figure 1. Reusability of the H β -75 in hydrations of 1,2-epoxycyclohexane and diphenylacetylene. Yields of 1,2-cyclohexanediol (white) and phenylbenzyl ketone (Black).

Table 3. Catalyst screening for hydration of diphenylacetylene (**3a**)

Entry	Catalyst	4a yield (%) ^a
1	none	0
2	HZSM5-11	2
3	HZSM5-75	11
4	HZSM5-150	15
5	H β -12.5	44
6	H β -20	51
7	H β -75	98
8	H β -255	11
9	HY-50	15
10	HMOR-45	78
11	SiO ₂ -Al ₂ O ₃	3
12	SiO ₂	16
13	ZrO ₂	2
14	TiO ₂	6
15	SnO ₂	4
16	CeO ₂	1
17	Nb ₂ O ₅	5
18	Niobic acid	43
19	Cs _{2.5} H _{0.5} PW ₁₂ O ₄₀	13
20	Mont. K10	55
21	Nafion-SiO ₂	76
22	Amberlyst-15	65
23	H ₂ SO ₄	43
24	PTSA	47
25	Sc(OTf) ₃	36

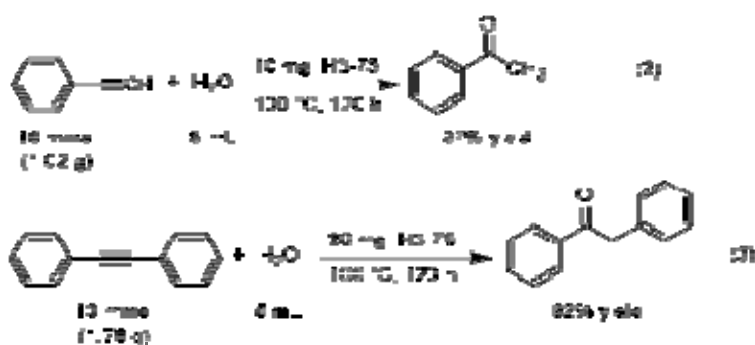
^aGC yield

Table 4. Hydration of various alkynes by H β -75

Entry	Alkynes	Products	t (h)	Yield (%) ^a
1			14	94
2			24	95
3			14	94
4			14	96
5			14	92
6			18	87
7 ^b			18	96
8 ^b			18	95

^aIsolated yield, ^bCatalyst 30 mg

Table 4 shows yields of the corresponding ketones for the hydration of various alkynes in water. Phenylacetylene (entry 1), its derivatives with electron-donating (entries 2-4) and electron-withdrawing functional groups (entry 5), and internal alkynes (entries 6-8) were transformed to the corresponding ketones with high yields (92-96%). **Figure 1** shows the result of catalyst reuse. After the first cycle for the hydration of **3a** to **4a** (**Table 3**, entry 7), the catalyst was separated, and washed, and then reused in the same manner as the case of hydration of epoxides. The yield for the fifth cycle (89%) is similar to that for the first cycle, showing the recyclability of the H β -75 catalyst. H β -75 was applicable to gram scale reactions of phenylacetylene and diphenylacetylene (10 mmol in each case) where the yields of the ketones were 97 and 92%, respectively (**eqs. 2 and 3**).



Hydrophobicity, Hydrophilicity and Acidity of H β and HZSM5 vs Si/Al ratio

The results of catalyst screening show that the catalytic activity of H β for hydration of hydrophilic epoxides and alkynes depends on Si/Al ratio; The H β with intermediate Si/Al ratio (H β -75) shows the highest yields of the products. To obtain the structural properties of zeolites for clarification of dominant factors which control the activity trends, we studied quantitative analysis of hydrophobicity, hydrophilicity, and acidity of zeolites including H β with different Si/Al ratio. The results were summarized in **Table 5**. It is well established that the amount of water adsorbed is a quantitative index for hydrophilicity of zeolites, which is strongly dependent on Si/Al ratio. Several papers reported that amount of water adsorbed on

Table 5. Acidity, hydrophilicity, and hydrophobicity of H β and the other catalysts for comparison.

Catalyst	nBA /mmol g ⁻¹	nLA /mmol g ⁻¹	nH ₂ O /mmol g ⁻¹	nDodecane /mmol g ⁻¹
H β -5	1.55	0.003	0.630	0.8
H β -12.5	0.46	0.005	0.434	1.0
H β -20	0.43	0.003	0.306	1.2
H β -75	0.28	0.001	0.084	1.4
H β -255	0.12	0.001	0.037	2.2
HZSM5-75	0.31	0.001	N/A	1.6
NaZSM5-45	0	0.006	N/A	N/A

The number of Lewis acid sites on the surface of oxides estimated by NH₃ adsorption at 200 °C (**Figure 4**).

H-MOR, H-ZSM5, and H β zeolites increased with increase in the Si/Al ratio.^[41-43] We have tested H₂O-TPD for quantification of hydrophilicity of zeolites and the results are shown in **Figure 2**. The profiles for the H β zeolites show a desorption peak in the range of 100-400 °C and that the peak centers shifted toward higher temperature with the decrease of Si/Al ratio. The amount of H₂O desorbed below 500 °C (n_{H₂O}) is used as a hydrophilicity index; the higher n_{H₂O} value implies higher hydrophilicity (**Table 5**). It is found that the hydrophilicity of H β zeolites decreases with increase in the Si/Al ratio, or in other word, hydrophobicity of H β zeolites increases with the Si/Al ratio. The result is consistent with the recent reports by Otomo et al.^[41] and Kobayashi et al.^[42,43], in which hydrophilicity of H β zeolites, estimated by vapor-phase water adsorption experiments, decreases with increase in the Si/Al ratio.

Hydrophilicity of the zeolites was evaluated by adsorption experiment of n-dodecane on/in water at room temperature. **Figure 3** shows kinetic curves and the equilibrium amount of n-dodecane adsorbed. Note that the amount of n-dodecane (1 mmol) with respect to water (170 g/L) is higher than the solubility of n-dodecane in water at 25 °C (3.7 mg/L), so the n-dodecane in the initial mixture is not dissolved in water but on water (oil droplets). Zeolite powders are initially present in water. During stirring the mixture, n-dodecane can move into zeolite via water/oil/zeolite interface. We have used n-dodecane on/in water for evaluation of hydrophobicity of zeolites, because the adsorption processes of n-dodecane should be similar to that of hydrophobic substrates during hydration reactions in this study. The amount of n-dodecane adsorbed to H β -75 increased with time, and the adsorption reached equilibrium within 15 h. The equilibrium adsorption value increased with the increase of Si/Al ration,

indicating that the hydrophilicity of H β zeolites increase with the increase of Si/Al. The similar kinetic curves and trend of equilibrium adsorption value were observed in the case of a series of HZSM5 zeolites. The minimum cross-diameter (size) of n-dodecane ($4.3 \text{ \AA} \times 4.9 \text{ \AA}$) is smaller than the pore sizes of H β and HZSM5 ($7.6 \text{ \AA} \times 7.3 \text{ \AA}$ and $5.6 \text{ \AA} \times 5.3 \text{ \AA}$, respectively), which is consistent with the similar adsorption rates and trends.

Acidity of the H β was analyzed by the IR spectroscopy for ammonia (NH $_3$) adsorbed on the zeolites. The spectra for H β with different Si/Al ratio and HZSM5-75 are shown in **Figure 4**. We determined the integrated molar extinction coefficient ($0.03 \text{ cm } \mu\text{mol}^{-1}$) of the NH $_4^+$ in zeolites. Using this coefficient combined with the area intensities of the bands around 1454 cm^{-1} , the numbers of Brønsted acid sites in H β -75 and HZSM5-75 were calculated to be 0.28 mmol g^{-1} and 0.31 mmol g^{-1} , respectively. The intensity of the band around 1454 cm^{-1} due to the NH $_4^+$ ^[50-53] decreases with increase in the Si/Al ratio, which shows that the number of the Brønsted acid site decreases with increase in the Si/Al ratio. The intensities of the band at 1640 cm^{-1} due to the coordinatively bound NH $_3$ on Lewis acid^[50-53] are relatively weak, revealing that the most of acid sites of H β and HZSM5-75 are Brønsted acid one. The IR spectrum for NH $_3$ adsorbed on NaZSM5-45 was recorded where only the peak around 1640 cm^{-1} was observed, indicating that NaZSM5-45 is Lewis acidic.

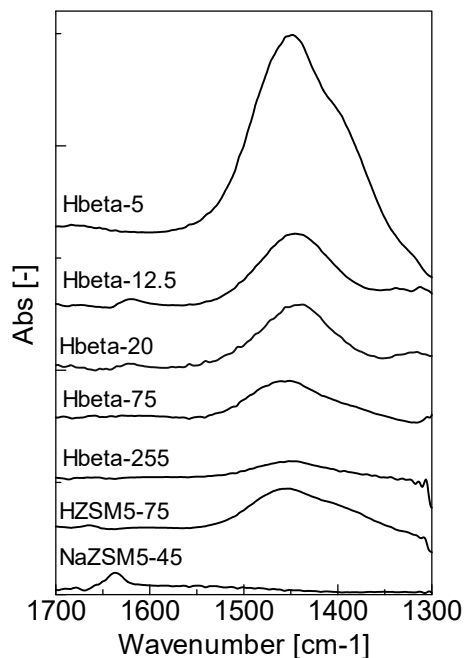


Figure 4. IR spectra of NH $_3$ adsorbed on H β zeolites (40 mg) at 200 °C

Effect of Hydrophobicity of Zeolites and Substrates on the Reaction Rates

To clarify main factors which control the activity trends in the zeolite-catalyzed hydration reactions, first, we discuss the role of Brønsted and Lewis acid sites using HZSM5-75 and NaZSM5-45. HZSM5-75 showed much higher initial rate ($34 \text{ mmol g}^{-1}\text{h}^{-1}$) than NaZSM5-45 ($6 \text{ mmol g}^{-1}\text{h}^{-1}$) in the hydration of 1,2-epoxycyclohexane. The similar result was also obtained in the hydration of phenylacetylene where the initial rates of HZSM5-75 and NaZSM5-45 were 58 and $4 \text{ mmol g}^{-1}\text{h}^{-1}$, respectively. Considering the result that HZSM5-75 is dominantly Brønsted acidic while NaZSM5-45 is Lewis acidic, Brønsted acid sites are the active sites for the hydration of epoxides and alkynes.

Next, the hydrations of several hydrophilic and hydrophobic substrates were carried out using H β with different Si/Al ratio. The octanol/water partition coefficient ($\log K_{ow}$) and the solubility in water are shown as quantitative indexes for hydrophobicity and hydrophilicity indexes for each molecule, respectively, in Table 6 (as shown in the next section). **Figure 5** summarizes the reaction rates for various epoxides and alkynes for H β as a function of Si/Al ratio. As shown in **Figure 5a-c**, the rates in hydration of hydrophobic epoxides (1,2-epoxycyclohexane and 1,2-epoxycyclooctane) show volcano-type dependence on the Si/Al ratio, whereas the rate in hydration of hydrophilic epoxide (propylene oxide) monotonically decreases with Si/Al ratio. The same trends are observed for hydration of hydrophobic alkynes (phenylacetylene, diphenylacetylene, and 1-ethynyl-3,5-dimethoxybenzene) and hydrophilic alkyne (3-butyne-2-ol) (**Figure 5d-g**).

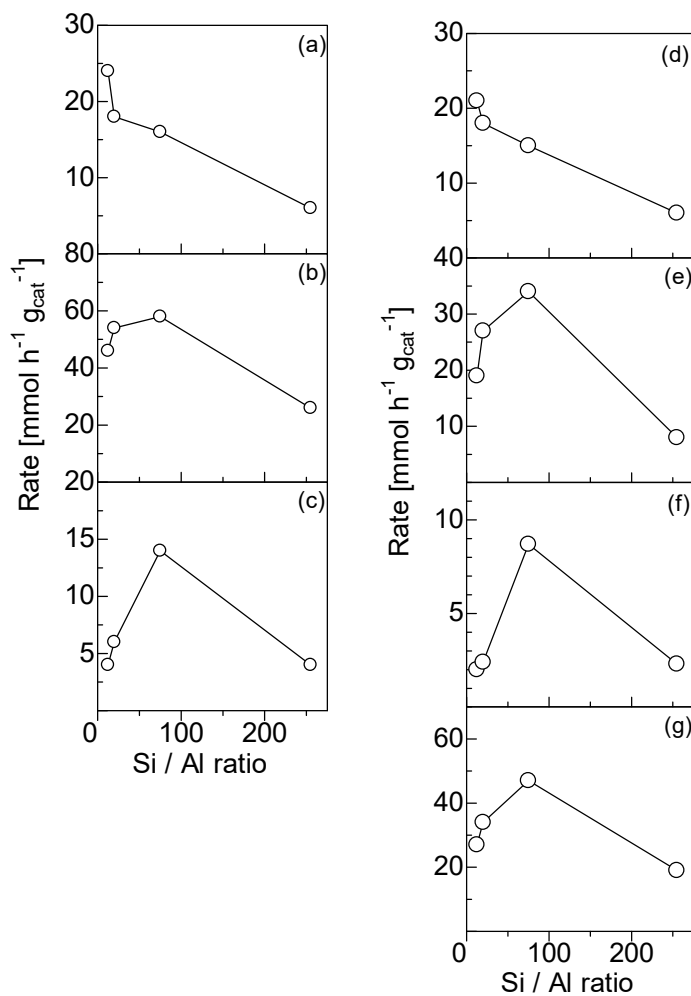

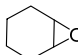
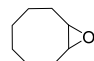
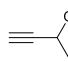
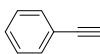
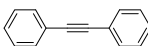
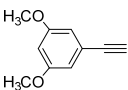


Figure 5. Initial rates for H β -catalyzed hydration of epoxides ((a) propylene oxide, (b) cyclohexane oxide, (c) 1,2-epoxycyclooctane) and alkynes ((d) 3-butyn-2-ol, (e) phenylacetylene, (f) diphenylacetylene, (g) 1-ethynyl-3,5-dimethoxybenzene) versus the Si/Al ratio in H β (Si/Al = 12.5, 20, 75, and 225).

Table 6. Size, hydrophilicity, and hydrophobicity of substrates and initial reaction rates by two-kind of zeolites.

Entry	Substrate	Size (Å) ^a	log K _{ow} ^b	Solubility (mmol/L) ^b	V _{β75} ^d (mmol g ⁻¹ h ⁻¹)	V _{ZSM} ^e (mmol g ⁻¹ h ⁻¹)	V _β /V _{ZSM}
1		4.4 × 4.7	0.03	2229	16	43	0.37
2		5.7 × 7.6	1.33	46.19	58	36	1.61
3		6.1 × 7.8	2.64	4.18	14	4	3.5
4		5.3 × 5.4	-0.00	6307	15	34	0.44
5		3.6 × 6.8	2.53	7.81	34	65	0.52
6		5.2 × 6.8	4.78	0.03	4.4	0.46	9.56
7		4.1 × 10.1	2.42	3.53	47	1	47
8	<i>n</i> -dodecane	4.3 × 4.9	6.10	0.0006			

^aMinimum cross-diameter of the molecules (The details were described in supporting materials)

^bOctanol/water partition coefficient (log K_{ow}) and solubility in water (mmol/L) at 25 °C were taken from ChemSpider Database, <http://www.chemspider.com> (Royal Society of Chemistry)

^cRates for hydration of the substrates per weight of Hβ-75

^dRates for hydration of the substrates per weight of H-ZSM5-75

Taking into account the dependencies of hydrophilicity, hydrophobicity and acidity of Hβ on Si/Al ratio, the trends of reaction rates can be explained as follows. The higher yield of the Si-rich Hβ for hydrophobic substrates is due to the strong interaction of hydrophobic pores with substrates and the moderate number of active acid sites. On the other hand, the higher yield of Al-rich Hβ for hydration of hydrophilic substrates is derived from the hydrophilic interaction between zeolite pore and substrates as well as the higher number of acid sites. To support the above consideration, we further carried out the hydration of propylene oxide using Hβ-5, which is expected to show higher activity for hydrophilic substrate. Hβ-5 exhibited much higher initial reaction rate and TOF compared to the Hβ with higher Si/Al

ratio (eq.4).

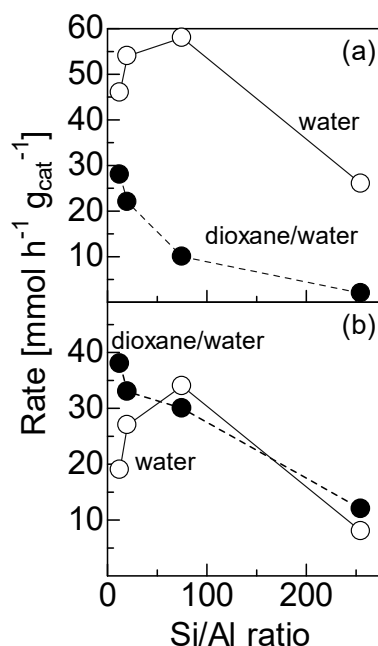


Figure 6. Comparison of reaction rates in water (o) and dioxane/water (●) versus the Si/Al ratio in H β for (a) cyclohexane oxide and (b) phenylacetylene

The hydration of hydrophobic epoxide (1,2-epoxycyclohexane) and alkyne (phenylacetylene) in dioxane/water mixture was also examined. The rates in both reactions monotonically decreased with increase of Si/Al ratio (**Figure 6**). In the presence of dioxane, the hydrophobic interaction between H β pores and substrates is weakened through the competitive interaction of dioxane with the pore and the solvation of substrates in dioxane, resulting in the change of dependencies of rates on Si/Al ratio from volcano. Furthermore, the TOF values for hydration of hydrophobic substrates in water were calculated from the yield and the amount of acid sites of H β . The trends of TOF values as a function of Si/Al ratio combined with acidity, hydrophilicity, and hydrophobicity were summarized in **Figure 7**. The trend of hydrophilicity is close to those of TOF values while the trends of acidity and hydrophobicity are completely different. Totally, hydrophobicity is a key factor affecting catalytic activity of H β zeolites in hydrations and the highest yield of H β -75 among the H β tested was ascribed to the strong hydrophobic interaction between the pore and substrates.

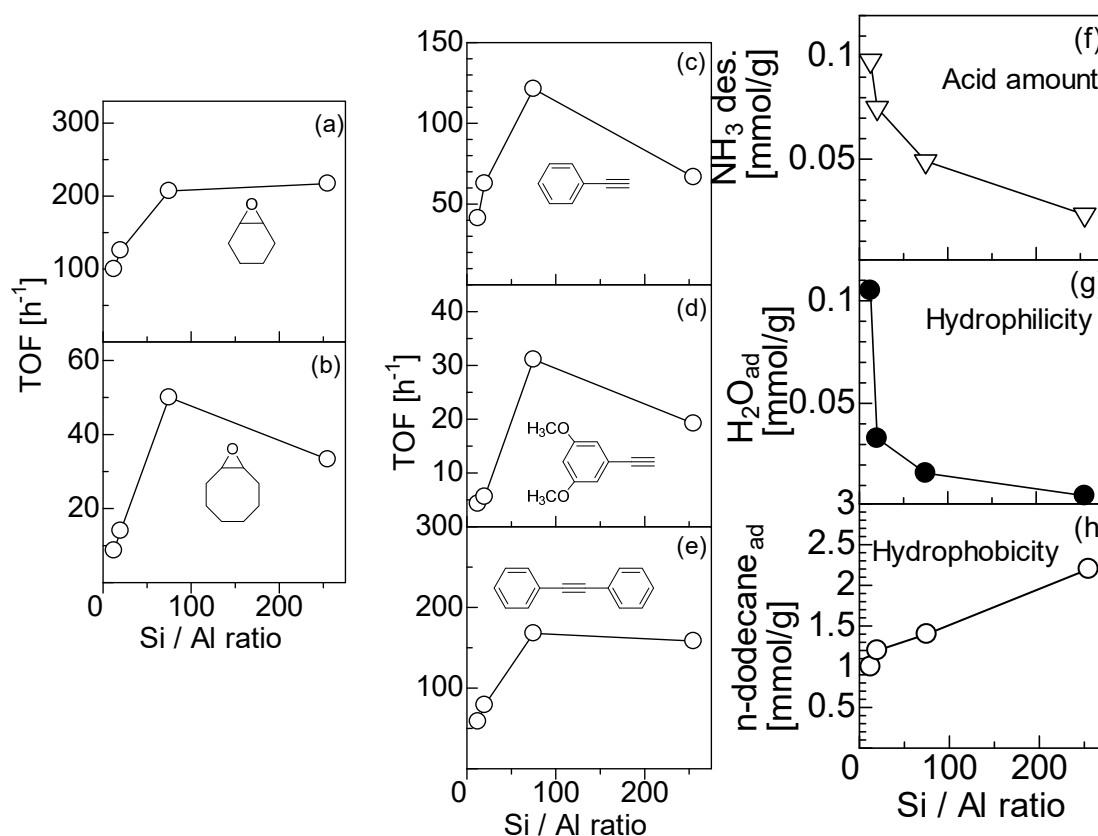


Figure 7. Turnover frequencies for hydrophobic substrates ((a)-(e)) and property of zeolites ((f) acidity, (g) hydrophilicity, (h) hydrophobicity) versus the Si/Al ratio in H β .

Effect of Zeolite Pore Size, Substrate Size on the Catalytic Activity

The effect of zeolite pore size was also investigated through hydration of epoxides and alkynes using zeolite H β -75 (7.3 Å × 7.6 Å) and HZSM5-75 (5.3 Å × 5.6 Å) with different pore size. We summarized the initial rates by two-type of zeolites and the estimated minimum cross-diameters of substrates (**Table 6**). For the substrates having larger sizes than the pore size of HZSM5-75, such as 1,2-epoxycyclohexane (5.7 Å × 7.6 Å), 1,2-epoxycyclooctane (6.1 Å × 7.8 Å), and diphenylacetylene (5.2 Å × 6.8 Å), H β -75 showed higher initial reaction rates compared to HZSM5-75 (entries 2, 3 and 6). Especially, the rate by H β -75 for 1-ethynyl-3,5-dimethoxybenzene (4.1 Å × 10.1 Å) much higher than that of HZSM5-75 (entry 7). In the case of propylene oxide (5.1 Å × 5.7 Å), 3-butyne-2-ol (5.8 Å × 6.2 Å), and phenylacetylene (3.6 Å × 6.8 Å), having similar to or smaller sizes than the pore size of HZSM5-75, the reaction rates by HZSM5-75 were higher than those of H β -75 (entries 1, 4, and 5). These results indicate that the pore size of zeolite has an effect on its activity for hydration. The higher yield of H β -75 compared to that of HZSM5-75 for bulky model

substrates (cyclohexane oxide (entry 2) and diphenylacetylene (entry 6)) is ascribed to its larger pore where the substrates can more smoothly access into the acid sites.

Adsorption experiments.

Adsorption of *n*-dodecane in liquid phase (**Figure 8**) was carried out as follows. *n*-Dodecane (1 mmol) in/on 1 mL water was stirred with zeolite powder (50 mg) for 15 h at room temperature, followed by centrifugation to separate the solids from the liquid. Then, acetone (6 mL) and the internal standard were added to the liquid, and the mixture was analyzed by GC-FID.

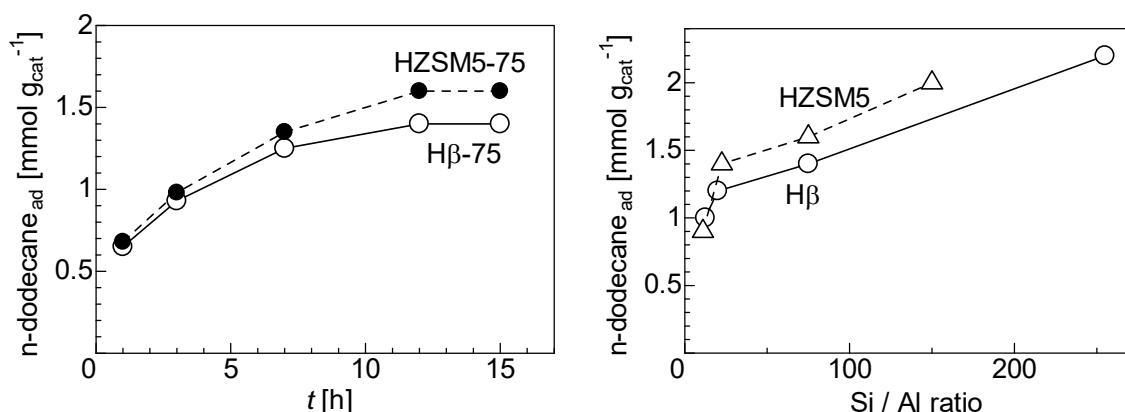


Figure 8. Adsorption kinetics (left) and the amount of *n*-dodecane adsorbed on the zeolite after 15 h at room temperature (right).

4.4 Conclusion

H β -75 acted as an effective heterogeneous catalyst for hydration of hydrophobic epoxides and alkynes in water. This catalyst showed high TONs, wide substrate scopes, and reusability with maintaining its activity. The effects of hydrophobicity, number of Brønsted acid sites, and pore size of zeolite on its activity were quantitatively studied by the hydration of diverse epoxides and alkynes with different hydrophilicity and size using two-type of zeolites with different Si/Al ratio. The key factor for high yields by H β -75 for hydration of hydrophobic substrates is hydrophobic interaction of the zeolite pore with substrates. The larger pore of H β -75 compared to HZSM5-75 also plays an important role to achieve high yields.

References

- (1) Izumi, Y. *Catal. Today* **1997**, *33* (4), 371–409.
- (2) Okuhara, T. *Chem. Rev.* **2002**, *102* (10), 3641–3666.
- (3) Zhong, M.; Zhao, Y.; Yang, Q.; Li, C. *J. Catal.* **2016**, *338*, 184–191.
- (4) Dai, W.; Wang, C.; Tang, B.; Wu, G.; Guan, N.; Xie, Z.; Hunger, M.; Li, L. *ACS Catal.* **2016**, *6* (5), 2955–2964.
- (5) Zhong, M.; Li, H.; Chen, J.; Tao, L.; Li, C.; Yang, Q. *Chem. - A Eur. J.* **2017**, *23* (48), 11504–11508.
- (6) van Hal, J. W.; Ledford, J. S.; Zhang, X. *Catal. Today* **2007**, *123* (1–4), 310–315.
- (7) Wu, X. F.; Bezier, D.; Darcel, C. *Adv. Synth. Catal.* **2009**, *351* (3), 367–370.
- (8) Reed, L. M.; Wenzel, L. A.; O'Hara, J. B. *Ind. Eng. Chem.* **2005**, *48* (2), 205–208.
- (9) Zhang, X.; Wang, M.; Zhang, C.; Lu, J.; Wang, Y.; Wang, F. *RSC Adv.* **2016**, *6* (75), 70842–70847.
- (10) *Reactions* **1990**, *8*, 123–132.
- (11) Ogawa, H.; Sawamura, K.; Chihara, T. *Catal. Letters* **1993**, *18* (4), 367–371.
- (12) Tang, B.; Dai, W.; Wu, G.; Guan, N.; Li, L.; Hunger, M. *ACS Catal.* **2014**, *4* (8), 2801–2810.
- (13) Das, S.; Asefa, T. *ACS Catal.* **2011**, *1* (5), 502–510.
- (14) Li, B.; Bai, S.; Wang, X.; Zhong, M.; Yang, Q.; Li, C. *Angew. Chemie - Int. Ed.* **2012**, *51* (46), 11517–11521.
- (15) Dai, Z.; Sun, Q.; Chen, F.; Pan, S.; Wang, L.; Meng, X.; Li, J.; Xiao, F. S. *ChemCatChem* **2016**, *8* (4), 812–817.
- (16) Tachinami, T.; Nishimura, T.; Ushimaru, R.; Noyori, R.; Naka, H. *J. Am. Chem. Soc.* **2013**, *135* (1), 50–53.
- (17) Thuong, M. B. T.; Mann, A.; Wagner, A. *Chem. Commun.* **2012**, *48* (3), 434–436.
- (18) Wang, S.; Miao, C.; Wang, W.; Lei, Z.; Sun, W. *ChemCatChem* **2014**, *6* (6), 1612–1616.
- (19) Hou, S.; Yang, H.; Cheng, B.; Zhai, H.; Li, Y. *Chem. Commun.* **2017**, *53* (51), 6926–6929.
- (20) Wong, W. L.; Ho, K. P.; Lee, L. Y. S.; Lam, K. M.; Zhou, Z. Y.; Chan, T. H.; Wong, K. Y. *ACS Catal.* **2011**, *1* (2), 116–119.
- (21) Da Silva, C. X. A.; Goncalves, V. L. C.; Mota, C. J. A. *Green Chem.* **2009**, *11* (1), 38–41.
- (22) Iimura, S.; Manabe, K.; Kobayashi, S. *Org. Biomol. Chem.* **2003**, *1* (entry 7), 2416–2418.
- (23) Jin, X.; Oishi, T.; Yamaguchi, K.; Mizuno, N. *Chem. - A Eur. J.* **2011**, *17* (4), 1261–1267.
- (24) Venkateswara Rao, K. T.; Sai Prasad, P. S.; Lingaiah, N. *Green Chem.* **2012**, *14* (5),

- 1507–1514.
- (25) Liang, S.; Jasinski, J.; Hammond, G. B.; Xu, B. *Org. Lett.* **2015**, *17* (1), 162–165.
 - (26) Huang, J.; Zhu, F.; He, W.; Zhang, F.; Wang, W.; Li, H. *J. Am. Chem. Soc.* **2010**, *132* (5), 1492–1493.
 - (27) Finiels, A.; Geneste, P.; Lecomte, J.; Marichez, F.; Moreau, C.; Moreau, P. *J. Mol. Catal. A Chem.* **1999**, *148* (1–2), 165–172.
 - (28) Mamede, N.; Peraka, S.; Marri, M. R.; Kodumuri, S.; Chevella, D.; Gutta, N.; Nama, N. *Appl. Catal. A Gen.* **2015**, *505*, 213–216.
 - (29) Liu, T.; Fu, W.; Zheng, X.; Jiang, J.; Hu, M.; Tang, T. *RSC Adv.* **2014**, *4* (35), 18217–18221.
 - (30) Siddiki, S. M. A. H.; Toyao, T.; Kon, K.; Touchy, A. S.; Shimizu, K. ichi. *J. Catal.* **2016**, *344*, 741–748.
 - (31) Nakajima, K.; Baba, Y.; Noma, R.; Kitano, M.; N. Kondo, J.; Hayashi, S.; Hara, M. *J. Am. Chem. Soc.* **2011**, *133* (12), 4224–4227.
 - (32) Kobayashi, S.; Manabe, K. *Acc. Chem. Res.* **2002**, *35* (4), 209–217.

Supporting Figures and Tables

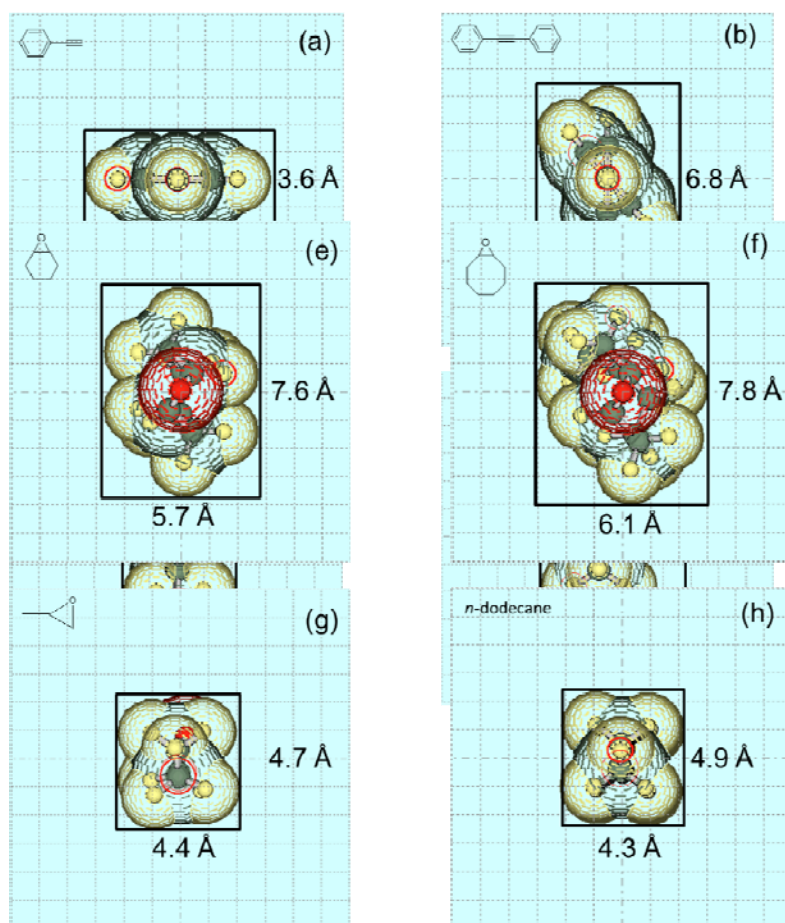


Figure S1. Space-filling models of (a) phenylacetylene, (b) diphenylacetylene, (c) 1-ethynyl-3,5-dimethoxybenzene, (d) 3-butyne-2-ol, (e) 1,2-epoxycyclohexane, (f) 1,2-epoxycyclooctane, (g) propylene oxide, and (h) *n*-dodecane. The minimum cross-sections of the ester based on van der Waals radius for sorbitol and isosorbide are shown. 1 mesh = 1 Å.

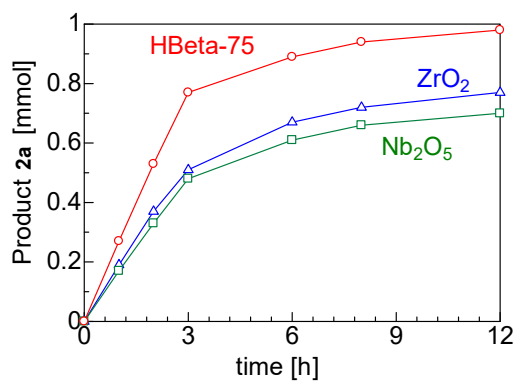


Figure S2. Time course in hydration of 1,2-epoxycyclohexane (**1a**) to 1,2-cyclohexanediol (**2a**) for Hβ-75 (red), ZrO₂ (blue), and Nb₂O₅ (green). Condition: **1a** (1 mmol), H₂O (1 mL), catalyst (5 mg), 50 °C, 1-12 h.

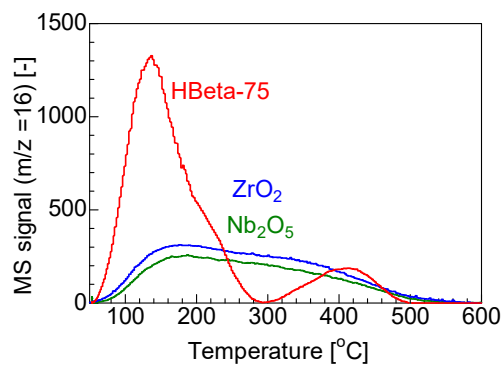


Figure S3. NH₃-TPD profiles of Hβ-75 (red), ZrO₂ (blue), and Nb₂O₅ (green).

Table S1. Specific surface areas of heterogeneous catalysts tested in this study

Catalyst	Specific surface area [m ² /g]
HZSM5-11	510
HZSM5-75	380
HZSM5-150	385
Hβ-12.5	400
Hβ-20	530
Hβ-75	500
Hβ-255	500
HY-50	600
HMOR-45	450
SiO ₂ -Al ₂ O ₃	560
SiO ₂	300
ZrO ₂	72
TiO ₂	47
SnO ₂	28
CeO ₂	81
Nb ₂ O ₅	70
Niobic acid	75
Cs _{2.5} H _{0.5} PW ₁₂ O ₄₀	116
Mont. K10	220
Nafion-SiO ₂	200
Amberlyst-15	45

Table S2. Comparison of initial formation rates of **2a** in hydration of **1a**, acidity determined by NH₃-TPD measurements, and TOF among H β -75, Zr₂O, and Nb₂O₅

Catalyst	Rate [g ⁻¹ h ⁻¹]	[mmol	Number of acid sites [mmol g ⁻¹] ^a	TOF [h ⁻¹] ^b
H β -75	54		0.508	106
Zr ₂ O	38		0.278	136
Nb ₂ O ₅	34		0.236	144

^a Determined by NH₃-TPD. ^b Calculated from the values of rate and acidity.

Chapter 5

**Acetalization of glycerol with ketones and aldehydes
catalyzed by high silica H-Beta zeolite**

5.1 Introduction

Glycerol is considered as a common renewable biomass material, which is the main by-product in natural triglyceride methanolysis for biodiesel production.¹ Increased glycerol production, together with a concomitant decreasing commodity price, has resulted in glycerol becoming a promising substrate in numerous chemical processes across a broad range of industrial sectors, such as personal care products, soaps, pharmaceuticals and foods. However, the glycerol demand in the aforementioned sectors is not able to consume all the glycerol produced from the biodiesel industries. New opportunities for the conversion of glycerol into value-added chemicals have emerged in recent years. In this context, catalysts play an important role in realizing the selective transformation of glycerol. Various catalytic transformations have, hitherto, been developed to obtain valuable chemicals, such as acrolein, glycidol carbonate, syngas, propanediols, and epichlorohydrin.²⁻¹⁰

Among the developed catalytic processes, the condensation of glycerol with carbonyl compounds to synthesize acetals (acetalization) has attracted significant attention because valuable cyclic acetals for diesel fuels and flavor compounds are obtained with the formation of H₂O as a non-toxic co-product.¹¹⁻³⁸ Additionally, this reaction offers a sustainable alternative to the present acetal technology in organic synthesis. Homogeneous acid catalysts, including *p*-toluenesulfonic acid (PTSA), HCl, H₃PO₄, and metal complex catalysts¹¹⁻¹³ have been utilized for the acetalization of glycerol with carbonyl compounds. However, after the reaction using these catalytic systems, neutralization or tedious separation of homogeneous catalysts are required, which results in both environmental issues and poor techno-economics. To circumvent these issues, various heterogeneous catalyst systems, for example, transition metal catalysts¹⁴⁻¹⁹, heteropoly acids²⁰⁻²², transition metal-oxides or phosphates²³⁻²⁶, sulfonic acid-functionalized carbon materials²⁷⁻³¹, metal-organic frameworks^{32,33}, and aluminosilicate zeolites³⁴⁻³⁸ have been developed. Among them, proton-exchanged aluminosilicate zeolites are promising materials as durable and practical heterogeneous catalysts, owing to their all-inorganic frameworks and commercial availabilities, as well as the absence of transition metal species.³⁹ For example, Mota et al. compared the activities of several proton-exchanged zeolites with Amberlyst-15 toward the acetalization of glycerol with acetone and formaldehyde.³⁴ In their experiments, Amberlyst-15 afforded the highest reaction yield in the presence of acetone, while higher yields were obtained in the presence of formaldehyde using proton-exchanged *BEA zeolite (H β), with a Si/Al ratio of 16, compared with Amberlyst-15 as well as ZSM5 and Y zeolites. Dealuminated and desilicated H β s were synthesized and then applied to the acetalization of glycerol by Venkatesha et al.³⁵ and Bokade et al.³⁶, respectively.

Both groups concluded that the enhanced catalytic performances were as a result of the increased pore volumes by dealumination or desilication. Very recently, Corma et al. demonstrated the acetalization of glycerol with 5-(alkyloxymethyl)furfural for the one-pot synthesis of biomass-derived surfactants using various H β zeolites and observed that the H β with a high Si/Al ratio of 100 exhibited high activity.³⁷ The aforementioned studies demonstrate the high potential of H β for the acetalization of glycerol with carbonyl compounds. However, quantitative studies, which focus on the effects of surface properties/acidity and substrate scope for carbonyl compounds, have not been reported, hitherto. Such studies would help elucidate zeolite catalysis including H β .

Our research group has previously developed efficient heterogeneous catalyst systems using H β zeolites for ester hydrolysis⁴⁰ and the hydration of alkynes/epoxides.⁴¹ Furthermore, we have also quantitatively reported how this type of catalysis is influenced by acid site concentration and the catalyst surface hydrophobic/hydrophilic properties based on various adsorption experiments and kinetic studies. In this work, we investigated the glycerol acetalization efficiency of H β as a function of Si/Al ratio by comparing with other heterogeneous and homogeneous catalysts, and observed that H β , with relatively high Si/Al ratio of 75 (H β -75), showed the highest efficiency. The substrate scope for carbonyl compounds and the reusability of H β -75 were also examined. Furthermore, the effect of hydrophobicity and acid site concentration on the acetalization efficiency is discussed to provide insight into the high efficiency of H β -75.

5.2 Experimental

5.2.1 General

Commercial compounds (Tokyo Chemical Industry or Kanto Chemical Company) were used without further purification. GC-MS (Shimadzu GCMS-QP2010) analyses were performed using an Ultra ALLOY⁺-1 capillary column (Frontier Laboratories Ltd.) with N₂ and He as the carrier gases. ¹H NMR analyses were performed using a JEOL-ECX 600 spectrometer operating at 600.17 MHz.

5.2.2 Catalyst preparation

H β -75 (JRC-Z-HB150, originally supplied from Clariant), H β -12.5 (JRC-Z-HB25), HMOR-45 (JRC-Z-HM90, originally supplied from Clariant), TiO₂ (JRC-TIO-4), CeO₂ (JRC-CEO-3), and amorphous SiO₂-Al₂O₃ (JRC-SAL-2) were provided by the Catalysis Society of Japan. H β -20 (HSZ-940HOA), H β -255 (HSZ-980HOA), HZSM5-20

(HSZ-840HOA) and HY-50 (HSZ-385HUA) were purchased from Tosoh Co. As-synthesized H β -5 (HSZ-940HOA), based on a previous report⁴², was supplied from Uni Zeo Co., Ltd. HZSM5-11 was obtained by calcination of NH₄-ZSM5 having a Si/Al ratio of 11 (HSZ-820NHA, purchased from Tosoh Co.), at 550 °C for 3 h. HZSM5-75 and HZSM5-150 were obtained from N.E. CHEMCAT Co. Niobic acid (Nb₂O₅·*n*H₂O, HY-340) was kindly provided by CBMM. Nb₂O₅ was synthesized by calcination of the niobic acid (500 °C for 3 h). SiO₂ (Q-10) was provided by Fuji Silysia Chemical Ltd. ZrO₂ and SnO₂ were obtained by calcination of ZrO₂·*n*H₂O and H₂SnO₃ (Kojundo Chemical Laboratory Co., Ltd.), at 500 °C for 3 h. Sulfonic acid-functionalized resin (Amberlyst-15) was commercially purchased from Sigma-Aldrich.

5.2.3 Catalytic tests

For a typical catalytic reaction, glycerol (1 mmol) was subjected to acetalization with aldehydes or ketones (1.5 mmol) in the presence of a catalyst (25 mg) and toluene (1 mL). The reaction mixture was added to a reaction tube (cylindrical Pyrex glass tube, 17 cm³), containing a magnetic stirrer bar and placed in a heated reactor, at reflux conditions, under a nitrogen atmosphere with stirring at 400 rpm. After completion of the reaction, methanol (2 mL) was added and catalyst was removed by filtration. The solvent was evaporated from the reaction mixture, and the acetal/ketal product yield and glycerol conversion in the crude mixture determined by ¹H NMR analysis (JEOL-ECX 600 spectrometer operating at 600.17 MHz, solvent CD₃OD) using mesitylene as an internal standard.

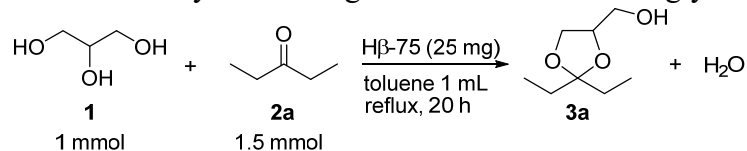
5.3 Results and Discussion

Comparison of H β zeolites with various acid catalysts

Initially, the acetalization of glycerol (**1**) with 3-pentanone (**2a**) was investigated using a wide matrix of 24 heterogeneous and homogenous catalyst types, by refluxing in toluene for 20 h. The results are summarized in **Table 1**. Under these conditions, the reaction does not proceed in the absence of any catalyst (entry 1). Among the catalysts tested, H β -75 afforded the highest yield (96%) of the five-membered cyclic acetal (**3a**) (entry 4), without the formation of the corresponding six-membered cyclic acetal. The Si/Al ratio of H β is observed to influence the **3a** yield, which increased as a function of increased Si/Al ratio from 12.5 to 75 (entries 2–4), while the use of H β -255 resulted in a lower yield compared with H β -75 (entry 5). A similar dependency on the Si/Al ratio was observed using a series of proton-exchanged ZSM5 (HZSM5) zeolites having Si/Al ratios between 11 and 150 (entries 6–9). HZSM5-75

exhibited a higher yield compared with the other HZSM5 catalysts (entry 8), although HZSM5-75 was inferior to H β -75. The zeolites possessing a relatively high Si/Al ratio of 75

Table 1. Catalyst screening for the acetalization of glycerol (**1**) with 3-pentanone (**2a**).



Entry	Catalyst	Yield (%) ^a
1	none	0
2	H β -12.5	44
3	H β -20	48
4	H β -75	96
5	H β -255	77
6	HZSM5-11	43
7	HZSM5-20	46
8	HZSM5-75	68
9	HZSM5-150	62
10	HY-50	58
11	HMOR-45	61
12	Al ₂ O ₃	48
13	ZrO ₂	61
14	TiO ₂	43
15	SnO ₂	67
16	Nb ₂ O ₅	54
17	Nb ₂ O ₅ · <i>n</i> H ₂ O	65
18	SiO ₂	16
19	CeO ₂	13
20	Cs _{2.5} H _{0.5} PW ₁₂ O ₄₀	62
21	Amberlyst-15	2
22	Montmorillonite K10	56
23 ^b	H ₂ SO ₄	25
24	PTSA	44
25	Sc(OTf) ₃	28

^a Yields of **3a** were determined by ¹H NMR spectroscopy, ^b 40 wt.% aqueous solution.

exhibited high catalytic performance. The performance of H β -75 with other heterogeneous acid catalysts was compared, including other proton-exchanged zeolites (HY-50 and HMOR-45), metal oxides (Al₂O₃, ZrO₂, TiO₂, SnO₂, Nb₂O₅, Nb₂O₅·*n*H₂O, SiO₂, and CeO₂), a heteropoly acid (Cs_{2.5}H_{0.5}PW₁₂O₄₀), and commercially-available solid acid catalysts (Amberlyst-15 and Montmorillonite K10). Moderate-to-good yields (43–67%) of **3a** were

obtained in the presence of Al₂O₃, ZrO₂, TiO₂, SnO₂, and Nb₂O₅ (entries 12–16). Nb₂O₅·*n*H₂O, known as a water-tolerant solid acid ⁴⁹, also exhibited an acceptable yield of 65% (entry 17). However, all **3a** yields were lower when compared with the yield for Hβ-75. Conversely, the yields for SiO₂ and CeO₂ were significantly lower (entries 18 and 19). Cs_{2.5}H_{0.5}PW₁₂O₄₀ and montmorillonite K10 exhibited moderate activity, forming **3a** in 62% and 56% yields (entries 20 and 22), respectively, while the use of Amberlyst-15 resulted in a poor yield (entry 21). Furthermore, typical homogeneous catalysts, such as H₂SO₄, PTSA, and Sc (OTf)₃, were applied to this reaction, however, the resultant yields of **3a** were low (25%, 44%, and 28%, respectively). From the above results, Hβ-75 is deemed the most effective catalyst for the acetalization of glycerol with ketone **2a**.

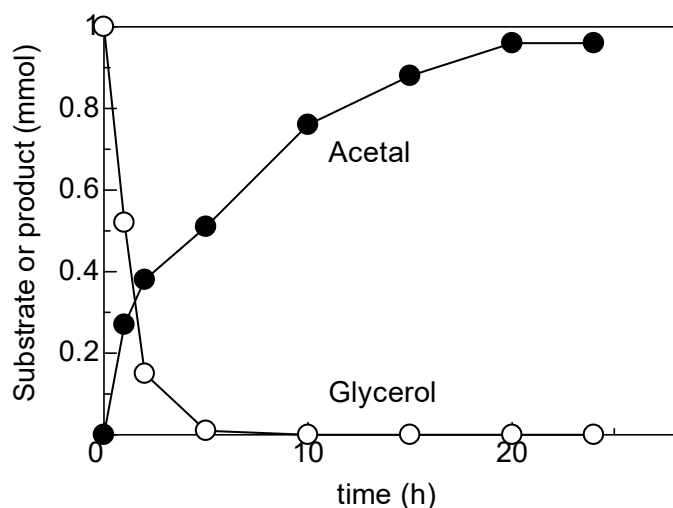


Figure 1. Acetalization of glycerol (**1**) with 3-pentanone (**2a**) to the corresponding acetal (**3a**) as a function of time-on-stream. Reaction conditions: Hβ-75 (25 mg), **1** (1 mmol), **2a** (1.5 mmol), toluene (1 mL), refluxed under a N₂ atmosphere for 0–24 h.

Optimization of reaction conditions

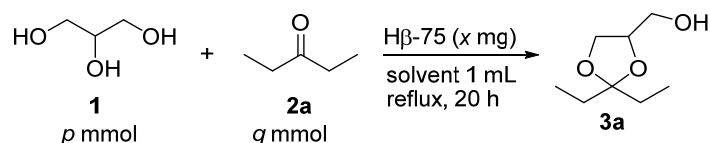
Using the most effective catalyst, Hβ-75, the optimal reaction conditions were determined for the acetalization of **1** with **2a** (Table 2). In the presence of **1** (1 mmol), **2a** (1 mmol), and toluene (1mL), the use of Hβ-75 (25 mg) afforded the highest yield (entries 1–5). The influence of ketone **2a** content was studied (0.5–1.5 mmol) using Hβ-75 (25 mg) and **1** (1 mmol) in toluene (entries 5–8). Although the use of an equimolar amount of **2a** gave **3a** in 85% yield (entry 5), **2a** in slight excess (1.25–1.5 mmol) is required to achieve >90% yield (entries 7 and 8). Furthermore, the influence of the solvent was examined through a series of

experiments comprising **1** (1 mmol), **2a** (1.5 mmol), and H β -75 (25 mg) for 20 h (entries 8–12). The aromatic solvents, such as toluene, *o*-xylene, and mesitylene, were effective (entries 8–10), with toluene being observed to be the most efficient solvent studied (entry 8). The use of 1,4-dioxane resulted in a significantly lower yield of **3a** (entry 11). Conversely, acetalization did not proceed using H₂O as a solvent (entry 12). Furthermore, time-on-stream was also investigated, as shown in **Figure 1**. Glycerol was not observed after 10 h, while the yield of **3a** reached the highest value of 96% after 20 h. Based on these results, the optimized reaction conditions were determined as follows: **1** (1 mmol), **2a** (1.5 mmol), H β -75 (25 mg), and toluene (1 mL) under reflux for 20 h.

Substrate scope and reusability of H β -75

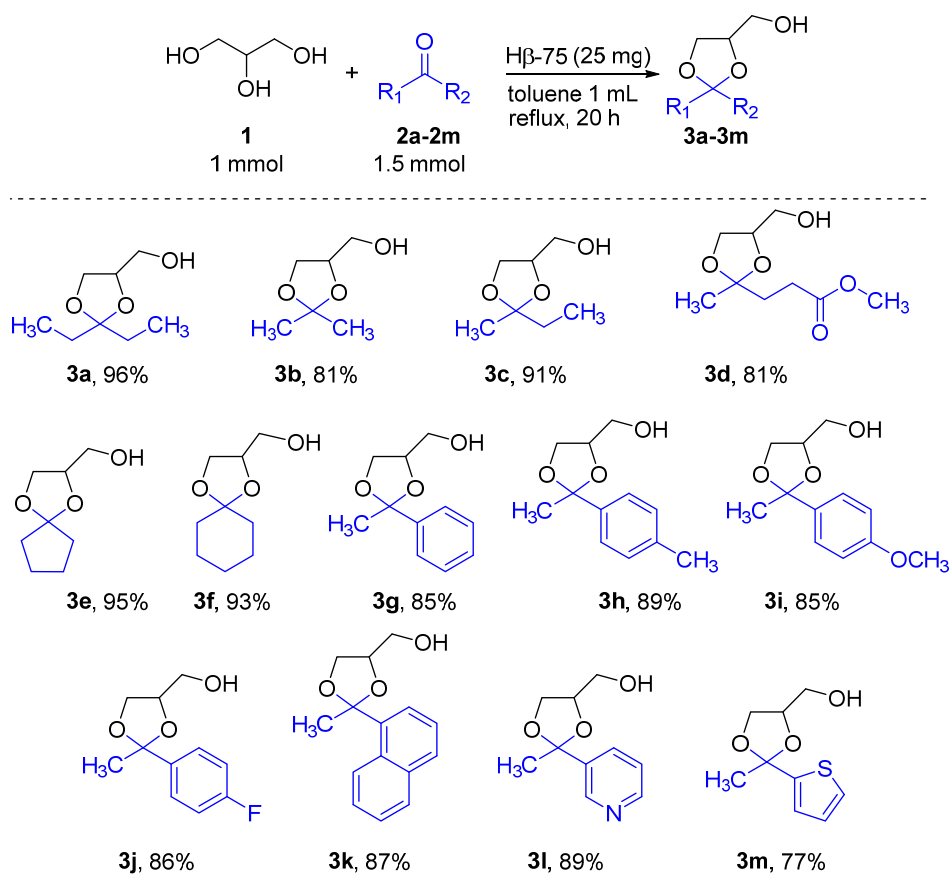
After establishing the optimized reaction conditions, the substrate scope toward ketones amenable to the H β -75-catalyzed acetalization with glycerol **1** was studied. The products **3a–3m**, together with their respective yields, are summarized in **Scheme 1**. Various acyclic

Table 2. Optimization of the acetalization reaction conditions using H β -75 catalyst.



Entry	H β -75 (mg)	1 (<i>p</i> mmol)	2a (<i>q</i> mmol)	Solvent	Yield (%) ^a
1	5	1	1	toluene	42
2	10	1	1	toluene	51
3	15	1	1	toluene	73
4	20	1	1	toluene	81
5	25	1	1	toluene	85
6	25	1	0.5	toluene	41
7	25	1	1.25	toluene	91
8	25	1	1.5	toluene	96
9	25	1	1.5	<i>o</i> -xylene	88
10	25	1	1.5	mesitylene	83
11	25	1	1.5	1,4-dioxane	23
12	25	1	1.5	H ₂ O	0

^a Yields of **3a** were determined by ¹H NMR spectroscopy.

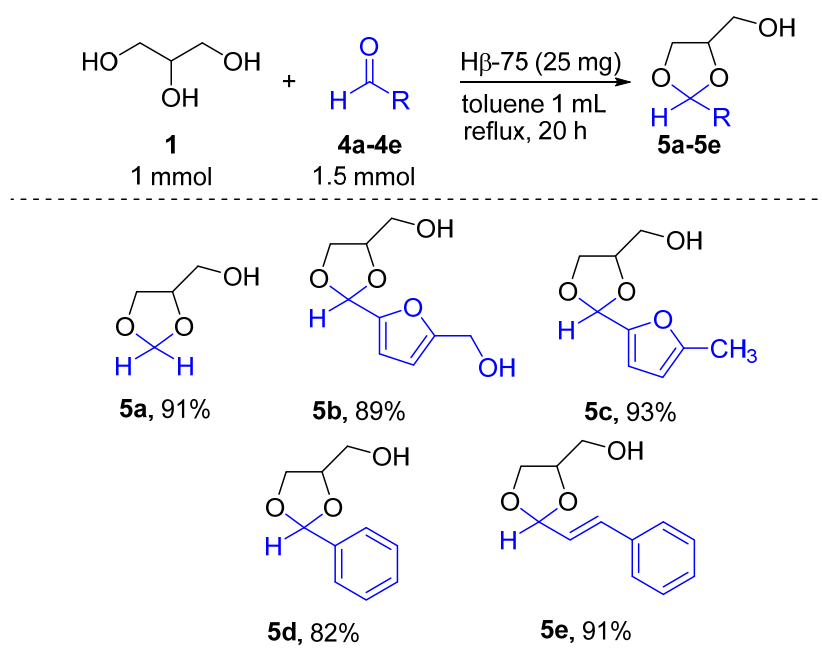


Scheme 1. Acetalization of glycerol with different ketones. Ketal yields were determined by ^1H NMR spectroscopy.

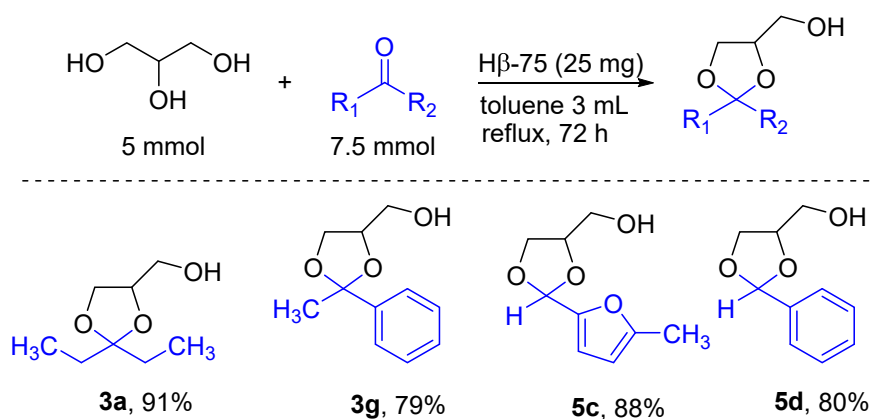
(**2a-2d**) and cyclic (**2e,2f**) ketones reacted efficiently with **1** to give the corresponding ketals **3a-3f** in 81%–96% yield. Acetophenone (**2g**) and its derivatives, possessing either electron-donating (**2h** and **2i**) or electron-withdrawing groups (**2j**), were also amenable to acetalization with glycerol. During the acetalization, the ester and methoxy moieties in the products (**3d** and **3i**) were retained. Furthermore, Hβ-75 promoted the acetalization of ketones having a bulky naphthalene ring (**2k**) as well as heterocycles (**2l** and **2m**), affording the desired products in good yields. Additionally, the substrate scope toward aldehydes in the present catalyst system was also studied (**Scheme 2**). The reaction of formaldehyde (**4a**) with **1** efficiently occurred, giving 1,3-dioxolane-4-methanol (**5a**) in 91% yield. The aldehydes incorporating furan (**4b** and **4c**) or phenyl rings (**4d**, **4e**) underwent acetalization with **1** to form the corresponding products **5b-5e** in 82%–93% yields. During the acetalization of cinnamaldehyde (**4e**), the olefinic moiety was tolerant. Overall, Hβ-75 efficiently promoted the acetalization of various ketones and aldehydes possessing numerous functional groups.

After the acetalization of glycerol and ketone **2a**, Hβ-75 was easily separated from the reaction mixture by centrifugation. The recovered catalyst was washed with acetone, dried at

90 °C for 3 h, and then reused for another reaction. Although product yields decreased slightly, H β -75 was recyclable in at least four reuse experiments (**Figure 2**). Furthermore,



Scheme 2. Acetalization of glycerol with different aldehydes. Acetal yields were determined by ^1H NMR spectroscopy.



Scheme 3. 5 mmol-scale acetalization of glycerol catalyzed by H β -75.

acetalization reactions of glycerol with **2a**, **2g**, **4c**, and **4d** were performed on a 5 mmol scale. As summarized in Scheme 3, the desired products (**3a**, **3g**, **5c**, and **5d**) were successfully obtained in 79%–91% yield. These results demonstrate the promising potential of H β -75 for practical applications in the acetalization of glycerol.

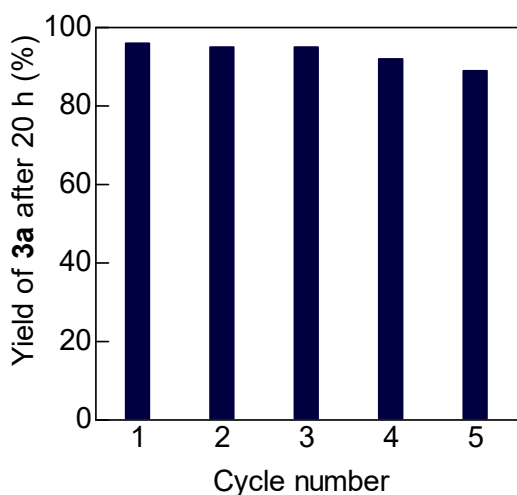


Figure 2. Catalyst reusability for the H β -75-catalyzed acetalization of glycerol (**1**) with 3-pentanone (**2a**). Reaction conditions: H β -75 (25 mg), **1** (1 mmol), **2a** (1.5 mmol), toluene (1 mL), refluxed under a N₂ atmosphere for 20 h.

Relationship between activity and hydrophobicity/acidity

Previously, we determined the hydrophobicity/hydrophilicity of H β as a function of Si/Al ratio (Si/Al = 12.5–255) by *n*-dodecane/H₂O adsorption experiments and revealed that hydrophobicity monotonically increases with increased Si/Al ratio(**Figure 3C**).⁴¹ A similar dependency of hydrophobicity on the Si/Al ratio was reported by Fukuoka et al.⁵⁰ and Yokoi et al.⁵¹. The quantitative determination of acid sites was also studied by NH₃ adsorption experiments using IR spectroscopy^{41,52}. The acid sites in H β (Si/Al = 12.5–255) comprised principally of Brønsted acid sites, and the Brønsted acid site concentration decreases with increasing Si/Al ratio (**Figure 3D**).⁴¹ Based on such adsorption experiments and kinetic studies, we further reported the influence of hydrophobicity/acidity on the hydration catalysis⁴¹.

During the acetalization of glycerol with ketone **2a**, as shown in **Table 1**, H β -75, with relatively high Si/Al ratio, is observed to be the most effective catalyst among the H β zeolites having Si/Al ratios ranging from 12.5 to 255 (entries 2–5). Similar phenomena were observed in the experiments using HZSM-5 having a broad range of Si/Al ratios (entries 6–9). To elucidate the origin of the high efficiency observed for H β -75, the initial reaction rates (V_{init}) of a series of H β catalysts were measured at below 20% conversion. The reaction rate exhibited a volcano-type dependency on the Si/Al ratio (**Figure 3A**), with H β -75 exhibiting the highest V_{init} value (11.3 mmol h⁻¹g_{cat}⁻¹). Conversely, the turnover frequency value, determined based on the Brønsted acid site concentration³⁴, monotonically increased with

increasing Si/Al ratio (**Figure 3B**), which is similar to the dependency of hydrophobicity on the Si/Al ratio (**Figure 3C**). Based on these results obtained by kinetic studies and adsorption experiments, the hydrophobic nature of the H β catalysts is suggested to accelerate the acetalization effectively. On the hydrophobic inner pore surface, the generated H₂O molecule, as a co-product, easily desorbs, thus accelerating the acetalization reaction. H β -75 is tailored to possess both a suitable hydrophobic nature and a sufficient acid site concentration in the pores, which promotes acetalization. The higher efficiency observed for H β -75, compared with HZSM5-75, is interpreted by a difference of pore size. The H β pore size (7.6 Å × 7.3 Å) is larger than HZSM-5 (5.6 Å × 5.3 Å). As a consequence, the product **3a**, having the minimum cross-section diameter of 5.7 Å × 9.3 Å (See Supporting Information), can more effectively ingress and diffuse within the larger pores of H β , resulting in enhanced catalytic performance of H β -75, compared with HZSM5-75⁴⁰.

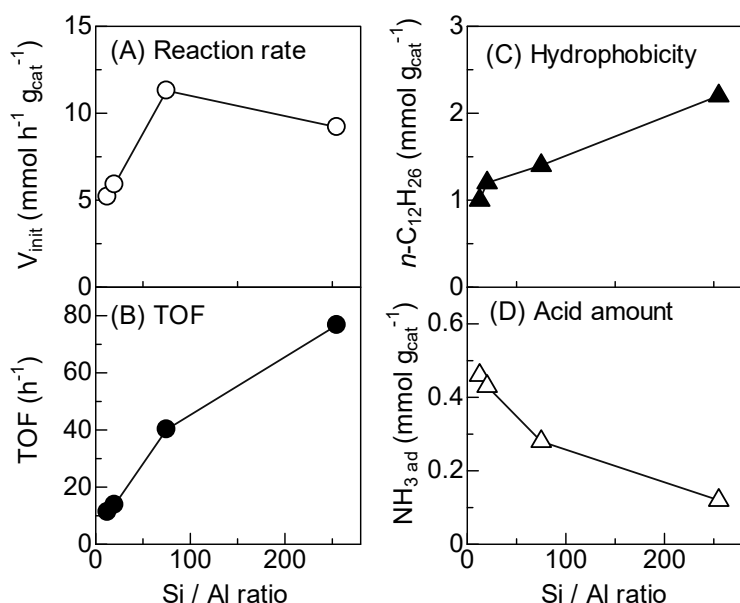


Figure 3. Results of the kinetic studies and adsorption experiments. (A) Initial reaction rate and (B) turnover frequencies (TOF), normalized to Brønsted acid site concentration, versus H β Si/Al ratio, for the acetalization of glycerol (**1**) with 3-pentanone (**2a**). (C) Hydrophobicity, as estimated by n -dodecane adsorption [41] and (D) total H β Brønsted acid site concentration [41] as a function of Si/Al ratio.

5.4 Conclusions

H β -75 exhibited the highest catalytic performance toward acetalization using glycerol among 21 various types of heterogenous acid catalysts. The present catalyst system was amenable to the acetalization of numerous ketones and aldehydes to afford the corresponding products in

good yields. The catalyst was also observed to be easily separated from the catalytic process and recyclable without demonstrating a significant loss in activity. The wide substrate scope and high recyclability of H β -75 offer advantages from a practical viewpoint. The kinetic studies and adsorption experiments using H β , as a function of Si/Al ratio, indicated that the acid sites present at the hydrophobic pore surface promoted acetalization more efficiently. The data provide a platform to develop further efficient acid catalysts for acetalization. The high activity of H β -75 is realized by the tailored hydrophobic nature of the catalyst surface, a sufficient number of accessible acid sites and in having a larger pore size compared with HZSM5.

References

- (1) Zhou, C. H.; Beltramini, J. N.; Fan, Y. X.; Lu, G. Q. *Chem. Soc. Rev.* **2008**, *37* (3), 527–549.
- (2) Pagliaro, M.; Ciriminna, R.; Kimura, H.; Rossi, M.; Della Pina, C. *Angew. Chemie - Int. Ed.* **2007**, *46* (24), 4434–4440.
- (3) Sun, D.; Yamada, Y.; Sato, S.; Ueda, W. *Appl. Catal. B Environ.* **2016**, *193*, 75–92.
- (4) Tomishige, K.; Nakagawa, Y.; Tamura, M. *Green Chem.* **2017**, *19* (13), 2876–2924.
- (5) Nishimura, S.; Takagaki, A.; Ebitani, K. *Green Chem.* **2013**, *15* (8), 2026–2042.
- (6) Vaidya, P. D.; Rodrigues, A. E. *Chem. Eng. Technol.* **2009**, *32* (10), 1463–1469.
- (7) Mizugaki, T.; Kaneda, K. *Chem. Rec.* **2018**, 1–21.
- (8) Katryniok, B.; Kimura, H.; Skrzyńska, E.; Girardon, J. S.; Fongarland, P.; Capron, M.; Ducoulombier, R.; Mimura, N.; Paul, S.; Dumeignil, F. *Green Chem.* **2011**, *13* (8), 1960–1979.
- (9) Katryniok, B.; Paul, S.; Bellière-Baca, V.; Rey, P.; Dumeignil, F. *Green Chem.* **2010**, *12* (12), 2079–2098.
- (10) Jérôme, F.; Pouilloux, Y.; Barrault, J. *ChemSusChem* **2008**, *1* (7), 586–613.
- (11) Rueping, M.; Phapale, V. B. *Green Chem.* **2012**, *14* (1), 55–57.
- (12) Crotti, C.; Farnetti, E.; Guidolin, N. *Green Chem.* **2010**, *12* (12), 2225–2231.
- (13) Scamardella, C.; Cucciolito, M. E.; Ruffo, F.; Raucci, U.; Rega, N.; Esposito, R.; Di Guida, R. *ACS Omega* **2019**, *4* (1), 688–698.
- (14) Mitsudome, T.; Matsuno, T.; Sueoka, S.; Mizugaki, T.; Jitsukawa, K.; Kaneda, K. *Heterocycles* **2011**, *84* (1), 371–376.
- (15) Li, X.; Zheng, L.; Hou, Z. *Fuel* **2018**, *233* (January), 565–571.
- (16) Feliczak-Guzik, A.; Nowak, I. *Microporous Mesoporous Mater.* **2019**, *277* (October 2018), 301–308.
- (17) Ammaji, S.; Rao, G. S.; Chary, K. V. R. *Appl. Petrochemical Res.* **2018**, *8* (2), 107–118.

- (18) Fonseca, A. M.; Ferreira, C.; Rombi, E.; Araujo, A.; Cutrufello, M. G.; Calvino-Casilda, V.; Bañares, M. A.; Neves, I. C. *Microporous Mesoporous Mater.* **2018**, *271* (February), 243–251.
- (19) Malleshram, B.; Sudarsanam, P.; Raju, G.; Reddy, B. M. *Green Chem.* **2013**, *15* (2), 478–489.
- (20) Chen, L.; Nohair, B.; Kaliaguine, S. *Applied Catal. A, Gen.* **2016**, *509*, 143–152.
- (21) Chen, L.; Nohair, B.; Zhao, D.; Kaliaguine, S. *ChemCatChem* **2018**, *10* (8), 1918–1925.
- (22) Chen, L.; Nohair, B.; Zhao, D.; Kaliaguine, S. *Appl. Catal. A Gen.* **2018**, *549* (June 2017), 207–215.
- (23) Nair, G. S.; Adrijanto, E.; Alsalmeh, A.; Kozhevnikov, I. V.; Cooke, D. J.; Brown, D. R.; Shiju, N. R. *Catal. Sci. Technol.* **2012**, *2* (6), 1173–1179.
- (24) Reddy, P. S.; Sudarsanam, P.; Malleshram, B.; Raju, G.; Reddy, B. M. *J. Ind. Eng. Chem.* **2011**.
- (25) Oliveira, A. C.; do Carmo, J. V. C.; Pinheiro, A. L. G.; Rodríguez-Castellón, E.; Carvalho, D. C.; Lang, R.; Otubo, L.; Tehuacanero-Cuapa, S. *Fuel Process. Technol.* **2018**, *184* (November 2018), 45–56.
- (26) Kanai, S.; Nagahara, I.; Kita, Y.; Kamata, K.; Hara, M. *Chem. Sci.* **2017**, *8* (4), 3146–3153.
- (27) Faria, R. P. V.; Pereira, C. S. M.; Silva, V. M. T. M.; Loureiro, J. M.; Rodrigues, A. E. *Ind. Eng. Chem. Res.* **2013**, *52* (4), 1538–1547.
- (28) Konwar, L. J.; Samikannu, A.; Mäki-Arvela, P.; Boström, D.; Mikkola, J. P. *Appl. Catal. B Environ.* **2018**, *220* (July 2017), 314–323.
- (29) Oger, N.; Lin, Y. F.; Le Grogne, E.; Rataboul, F.; Felpin, F. X. *Green Chem.* **2016**, *18* (6), 1531–1537.
- (30) Güemez, M. B.; Arias, P. L.; Cambra, J. F.; García, I.; Agirre, I.; Barrio, V. L.; Requies, J. *Biomass and Bioenergy* **2011**, *35* (8), 3636–3642.
- (31) Deutsch, J.; Martin, A.; Lieske, H. *J. Catal.* **2007**, *245* (2), 428–435.
- (32) Li, L.; Korányi, T. I.; Sels, B. F.; Pescarmona, P. P. *Green Chem.* **2012**.
- (33) Bakuru, V. R.; Churipard, S. R.; Maradur, S. P.; Kalidindi, S. B. *Dalt. Trans.* **2019**, *48* (3), 843–847.
- (34) Da Silva, C. X. A.; Gonalves, V. L. C.; Mota, C. J. A. *Green Chem.* **2009**, *11* (1), 38–41.
- (35) Venkatesha, N. J.; Bhat, Y. S.; Jai Prakash, B. S. *RSC Adv.* **2016**, *6* (23), 18824–18833.
- (36) Sonar, S. K.; Shinde, A. S.; Asok, A.; Niphadkar, P. S.; Mayadevi, S.; Joshi, P. N.; Bokade, V. V. *Environ. Prog. Sustain. Energy* **2018**, *37* (2), 797–807.
- (37) Garcia-Ortiz, A.; Arias, K. S.; Climent, M. J.; Corma, A.; Iborra, S. *ChemSusChem* **2018**, *11* (17), 2870–2880.

- (38) Arias, K. S.; Garcia-Ortiz, A.; Climent, M. J.; Corma, A.; Iborra, S. *ACS Sustain. Chem. Eng.* **2018**, *6* (3), 4239–4245.
- (39) Chester, A. W.; Derouane, E. G. *Zeolite characterization and catalysis: A tutorial*; Springer-Verlag New York Inc.: New York, 2010.
- (40) Toyao, T.; Shimizu, K.; Siddiki, S. M. A. H.; Kon, K.; Touchy, A. S. *J. Catal.* **2016**, *344*, 741–748.
- (41) Sultana Poly, S.; Hakim Siddiki, S. M. A.; Touchy, A. S.; Yasumura, S.; Toyao, T.; Maeno, Z.; Shimizu, K. *J. Catal.* **2018**, *368*, 145–154.
- (42) Kamimura, Y.; Chaikittisilp, W.; Itabashi, K.; Shimojima, A.; Okubo, T. *Chem. - An Asian J.* **2010**, *5* (10), 2182–2191.
- (43) Li, X.; Zheng, L.; Hou, Z. *Fuel* **2018**, *233* (January), 565–571.
- (44) Guidi, S.; Noè, M.; Riello, P.; Perosa, A.; Selva, M. *Molecules* **2016**, *21* (5).
- (45) Corma, A.; Ruiz, V. R.; Leyva-Pérez, A.; Sabater, M. J. *Adv. Synth. Catal.* **2010**, *352* (10), 1701–1710.
- (46) Almeida, M.; Klein, S.; Lopes, N.; dos Santos, W.; Zanatta, L.; Clososki, G.; Nelson, D.; de Almeida, M.; Barbosa, S.; Lage, G.; Ottone, M. *J. Braz. Chem. Soc.* **2018**, *29* (8), 1663–1671.
- (47) Mallesham, B.; Sudarsanam, P.; Reddy, B. M. **2014**, 803–813.
- (48) Barbasiewicz, M.; Mąkosza, M. *Org. Lett.* **2006**, *8* (17), 3745–3748.
- (49) Baba, Y.; Hayashi, S.; N. Kondo, J.; Hara, M.; Kitano, M.; Noma, R.; Nakajima, K. *J. Am. Chem. Soc.* **2011**, *133* (12), 4224–4227.
- (50) Yokoyama, H.; Kobayashi, H.; Hasegawa, J. Y.; Fukuoka, A. *ACS Catal.* **2017**, *7* (7), 4828–4834.
- (51) Otomo, R.; Yokoi, T.; Tatsumi, T. *Appl. Catal. A Gen.* **2015**, *505*, 28–35.
- (52) Katada, N.; Tamagawa, H.; Niwa, M. *Catal. Today* **2014**, *226*, 37–46.

Chapter 6

**Methylation of xylene by hydrogenation of CO₂ using
TiO₂-supported Re and HBEA zeolite catalysts**

6.1 Introduction

The growing concerns about global climate change and increasing social awareness of the environmental problems have created a need for more sustainable development.¹ Thus, our society needs to face new challenges, such as mitigation of climate change, preservation of the environment, usage of renewable energy and replacement of fossil fuels.² The realization of these challenges requires new breakthrough solutions in order to be successfully addressed. Carbon dioxide (CO₂) is one of the major components of greenhouse gases emitted into the Earth's atmosphere due to human activities. This increase in CO₂ concentration is largely due to the combustion of fossil fuels, which are required to meet the world's energy demand.³ Not only the use of CO₂ as a chemical feedstock is a way to reduce atmospheric CO₂ concentration, it is also abundant, nontoxic, and easily available. There is no doubt that carbon dioxide (CO₂) is a common factor in these great challenges. Therefore, the valorization of CO₂ is advantageous from both environmental and economical point of view. The use of carbon dioxide (CO₂) as a building block for the production of chemicals is a topic of high interest and nowadays heavily discussed and investigated.⁴ So far, much attention has been directed towards the catalytic transformation of CO₂ via hydrogenation to produce value-added chemicals, especially CH₃OH, due to the popularity of "methanol economy".⁵ CH₃OH, one of the most important product chemicals, is widely used as a C₁ source for industrial purpose, especially for the formation of C-N and C-C bond. In recent years, several studies on the direct methylation of C-N and C-H bonds by employing using CO₂/H₂ has been reported.⁶⁻¹³ Although these studies are highly impactful, the substrate scope are mostly limited to molecules which contain activated C-N or C-H bonds such as amines, imines and heteroarenes. In the past decades, great efforts have been paid to develop efficient technologies for CO₂ hydrogenation, to various C₁ products, such as methane, methanol, carbon monoxide and formic acid. Recently, the hydrogenation of CO₂ to liquid fuels and lower olefins has also made great progress, which advances the frontier of CO₂ utilization.¹⁴ A variety of reports on the catalytic methylation of C-H bonds for unactivated aromatic hydrocarbons, by using fossil-based methylating agents such as methanol, dimethyl ether, methane, and syngas are widely available.^{14,15} These reactions are mainly carried out by using a bifunctional catalyst system which includes a methanol synthesis catalyst coupled with acidic zeolite, which act as a methanol conversion catalyst.¹⁶ The methylation of aromatic hydrocarbons is of great importance as aromatics such as benzene, toluene, and xylenes are one of the most important platform molecules for the petrochemical industry.¹⁷ Therefore, the direct methylation of aromatic hydrocarbons to polymethyl benzenes (Tri, Tetra, Penta, Hexa

methyl benzenes) by using CO₂/H₂ is highly challenging.

In this report, a mix catalyst consists of a Re/TiO₂ catalyst, which exhibits high activity and product selectivity for i) the hydrogenation of carboxylic acid derivatives, ii) the *N*-methylation of amines using CO₂ and H₂, and iii) the *N*-alkylation of amines with carboxylic acids or esters in the presence of H₂, iv) the low temperature methanol synthesis using CO₂ and H₂¹⁸, and H-beta (Si/Al = 20), was employed for the direct methylation of xylene by using CO₂ and hydrogen in a batch reactor ($p_{\text{CO}_2} = 1 \text{ MPa}$; $p_{\text{H}_2} = 5 \text{ MPa}$; $T = 240 \text{ }^\circ\text{C}$). Catalyst screening was conducted on various combination of supported metal catalysts and different zeolites with a wide range of Si/Al ratio.

6.2 Experimental

Re (1)/TiO₂ was synthesized using a simple wet impregnation method employing NH₄ReO₄ and TiO₂. Commercially available zeolite catalysts are used directly without further treatment. For each experiment, the active catalyst was prepared by physically mixing both catalysts and followed by reduction in a quartz tube ($T = 500 \text{ }^\circ\text{C}$; $t = 0.5 \text{ h}$) under a flow of H₂ ($20 \text{ cm}^3 \text{ min}^{-1}$). A powder X-ray diffraction (XRD) pattern of the reduced Re (1)/TiO₂ catalyst was essentially identical to that of pristine TiO₂ (**Figure 1**). High-angle annular dark-field scanning transmission electron microscopy (HAADF-STEM) images of Re (1)/TiO₂ (**Figure 2**) show that the Re loaded on the TiO₂ support forms highly dispersed sub-nanometer clusters.

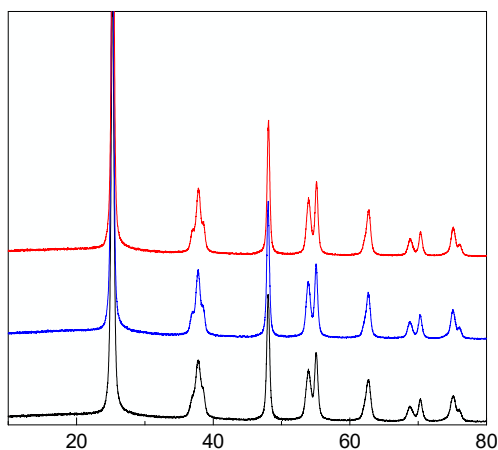


Figure 1. X-ray diffraction (XRD) pattern of the reduced Re (1)/TiO₂ catalyst

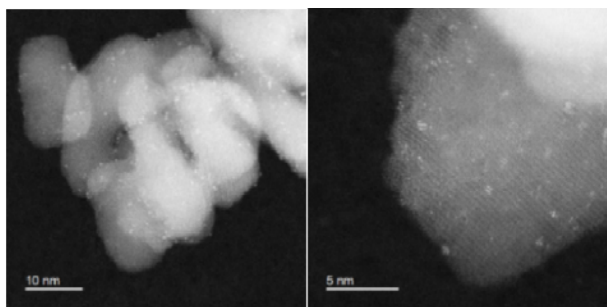


Figure 2. HAADF-STEM images of Re(1)/TiO₂.

6.3 Results and Discussion

In the early stage of this project, methylations of xylene by using CO₂/H₂ were carried out to screen the properties of various methanol synthesis catalysts. The obtained results are summarized in (Figure 3 and Figure 4). A combination of Re (1)/TiO₂ and H-BEA (Si/Al = 20) afforded the highest yield (70%) of methylated products at a CO₂ conversion of 48%, with lowest number of undesired byproducts such as CO, CH₄. In contrast, other TiO₂-supported metal catalysts afforded a much lower yield of methylated products. From these results, it is clear that Re (1)/TiO₂ is the best candidate as the methanol synthesis component for the mix catalyst used in this reaction, which is consistent with our previous study.

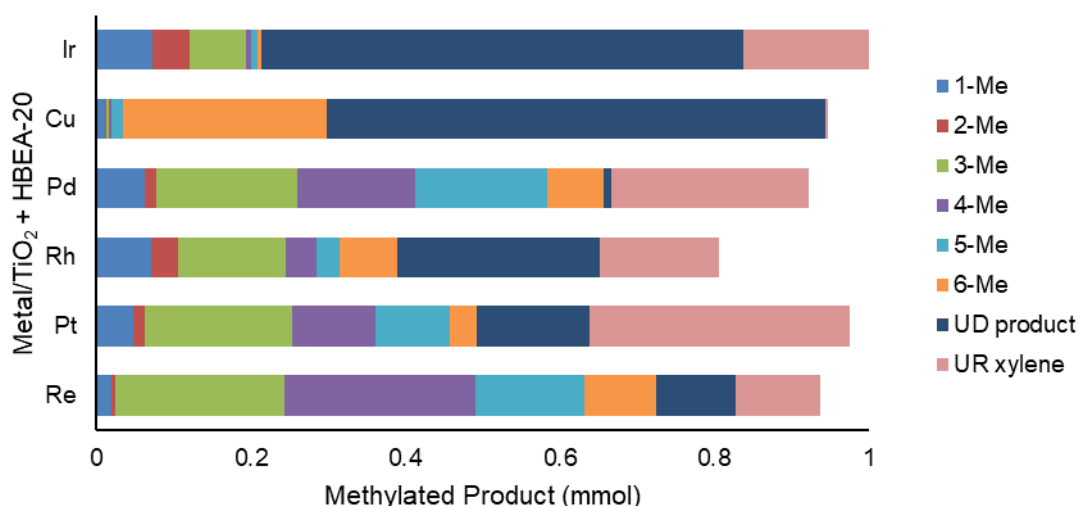


Figure 3. Reductive methylation of *m*-xylene with CO₂ using mixed catalysts (Metal (1)/TiO₂ + HBEA-20 with different metal) methylated yields are based on *m*-xylene, reaction time 20h. UD indicates undetected product, UR indicates unreacted product.

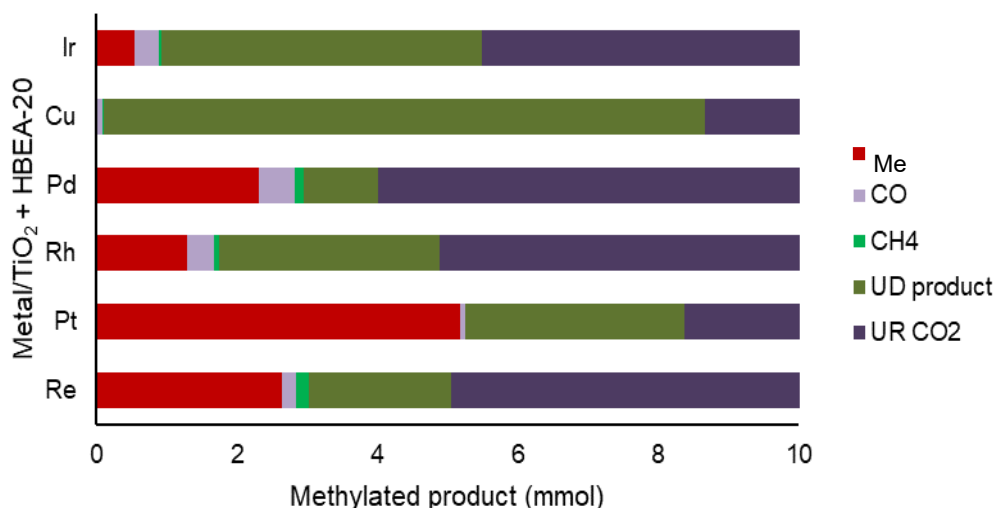


Figure 4. Reductive methylation of *m*-xylene with CO₂ using mixed catalysts (Metal (1)/TiO₂ + HBEA-20 with different metal) methylated yields are based on CO₂, reaction time 20h. UD indicates undetected product, UR indicates unreacted product.

After establishing Re (1)/TiO₂ as the methanol synthesis catalyst, we next explored the applicability of various zeolites with distinct framework type with a wide range of SiO₂/Al₂O₃ ratio for the methylation of xylene using CO₂/H₂.

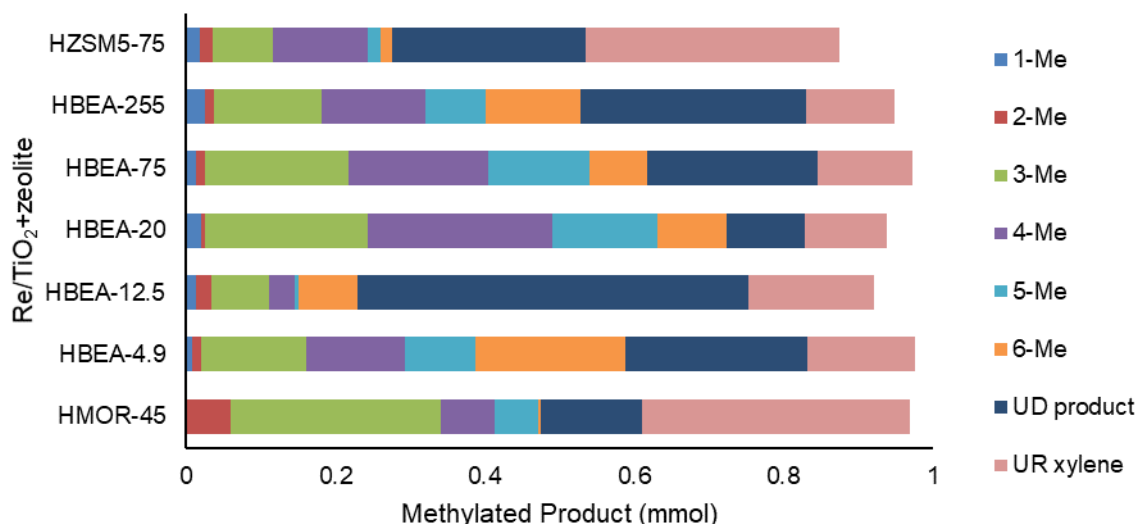


Figure 5. Reductive methylation of *m*-xylene with CO₂ using mixed catalysts (Re (1)/TiO₂ with different zeolite) methylated yields are based on *m*-xylene, reaction time 20h. UD indicates undetected product, UR indicates unreacted product.

Compared to other zeolites, H-beta is more favorable for the formation of polymethyl benzenes. The highest yield for methylated products was achieved by using H-beta (Si/Al = 20) (**Figure 5** and **Figure 6**). Even though there were no significant differences in terms of total yield of methylated products for all of H-beta zeolites (Si/Al = 4.9, 12.5, 75, 255), Meanwhile, H-ZSM-5 (Si/Al=75) which is typically used for the shape selective methylation of aromatics, were found to be less effective for the formation of polymethyl benzenes as compared to H-beta in our case. Based on these results, we concluded that H-beta (Si/Al= 20) is the most suitable methanol conversion catalyst for our bifunctional catalyst system. With the optimized catalyst system in hand, the effect of reaction temperature ($T = 220, 230, 240, 250, 280$ °C) on the methylation of xylene using CO₂ and H₂ was investigated (**Figure 7**). Reaction at 240 °C showed the best performance both in terms of total yield and product selectivity.

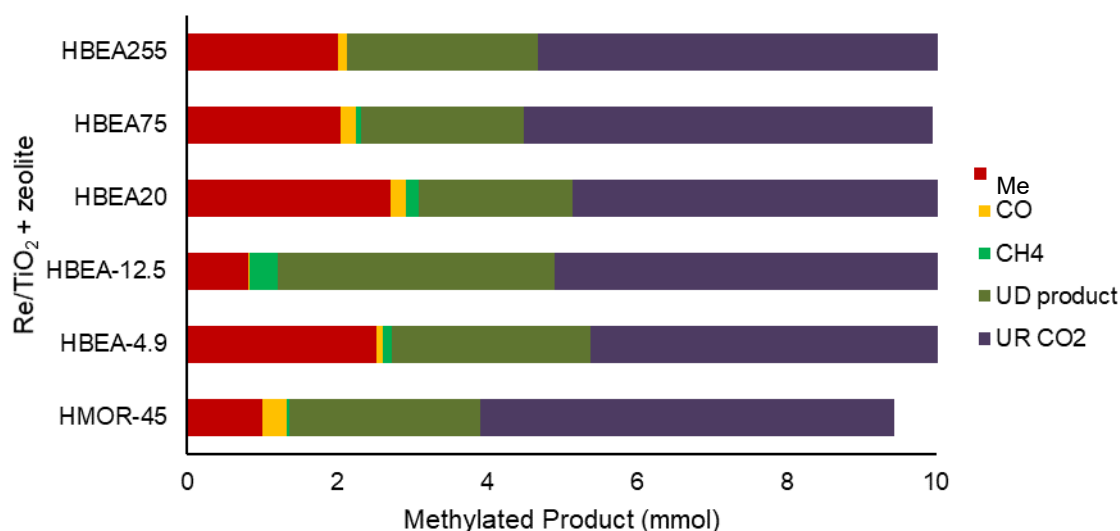


Figure 6. Reductive methylation of *m*-xylene with CO₂ using mixed catalysts (Re (1)/TiO₂ with different zeolite) methylated yields are based on CO₂, reaction time 20h. UD indicates undetected product, UR indicates unreacted product.

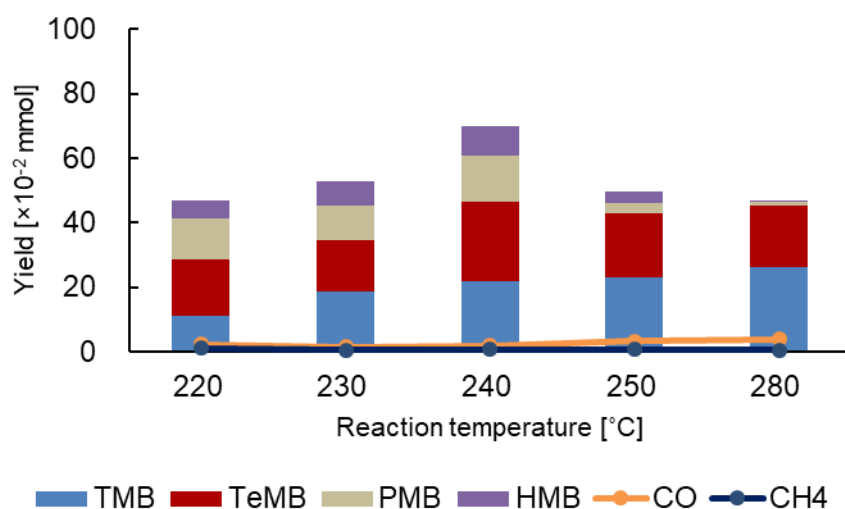


Figure 7. Effect of the reaction temperature on methylation of *m*-xylene using CO₂ and H₂ catalyzed by mixed catalyst consists of Re (1)/TiO₂ and HBEA (SiO₂/Al₂O₃=40). Pre-treatment: H₂ (20 mL min⁻¹), 500 °C, 0.5 h; reaction conditions: 0.0081 mmol of catalytically active metal and 100 mg of H-Beta (SiO₂/Al₂O₃=40), 1 mmol of substrate, CO₂ (1 MPa), H₂ (5 MPa), 20 h.

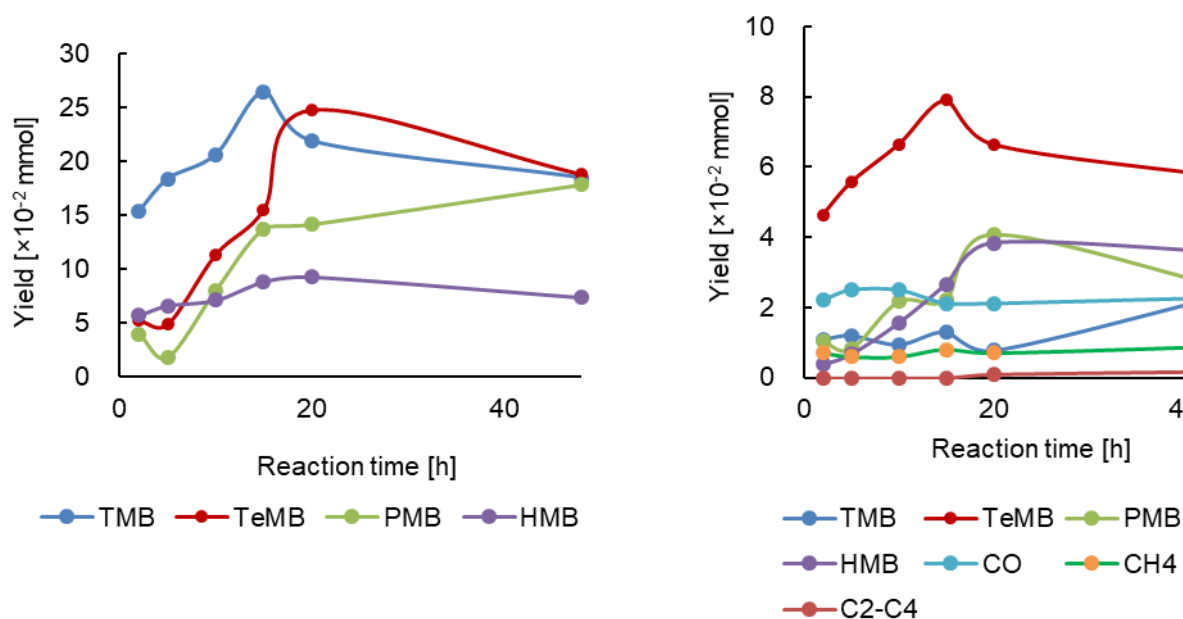
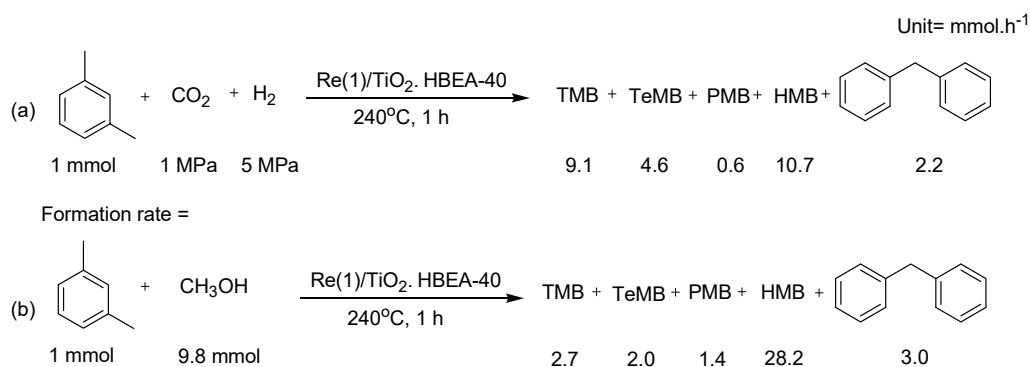


Figure 8. *m*-xylene-based (left) and CO₂-based (right) time-course plot of methylation of *m*-xylene over mixed catalyst composed of Re (1)/TiO₂ and HBEA (SiO₂/Al₂O₃=40). Pre-treatment: H₂ (20 mL min⁻¹), 500 °C, 0.5 h; reaction conditions: 0.0081 mmol of loaded metal and 100 mg of H-Beta (SiO₂/Al₂O₃=40), 1 mmol of substrate, CO₂ (1 MPa), H₂ (5 MPa), 240 °C.

The time course plot of the methylation of xylene is shown in **Figure 8**. Even though the initial time at 1 h HBEA-75 shows the highest yield of polymethyl benzene than the HBEA 20. But the final yield of polymethyl benzene is highest for the HBEA-20 after 20 h. The

product concentration increases gradually as the reaction proceeds.

In order to gain more insights into the specifics of the reaction, methylation reaction employing other possible methylation agent such as CH₃OH, was carried out under the standard reaction condition (**Scheme 1**). the reaction proceeds when CH₃OH was used instead of CO₂/H₂, suggesting that methanol is a possible intermediate for our system.



Scheme 1. Methylation of *m*-xylene over Re (1)/TiO₂ and HBEA (Si/Al=20) using several C₁ resources. (a) CO₂, (b) MeOH.

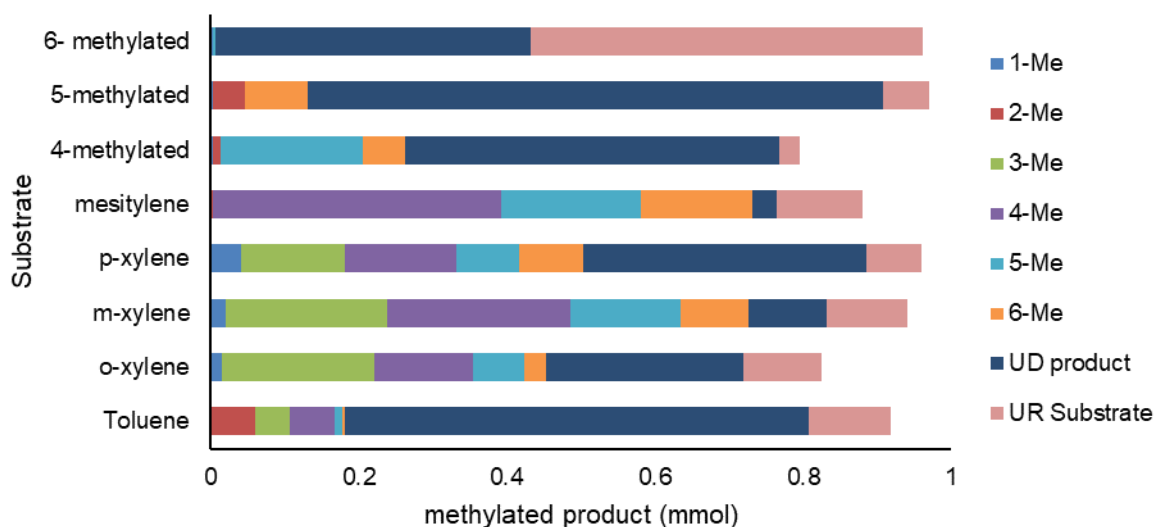


Figure 9. Substrate scope for the methylation reaction using CO₂ and H₂ catalyzed by mixed catalyst consists of Re (1)/TiO₂ and HBEA (SiO₂/Al₂O₃=40). Pre-treatment: H₂ (20 mL min⁻¹), 500°C, 0.5 h; reaction conditions: 0.0081 mmol of catalytically active metal and 100 mg of H-Beta (SiO₂/Al₂O₃=40), 1 mmol of substrate, CO₂ (1 MPa), H₂ (5 MPa), 20 h (based on different substrate). UD indicates undetected product, UR indicates unreacted product.

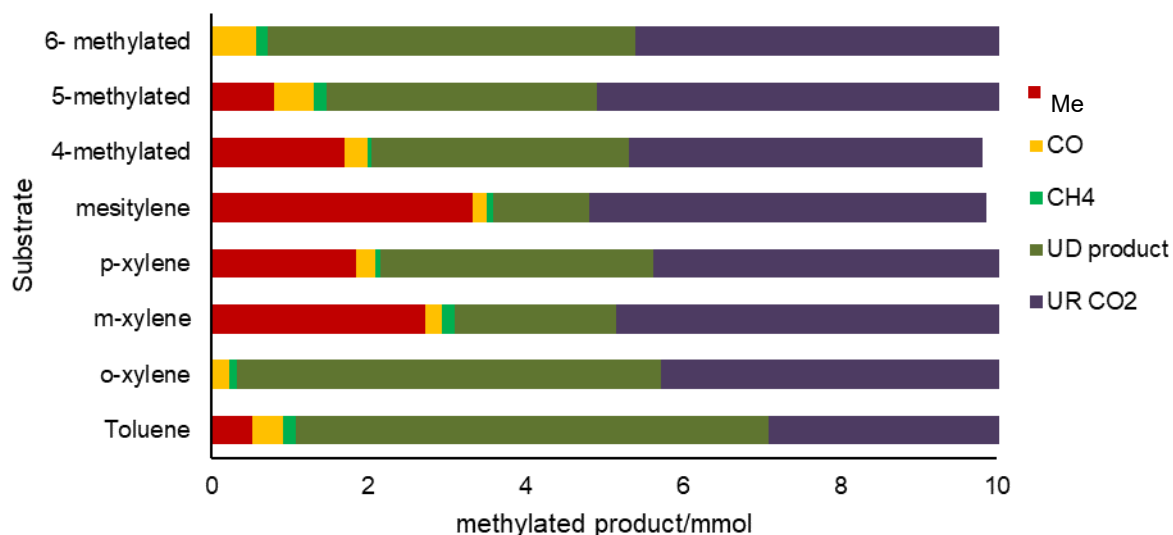


Figure 10. Substrate scope for the methylation reaction using CO₂ and H₂ catalyzed by mixed catalyst consists of Re (1)/TiO₂ and HBEA (SiO₂/Al₂O₃=40). Pre-treatment: H₂ (20 mL min⁻¹), 500°C, 0.5 h; reaction conditions: 0.0081 mmol of catalytically active metal and 100 mg of H-Beta (SiO₂/Al₂O₃=40), 1 mmol of substrate, CO₂ (1 MPa), H₂ (5 MPa), 20 h (based on CO₂). UD indicates undetected product, UR indicates unreacted product.

We also have investigated the methylation of different substrates with the mix catalysts Re (1)/TiO₂. HBEA-20 (**Figure 9** and **Figure 10**). The Results showed that *m*-xylene obtained the highest yield of poly methylated benzene than the other substrates.

6.4 Conclusion

The methylation of *m*-xylene by hydrogenation of CO₂, in the presence of H₂ was presented. Screening study showed that TiO₂-supported Re (Re/TiO₂) with Hbeta-20 (Si/Al=20) is the best combination for achieving high activity for this reaction. Under the optimized reaction conditions (PCO₂ = 1 MPa; PH₂ = 5 MPa; T = 513 K), this catalytic system achieved high yields of polymethyl benzenes. Re metal NPs catalyze a hydrogenation step, while the Hbeta-20 zeolite catalyzes alkylation step.

References

- (1) Hank, C.; Gelpke, S.; Schnabl, A.; White, R. J.; Full, J.; Wiebe, N.; Smolinka, T.; Schaadt, A.; Henning, H.-M.; Hebling, C. *Sustain. Energy Fuels* **2018**, *2* (6), 1244–1261.
- (2) Kattel, S.; Liu, P.; Chen, J. G. *J. Am. Chem. Soc.* **2017**, *139* (29), 9739–9754.
- (3) Liu, Q.; Wu, L.; Jackstell, R.; Beller, M. *Nat. Commun.* **2015**, *6*, 1–15.
- (4) Dabral, S.; Schaub, T. *Adv. Synth. Catal.* **2019**, *361* (2), 223–246.
- (5) Olah, G. A. *Angew. Chemie - Int. Ed.* **2005**, *44* (18), 2636–2639.
- (6) Karsten, B. P.; Bijleveld, J. C.; Viani, L.; Cornil, J. **2009**, 1–9.
- (7) Zalazar, M. F.; Paredes, E. N.; Romero Ojeda, G. D.; Cabral, N. D.; Peruchena, N. M. *J. Phys. Chem. C* **2018**, *122* (6), 3350–3362.
- (8) De Wispelaere, K.; Martínez-Espín, J. S.; Hoffmann, M. J.; Svelle, S.; Olsbye, U.; Bligaard, T. *Catal. Today* **2018**, *312* (February), 35–43.
- (9) Yang, F.; Zhong, J.; Liu, X.; Zhu, X. *Appl. Energy* **2018**, *226* (April), 22–30.
- (10) Bai, Y.; Yang, F.; Liu, X.; Liu, C.; Zhu, X. *Catal. Letters* **2018**, *148* (12), 3618–3627.
- (11) Zhao, X.; Zeng, F.; Zhao, B.; Gu, H. *China Pet. Process. Petrochemical Technol.* **2015**, *17* (1), 31–38.
- (12) Lee, S.; Kim, D.; Lee, J.; Choi, Y.; Suh, Y. W.; Lee, C.; Kim, T. J.; Lee, S. J.; Lee, J. K. *Appl. Catal. A Gen.* **2013**, *466*, 90–97.
- (13) Ahn, J. H.; Kolvenbach, R.; Al-Khattaf, S. S.; Jentys, A.; Lercher, J. A. *ACS Catal.* **2013**, *3* (5), 817–825.
- (14) Li, Y.; Cui, X.; Dong, K.; Junge, K.; Beller, M. *ACS Catal.* **2017**, *7* (2), 1077–1086.
- (15) Wang, Y.; Tan, L.; Tan, M.; Zhang, P.; Fang, Y.; Yoneyama, Y.; Yang, G.; Tsubaki, N. *ACS Catal.* **2019**, *9* (2), 895–901.
- (16) Kasipandi, S.; Bae, J. W. *Adv. Mater.* **2019**, *1803390*, 1–18.
- (17) Gong, J.; You, F. **2014**, *60* (9), 1531–1556.
- (18) Toyao, T.; Siddiki, S. M. A. H.; Touchy, A. S.; Onodera, W.; Kon, K.; Furukawa, S.; Ariga, H.; Asakura, K.; Shimizu, K. I.; Kamachi, T.; Yoshizawa, K.; Morita, Y. *Chemistry - A European Journal*. 2017.

Chapter 7

General Conclusion

7.1- Conclusion

The thesis reports investigations on the use of heterogeneous catalysts, particularly in the synthesis of fine chemicals. An introduction to the field of heterogeneous-catalyzed dehydrogenation, hydration and hydrogenation reactions of chemicals, mostly focusing on the mechanistic aspects of these processes, from the early investigations to the most recent developments. The objective of the thesis is to develop new heterogeneous catalysts for sustainable production of chemicals, as an atom-efficient synthetic method. However, most of the reports used homogeneous catalysts, which have serious drawbacks of difficulties in product/catalyst separation and catalyst reuse and needs of additives including expensive ligands. This newly developed simple, atom-efficient and environmentally benign method provides a practical and convenient route to synthesize chemicals from readily available starting materials with a wide range of substrate scope.

Chapter 2,3 showed one-pot, acceptorless dehydrogenative method, using a carbon-supported Pt catalyst (Pt/C) along with KO^tBu for the synthesis of substituted pyrimidines and pyridines from alcohols. The reaction takes place efficiently using a wide range of substrate scopes. The Pt/C catalyst that promotes this process is reusable and has a higher turnover number (TON) than those employed in previously reported methods.

Chapter 4,5 showed the transformation of hydrophobic substrates to important chemicals in polar environment. H β -75 showed wide substrate scope, good reusability, and applicability in gram-scale synthesis for these reactions. The effects of hydrophobicity, acidity, and the size of zeolite pores were also comprehensively studied through the hydration of hydrophilic and hydrophobic epoxides and alkynes with different molecular sizes using two types of zeolite (H β and HZSM5). Chapter 6 combined the previous chapters for the synthesis of polymethylated benzene from the starting material of *m*-xylene.

In conclusion, this work clarifies the syntheses of chemicals using various heterogeneous catalysts in three methodologies, (1) acceptorless dehydrogenative coupling reaction by metal nanoparticles (2) hydration of hydrophobic substrate in polar environment by Bronsted acidic zeolite and (3) Hydrogenation of CO₂ by metal nanoparticles and zeolite catalysts.

Acknowledgements

First, I would like to express my sincerest respect and gratitude to my supervisor Professor Kenichi Shimizu for his scholastic supervision, friendly collaboration, invaluable suggestions and thoughtful guidance at all stages of the present work, without which the present thesis paper might not have been completed.

I would like to thank specially appointed Asst. Prof. S.M.A. Hakim Siddiki for his scientific advises and numerous discussions which significantly contributed to the progress of my work. Without his support, this thesis would have not been accomplished.

I express my gratitude to Asst. Prof. Takashi Toyao for all the assistance, advices and valuable discussions. I am thankful to Professor Junya Hasegawa, Associate Professor Shinya Furukawa and specially appointed Lecturer Zen Maeno for their kind help and co-operation.

I am grateful to Dr. Abeda Sultana Touchy, Dr. Ken-ichi Kon & Mr. Wataru Onodera for their kind support and co-operation.

I would also like to thank my labmates for such an excellent place to work, Thanks for being more than friends. The completion of my present research would have not been made possible if not for the kind support of all the professors and lab mates in Shimizu Lab.

I would like to acknowledge the AGS (Advanced Graduate School) scholarship for financial support.

Finally, my heartfelt gratitude is extended to my beloved parents for their continuous support and encouragement. I also grateful to my husband, Md. Mahbub Alam Akanda for his understanding, constant support and encouragement of my research life.

Sharmin Sultana Poly